NASA Conference Publication 3185

Orbital, Rotational and Climatic Interactions

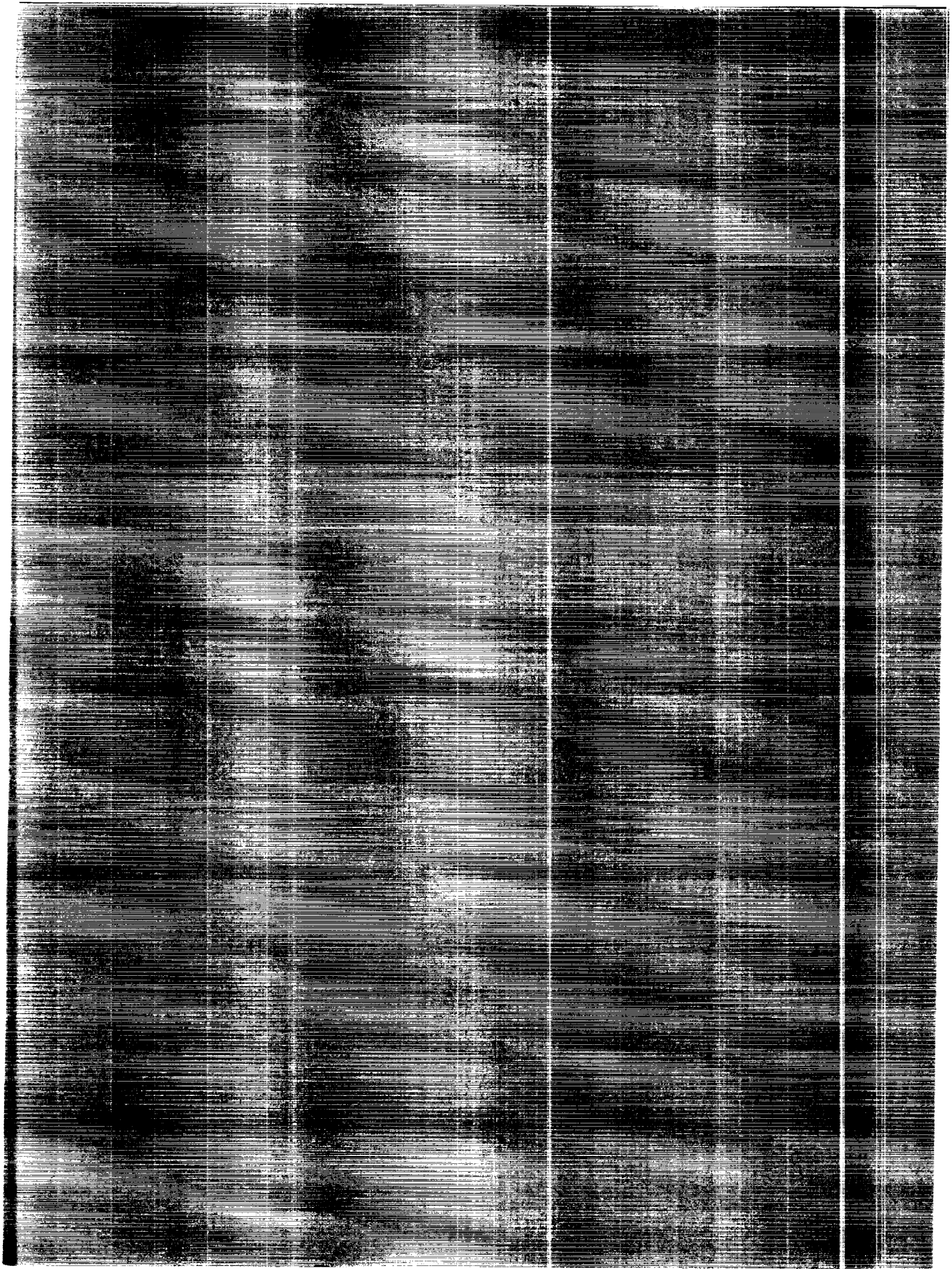

NASA Conference Publication 3185

Orbital, Rotational and Climatic Interactions

Edited by
Bruce G. Bills
Goddard Space Flight Center
Greenbelt, Maryland

Report of a workshop sponsored by the
NASA Goddard Space Flight Center,
Greenbelt, Maryland, and held at
The Johns Hopkins University
Baltimore, Maryland
July 9–11, 1991

National Aeronautics and
Space Administration
Office of Management
Scientific and Technical
Information Program
1993

CONTENTS

Background

It has long been recognized that subtle changes in the orbital and rotational parameters of the Earth directly modify the spatial and temporal patterns of incident solar radiation, and thus indirectly, but still quite significantly, influence climate. Though the time scales of climatic forcing via orbital and rotational change are far removed from the normal time scales of human awareness and public policy decisions, they are nonetheless important. The importance of astronomically forced climatic change stems from two considerations: the overall magnitude of the effect, and the potential for calibration of climate system response on other time scales. The dominant climatic signal on time scales from 10^4 years to 10^7 years is phase coherent with, and presumably causally linked to orbital and rotational variations. Because the astronomical forcing can be computationally reconstructed with considerable accuracy, and the climatic response is preserved in a myriad of proxy records, the system response function in this frequency band can be quite well constrained.

Objectives

The basic scientific goal of the Workshop was to arrive at a better understanding of the interactions between the orbital, rotational and climatic variations of the Earth. In order to accomplish that objective, the Workshop was structured so as to provide an opportunity for experts in the various sub-disciplines to vigorously interact and exchange ideas, in a rather informal setting.

A number of previous workshops and symposia have been held over the last decade on various aspects of orbital, rotational and climatic interactions. However, significant recent developments have taken place in a number of the scientific disciplines relevant to understanding the mechanisms associated with astronomical forcing and climatic response. As the field matures, discussion can shift from the issues associated with "whether" to those associated with "how". Some of these recent developments include:

improved models of planetary orbital evolution over 10^7 to 10^8 year timespans,

enhanced understanding of the Earth's deformational and rotational response to glacial loading

better appreciation for the role of core-mantle coupling in precessional dynamics

improved radiometric dating of key events of the last glacial cycle

acquisition of additional marine and continental climate records

implementation of improved statistical techniques for comparing climatic and astronomical time series

maturation of algorithms for modeling climatic states and processes

Until quite recently, most of the people actively working on astronomically forced climatic change were oceanographers or glaciologists. The simple explanation for this observation is that the best records of quasiperiodic climatic change came from marine sediments and glacial ice cores. However, as the field develops, one can expect participation from a wider range of disciplines. For example, it seems likely that significant progress can be made in understanding the precessional dynamics of the solid Earth by examining the paleoclimatic record. Though recent progress in space geodetic techniques has made it possible to precisely characterize the rotational response of the Earth on time scales from a few hours to the lunar nodal precession period (18.6 years), the details of the Earth's response on the spin precession

time scale (26 thousand years) are still poorly known, since the direct observations only span a short part of one period. In that case, high resolution spectral studies of long climatic records have already indicated subtle effects associated with glacial mass redistribution.

Because of the very interdisciplinary nature of the subject matter of the Workshop, it is difficult for any one person, or any small group of people to be really conversant with the latest results, techniques and opinions across the entire spectrum of relevant topics. However, by assembling a diverse and reasonably large group of people with complementary interests, it was anticipated that each of the participants would gain a better appreciation for those areas outside their immediate expertise. It was hoped that each participant would come away from the meeting with an improved understanding of *symplectic integration schemes, benthic foraminiferal taphonomy, isotopic fractionation dynamics, stochastic resonances, visco-elastic normal modes, Hopf bifurcations, quasi-geostrophic potential vorticity,* and many of the other topics represented.

However, the objectives of the workshop extended beyond educating the individual participants. It was also anticipated that collectively, we would take a critical look at what is now known in various specialty areas, and also take a broad look at how well all the little pieces fit together. This kind of examination is helpful in identifying promising new research directions which will eventually fill in the gaps in our present understanding.

Organization

On 9-11 July 1991, an international workshop on *Orbital, Rotational and Climatic Interactions* was held in Olin Hall, which houses the Department of Earth and Planetary Sciences, at the Johns Hopkins University, in Baltimore, Maryland. The workshop was hosted by the NASA Goddard Space Flight Center, and was convened by Bruce G. Bills, Head of the Geodynamics Branch at GSFC. The agenda consisted of five half-day sessions, in which each participant was given an opportunity to present a summary of their recent work, with ample time for discussion. The afternoon of the third day was devoted to informal discussion of directions for future research.

Acknowledgments

All workshop participants are thanked for the contributions to this report. Many others also provided valuable input. Financial support was provided by the NASA Biogeochemistry and Geophysics Program.

Workshop Participants

Bruce G. Bills
Geodynamics Branch
Goddard Space Flight Center
Greenbelt, MD 20771

Gerard Bond
Lamont-Doherty Geological Observatory
Columbia University
Palisades, NY 10964

Madeleine Briskin
Department of Geology
University of Cincinnati
Cincinnati, OH 45221

Benjamin F. Chao
Geodynamics Branch
Goddard Space Flight Center
Greenbelt, MD 20771

Steven C. Clemens
Department of Geological Sciences
Brown University
Providence, RI 02912

Thomas J. Crowley
Applied Research Corporation
305 Arguello Drive
College Station, TX 77840

Alfred G. Fischer
Department of Geological Sciences
University of Southern California
Los Angeles, CA 90089

L. Danny Harvey
Department of Geography
University of Toronto
Toronto, Ontario
M5S 1A1, Canada

Timothy D. Herbert
Scripps Institution of Oceanography
University of California
La Jolla, CA 92093

Linda Hinnov
Department of Earth and Planetary Sciences
The Johns Hopkins University
Baltimore, MD 21218

William T. Hyde
Department of Oceanography
Dalhousie University
Halifax, Nova Scotia
B3K 5T8, Canada

Jacques Laskar
Service de Mechanique Celeste
Bureau des Longitudes
77 Avenue Denfert-Rochereau
F75014 Paris, France

Marie-France Loutre
Institut d'Astonomie et Geophysique
Universite Catholique de Louvain
2, Chemin du Cyclotron
B1348 Louvain-la-Neuve, Belgium

Andrew McIntyre
Lamont-Doherty Geological Observatory
Columbia University
Palisades, NY 10964

Paul E. Olsen
Lamont-Doherty Geological Observatory
Columbia University
Palisades, NY 10964

Jeffrey Park
Department of Geology and Geophysics
Yale University
New Haven, CT 06511

W. Richard Peltier
Department of Physics
University of Toronto
Toronto, Ontario
M5S 1A7, Canada

David L. Richardson
Department of Aerospace Engineering
University of Cincinnati
Cincinnati, OH 45221

Barry Saltzman
Department of Geology and Geophysics
Yale University
New Haven, CT 06511

David J. Thomson
Mathematical Sciences Research Center
AT&T Bell Laboratories
Murray Hill, NJ 07974

Kenneth L. Verosub
Geology Department
University of California
Davis, CA 95616

Patrick Wu
Department of Geology and Geophysics
University of Calgary
Calgary, Alberta
T2N 1N4, Canada

Geodynamic Contributions to Global Climatic Change

Bruce G. Bills
Geodynamics Branch
NASA Goddard Space Flight Center
Greenbelt, MD 20771

Abstract

Orbital and rotational variations perturb the latitudinal and seasonal pattern of incident solar radiation, producing major climatic change on time scales of 10^4-10^6 years. The orbital variations are oblivious to internal structure and processes, but the rotational variations are not. The intent of this article is to describe a program of investigation whose objective would be to explore and quantify three aspects of orbital, rotational and climatic interactions. An important premise of this investigation is the synergism between geodynamics and paleoclimate. Better geophysical models of precessional dynamics are needed in order to accurately reconstruct the radiative input to climate models. Some of the paleoclimate proxy records contain information relevant to solid Earth processes, on time scales which are difficult to constrain otherwise.

Specific mechanisms which will be addressed include:

- climatic consequences of deglacial polar motion, and
- precessional and climatic consequences of
  - glacially induced perturbations in the gravitational oblateness, and
  - partial decoupling of the mantle and core.

The approach entails constructing theoretical models of the rotational, deformational, radiative and climatic response of the Earth to known orbital perturbations, and comparing these with extensive records of paleoclimate proxy data. Several of the mechanisms of interest may participate in previously unrecognized feed-back loops in the climate dynamics system. A new algorithm for estimating climatically diagnostic locations and seasons from the paleoclimate time series is proposed.

INTRODUCTION

It is widely recognized that mass redistributions associated with climatic change (glaciations) are an important source of crustal deformation and geodynamic change. It is much less widely appreciated that rates, phases and amplitudes of deformation of the deep interior of the Earth can influence climate. The objective of this investigation is to better characterize four aspects of this geodynamic contribution to global climatic change. The common theme among them has two threads: internal mass redistributions influence the rotational dynamics of the Earth, and changes in orbital and rotational parameters influence the latitudinal and seasonal pattern of insolation. Previous attempts to account for astronomically forced climatic change have usually only considered extremely simplisitic models for the response of the Earth to external torques and surface loads.

The focus of the proposed investigation will consist of three specific aspects of interaction between internal mass flow and rotational dynamics, and a new algorithm for comparing paleoclimatic proxy data with astronomically forced variations in insolation patterns.

The latitudinal and seasonal pattern of incident solar radiation depends on the eccentricity of the Earth's orbit and the orientation of the spin axis relative to both the orbit normal and the aspidal line. Unit vectors $\mathbf{s}$ and $\mathbf{n}$ characterize the directions of the spin axis and orbit normal, respectively. Two angles completely characterize the relative orientation of the spin axis. The obliquity ϵ is simply the angle between the orbit normal and the spin axis

$$\epsilon = cos^{-1}(\mathbf{n} \cdot \mathbf{s}) \tag{1}$$

The ascending node of the orbit plane on the instantaneous equator plane has an orientation given by $(\mathbf{s} \times \mathbf{n})$, and the longitude of perihelion ϖ is just the angle in the orbit plane from that node to perihelion. It is widely appreciated that secular variations in these three parameters (e,ϵ,ϖ) produce major climatic change (Hays et al., 1976; Berger et al., 1984). In fact, spectral analyses of long, high resolution marine sediment isotopic records show significant variance at periods near 100 kyr, 41 kyr and 19-23 kyr, which are generally attributed to spectral lines in the radiative forcing fluctuations associated with e, ϵ and e sin(ϖ), respectively.

The causes and effects of the orbital changes are quite well understood. Gravitational interactions with the other planets cause the shape and orientation of the orbit to change on time scales of 10^4-10^6 years. The inclination I and nodal longitude Ω determine the orientation of the orbit plane. The eccentricity e and perihelic longitude ω determine the shape of the orbit and its orientation within the plane. Note that ω is measured from an inertially fixed direction, rather than the moving

node as is the case for ϖ. The secular evolution of the orbital element pairs (I,Ω) and (e,ω) can be conveniently represented in terms of Poisson series

$$\begin{aligned} p &= sin(I)\ sin(\Omega) &&= \Sigma N_j\ sin(s_j\, t + g_j) \\ q &= sin(I) cos(\Omega) &&= \Sigma N_j\ cos(s_j\, t + g_j) \end{aligned} \tag{2}$$

$$\begin{aligned} h &= e\ \sin(\omega) &&= \Sigma M_j\ sin(r_j\, t + f_j) \\ k &= e\ \cos(\omega) &&= \Sigma M_j\ cos(r_j\, t + f_j) \end{aligned} \tag{3}$$

In the lowest order solution, there are as many frequencies r_j and s_j as there are planets. However, the frequencies r_j and s_j are characteristic modal frequencies (eigenvalues) of the coupled system of oscillators and are not each uniquely associated with a particular planet (Milani, 1988). The frequencies r_j are all positive, indicating that the perihelia advance. In the lowest order solution, the apsidal rates are all in the interval ($0.667 < r_j < 28.221$ arcsec/year). The corresponding periods are 45.92 kyr to 1.943 Myr. One of the frequencies s_j is zero, and all the others are negative, indicating that the nodes regress. In the lowest order solution, the non-zero nodal rates are all in the interval ($0.692 < s_j < 26.330$ arcsec/year). The corresponding periods are 49.22 kyr to 1.873 Myr. In higher order solutions, variations in (e,ω) become coupled to variations in (I,Ω), but the solutions can still be cast in terms of Poisson series like Equations (2) and (3).

Laskar (1988) has recently published a secular variation theory which is complete to fifth order in eccentricity and inclination. Agreement between this secular variation model and strictly numerical computations (Richardson and Walker, 1989; Quinn et al., 1991) is much better than for any previous analytical model. The inclination and eccentricity series for Earth each contain 80 distinct terms. Figures (1) and (2) illustrate the spectra and corresponding histories of variation in orbital inclination and eccentricity for the past 2 10^6 years.

In computing these secular orbital variations, the Earth, Moon and planets can all be treated as point masses. No internal structure or processes are relevant to orbital evolution. The physics of the process is simple, and well understood, though development of proper mathematical tools to represent the long term evolution remains an area of active research (Laskar, 1988, 1990; Quinn et al., 1991). On the other hand, the rotational evolution does depend rather sensitively on various aspects of the structure and dynamics of the interior.

Lunar and solar gravitational torques acting on the oblate figure of the Earth cause the spin axis $\mathbf{s}$ to precess about the instantaneous orbit normal $\mathbf{n}$. If the Earth is considered to be a rigid body,

the evolution of the spin axis orientation is given by

$$ds/dt = \alpha(\mathbf{n} \cdot \mathbf{s})(\mathbf{s} \times \mathbf{n}) \tag{4}$$

where

$$\alpha = \frac{3(C-A)}{2Cn} \sum \frac{Gm_i}{b_i^3}\{1 - 3sin^2(I_i)\} \tag{5}$$

is a scalar rate factor which depends on intrinsic properties of the Earth, such as polar and equatorial moments of inertia (C,A) and rotation rate n, and on extrinsic influences, such as masses m, orbital inclinations I, and semiminor axes b, of the Moon and Sun. The solar and lunar torques together produce a precession of the spin axis of the Earth at a rate of $\alpha(\mathbf{n} \cdot \mathbf{s}) = 50.38$ arcsec/year (Kinoshita, 1977, Williams et al., 1991).

Once the present spin axis direction s is known and orbital element histories are given via Equations (2) and (3), an obliquity history can be constructed from equation (4) in two different ways. The linear perturbation approach (Miskovic, 1931, Sharaf and Boudnikova, 1967; Vernekar, 1972, 1977; Ward, 1974; Berger, 1976) involves deriving coefficients of a trigonometric series, similar to Equations (2) and (3), which yield the obliquity and longitude of perihelion directly as functions of time. An alternative is to apply standard numerical algorithms for solving initial value problems to generate a vector time series s(t) and then compute the obliquity and longitude of perihelion directly (Ward, 1979; Laskar, 1986; Bills, 1990b). Figure (3a) shows the spectrum of obliquity variations, which in the linear perturbation model is simply obtained from the inclination spectrum by shifting each frequency s_j by the luni-solar precession rate (s = 50.38 arcsec/year) and multiplying each amplitude N_j by the spectral admittance

$$F_j = s_j/(s_j + s) \tag{6}$$

Figure (3b) shows the numerically integrated obliquity history of Laskar (1986,1988) for the last 2 Ma, using the rotational theory of Kinoshita (1977). The difference between the numerical and linear perturbation solution never exceeds 0.06 degree over that interval. It is clear that the linear perturbation solution gives a very adequate representation of the spin precession.

The influence of orbital and rotational variations on climate is operative through perturbations in the latitudinal and seasonal pattern of insolation. The diurnal average intensity of radiation at a point is inversely proportional to the squared solar distance and directly proportional to the diurnal average rectified solar direction cosine

$$F = (a/r)^2 \langle ||\mathbf{u} \cdot \mathbf{u}_s|| \rangle \tag{7}$$

where a and r are mean and instantaneous solar distance and $\mathbf{u}$ and $\mathbf{u}_s$ are unit vectors from the center of the Earth to the surface point of interest and the sub-solar point, respectively. The insolation pattern, as a function of latitude θ and mean anomaly M, can be readily computed once values are specified for the orbital and rotational parameters ϵ, e, and ϖ (Hargreaves, 1895; Milankovitch, 1920; Vernekar, 1972, 1977; Ward, 1974). Figure (4) illustrates that pattern for the present orbital and rotational configuration. This pattern can also be written in terms of a Fourier-Legendre series (Hargreaves, 1895; North and Coakley, 1979; Taylor, 1984; Bills, 1992)

$$F(\mu, M; \epsilon, e, \varpi) = \sum P_n(\mu) \sum exp(ip\,M)\; F_{n,p}(\epsilon, e, \varpi) \tag{8}$$

where $\mu = \cos(\theta)$, and P_n is a Legendre polynomial. The number of terms in the Fourier summation required to obtain a good representation of the seasonal pattern is greater in the polar regions than in the tropics and mid-latitudes. The primary difficulty in the polar regions is reproducing the abrupt change in slope of the insolation curve at times of transition to continual darkness or continual light. It is also true that the polar regions place the greatest demands on the Legendre summation, since the spatial pattern also has a discontinuous first derivative at the latitude where the transition occurs to continual darkness or light.

A significant fraction of the recent work on comparing paleoclimate proxy records to astronomically forced insolation changes has been based on the published insolation curves of Berger (1978, 1991). Common practice is to compare computed variations in some particular aspect of the seasonal and latitudinal insolation pattern (July insolation at 65° N is a particularly frequent choice) with an observational record of some climatic indicator ($\delta^{18}O$ variations versus age (depth) in a marine sediment core, for example). Comparisons of this sort enable estimates of amplitude, phase and coherence of climatic response to radiative forcing, and have unequivocally demonstrated that orbital and rotational variations are a dominant cause of climatic change on time scales of 10^4-10^6 years.

Despite obvious successes, several problems remain in the general methodology. For example, the orbit and rotation are both assumed to be perfect clocks and, as a result, data time series are often "tuned" to the astronomical time scale (Martinson et al., 1982; Shackleton et al., 1990; Hilgren, 1991). However, as we shall see in the next two sections, the rotational variations in particular do not keep very good time. Also, a number of significant observations remain without adequate explanation. One of the most perplexing of these is the mid-Pleistocene climatic switch in dominant oscillation frequency. The 41 kyr oscillation was dominant throughout the early Pleistocene, and the 100 kyr oscillation has been dominant since the Brunhes-Matuyama magnetic polarity reversal

(or thereabouts), whereas the standard July 65° N insolation curve shows no discernible change in spectral composition over the entire interval.

The intent of this article is to point out the need for a critical examination of this standard scenario, with the objective of improving the geodynamic component of the model enough to provide better radiative forcing time series to the paleoclimate community, use paleoclimate proxy data records to calibrate solid earth responses to applied loads and torques, and explore potential feed-back loops .

Two of the topics of study are perturbations to the simple precession model presented in Equation (4). The first topic concerns time variations in the precession rate occasioned by glacial mass transport and resulting changes in the difference between polar and equatorial moments of inertia (C-A). These fractional variations can likely reach 1% in magnitude and are fully competitive with changes in orbital eccentricity in terms of their effect on instantaneous precession rate. The second topic is the effect of differential precession in the deep interior, which is governed by the (poorly known) characteristics of the inertial and dissipative coupling torques which attempt to keep the rotation axes of the mantle and core aligned.

The third topic is the potentially significant geodynamic feed-back loop associated with deglacial mass transport, polar motion and ensuing perturbations to radiative equilibrium temperature patterns. The asymmetrical disposition of major ice sheets and ocean basins relative to the rotation axis implies that during growth or decay of these ice sheets the geographic location of the principal axis of greatest inertia will shift. If the hydrospheric and cryospheric changes are appreciably more rapid than can be compensated by asthenospheric flow, the rotation axis will shift, possibly by as much as ~ 1°. The primary climatic consequence is a shifting of the geographic distribution of continental and oceanic regions (which differ by a factor of 60 in heat capacity). The effect of a 1° change in the geographic position of the pole is different (but not necessarily less significant) than a 1° change in obliquity.

The fourth and final topic is a new modelling strategy in which climate proxy data records are used to estimate linear combinations of insolation pattern Fourier-Legendre coefficients which best duplicate the observed variations. This approach allows the data variance to be partitioned into global versus regional effects, and can distinguish between responses to annual average insolation and those due to seasonal cycle fluctuations.

PRECESSIONAL DYNAMICS WITH VARIABLE RATE FACTOR

Statement of Problem

All but the most recent reconstructions of the radiative forcing input to paleoclimate models have assumed that both the orbital and rotational dynamics could be readily and accurately reconstructed from their present configurations, via the simple analyses mentioned in the introduction. These expectations seem well founded in the case of orbital evolution, though the possibility of chaotic dynamics in the inner solar system (Laskar, 1990; Laskar et al., 1992) does seem to preclude confident extrapolation beyond 10^7 years. However, there are a number of processes, working in different locations and at different rates, which all serve to compound the difficulty of accurately computing the spin precessional evolution.

An important aspect of this problem is the synergism between geodynamics and paleoclimate. Better geophysical models are needed in order to accurately reconstruct the radiative input to climate models. Some of the paleoclimate proxy records contain information relevant to solid Earth processes on time scales which are difficult to constrain otherwise.

On the longest time scales of interest (10^7-10^9 years) the limiting uncertainty is variability in the tidal transfer of angular momentum from the rotation of the Earth to the orbit of the Moon. At present, these tidal torques are increasing the length of the day by 22.5 10^{-6} sec/year and increasing the size of the lunar orbit by 3.88 cm/year (Cazenave and Daillet, 1981; Christodoulidis et al., 1988). Berger et al. (1989) have made a useful first step towards including this effect in climatic time series. They computed the change in the major precession and obliquity frequencies due to lunar tidal evolution, assuming that the present rate of tidal energy dissipation is representative of the past 500 Myr. However, the present rates are considerably higher than the long term average (Hansen, 1982), largely due to a near resonance between sloshing modes of ocean basins and the diurnal and semidiurnal tidal periods (Platzman et al., 1981), and apparently compounded by a contribution from shallow seas (Wunsch, 1986; Dickman and Preisig, 1986). Sedimentary records which constrain lunar orbital evolution show some promise of resolving this problem (Olsen, 1986; Williams, 1989a,b; Herbert and D'Hondt, 1990), but the situation is definitely more complex than is suggested by Berger et al., (1989).

Another parameter which can vary, on rather shorter time scales and in an equally irregular

fashion, is the gravitational oblateness of the Earth (C-A)/C. Thomson (1990) has recently made three important contributions to the understanding of this source of variability. First, he pointed out that mass redistribution associated with major glaciations and compensating subsidence and crustal deformations (Le Treut and Ghil, 1983; Wu and Peltier, 1984) can cause fractional changes in oblateness of order 10^{-3}-10^{-2}. Second, he showed that high resolution spectral analyses of several climatic time series appear to indicate fluctuations of the luni-solar precession rate of this magnitude, and with a dominant period near 100 kyr. Finally, Thomson pointed out that the best fit to the paleoclimate proxy data was obtained using a mean lunisolar precession rate 0.6 arcsec/year less than the present observed value. He notes that the resulting value would correspond rather closely with that expected for a hydrostatic flattening (Nakiboglu, 1982). If these important results are corroborated, they will demonstrate that important feed-back loops exist in the orbital-rotational-climatic interactions system, further "up-stream" in the presumed causal chain than has been previously recognized.

Approach

The research design for this segment of the proposed investigation will address several issues. The primary focus will be an attempt to resolve two related questions. What are the precessional and paleoclimatic consequences of small (0.001-0.01) variations in oblateness (C-A)/C, over time scales of 10^3-10^6 years? Can such variations can be confidently inferred from paleoclimatic proxy data? These questions represent a forward modeling problem and a coupled inverse problem, respectively.

The first question is the easier to answer. Equation (4) describes the variations in orientation of the spin axis, as viewed in an inertial reference frame. However, since we are primarily interested in the orientation of the spin axis relative to orbit normal (obliquity) and the apsidal line (longitude of perihelion), the analysis will be made easier if we first transform to a coordinate system fixed in the orbit plane. If the rotation matrix is denoted by A, the transformed equation takes the form (Ward, 1974; Bills, 1990a)

$$d\mathbf{s}/dt = \{dA/dt\ A^{-1}\}\mathbf{s} + a(\mathbf{n}\cdot\mathbf{s})(\mathbf{s}\times\mathbf{n}) \tag{9}$$

where

$$\{dA/dt\ A^{-1}\} = B\ dI/dt + C\ dW/dt \tag{10}$$

$$B = \begin{bmatrix} 0 & 0 & 0 \\ 0 & 0 & 1 \\ 0 & -1 & 0 \end{bmatrix} \tag{11}$$

$$C = \begin{bmatrix} 0 & \cos(I) & -\sin(I) \\ -\cos(I) & 0 & 0 \\ \sin(I) & 0 & 0 \end{bmatrix} \tag{12}$$

Now define two complex quantities: P = sin(I) $e^{i\Omega}$, which represents components of the orbit normal on the invariable plane, and S = sin(ϵ) $e^{i\Psi}$, which represents components of the spin vector on the orbital plane. In this new notation, Equation (9) can be rewritten in the form

$$dS/dt + ia\ S = ib\ dP/dt \tag{13}$$

where

$$a = \alpha cos(\epsilon) + cos(I)\ d\Omega/dt \tag{14}$$

$$b = cos(\epsilon)e^{-i\Omega} \tag{15}$$

The complete solution to a nonhomogeneous linear differential equation consists of both "free" and "forced" modes of oscillation. The free modes, in this case, correspond to spin precession with the orbit plane fixed, and the forced modes correspond to motions of the spin axis as it attempts to precess about the instantaneous orbit normal, while the orbit normal itself is precessing. The forced modes make first order contributions to both ϵ and ϖ, whereas the free modes are only second order for ϵ but are first order for ϖ. As a result, in the standard linear series solutions (Berger, 1978; Ward, 1974), the obliquity terms include only the forced response to changes in (I,Ω), whereas the nodal longitude terms include both forced modes from (I,Ω), and free modes with variable (e,ω).

The result of variable oblateness will have exactly the same qualitative effect on spin precession as does a change in orbital eccentricity. Both effect the free modes only. It will thus be rather difficult to confidently distinguish oblateness variations from unmodeled eccentricity variations. However, that does not effect the forward modeling aspect of the problem. To the extent that oblateness variations occur, their effect should be included in the astronomical forcing to climate models.

An iterative approach to the problem seems promising. Orbital variations are uneffected by oblateness and need not directly concern us. As a first step, standard rotational variations (including eccentricity, but neglecting oblateness variations) will be used to generate radiative input to an energy balance climate model (North et al., 1981; Short et al., 1991), with a coupled ice-sheet model

(DeBlonde and Peltier, 1990). Time variations in oblateness can be simply estimated from the surface load and internal compensation. The resulting oblateness history is then fed back into the rotational calculation and the entire process is repeated. The inner-most loops of this algorithm are somewhat similar to the model of Peltier (1982). However, he did not allow the mass loading to influence the radiative forcing.

Even fairly modest changes in oblateness are rotationally significant. For comparison, the eccentricity perturbation influences precession rate via the factor $(a/b)^3$, where a and b are semimajor and semiminor axes, respectively. This amounts to $(1\text{-}e^2)^{-3/2}$, which differs from unity by only 0.0054 for a near-maximum value of $e = 0.06$,

DIFFERENTIAL PRECESSION: INERTIAL AND DISSIPATIVE COUPLING OF THE MANTLE AND CORE

Statement of Problem

The hydrostatic figure of a planet represents a compromise between gravitation, which attempts to attain spherical symmetry, and rotation, which prefers cylindrical symmetry. Due to its higher mean density, the core of the Earth is more nearly spherical than the mantle. The direct luni-solar precessional torques on the core will thus be inadequate to make it precess at the same rate as the mantle. In fact, the core oblateness is only about 3/4 that required for coprecession with the mantle (Smith and Dahlen, 1981). However, it is clearly the case that the core and mantle precess at very nearly the same rate (Stacey, 1973). A variety of different physical mechanisms contribute to the torques which achieve this coupling, but a purely phenomenological partitioning is useful. The net torque can be described as a sum of inertial torques, which are parallel to $(\chi_m \times \chi_c)$, and dissipative torques, which are parallel to $(\chi_m - \chi_c)$. Here, χ_c and χ_m are the rotation vectors of the core and mantle, respectively. The two types of torques have qualitatively different results: inertial torques cause the core and mantle axes to precess at fixed angular separations and on opposite side of their combined angular momentum vector, whereas the effect of dissipative torques is to reduce the angle between the axes.

On short time scales it is appropriate to consider the core to be an inviscid fluid constrained to move within the ellipsoidal region bounded by the rigid mantle (Poincare, 1910; Toomre, 1966; Voorhies, 1991). The inertial coupling provided by this mechanism is effective whenever the ellipticity of the container exceeds the ratio of the precessional to rotational rates. If the mantle were actually rigid, or even elastic (Merriam, 1988; Smylie et al., 1990), this would be an extremely effective type of coupling. However, on sufficiently long time scales, the mantle will deform viscously and can accommodate the motions of the core fluid (Wu, 1990). The inertial coupling torque exerted by the core on the mantle will have the form

$$T_i = k_i[\chi_m \times \chi_c] \tag{16}$$

A fundamentally different type of coupling is provided by electromagnetic or viscous torques (Rochester, 1962; Sasao et al., 1977; Kubo, 1979). The dissipative coupling torque exerted by the

core on the mantle will have the form

$$T_d = k_d[\chi_m - \chi_c] \tag{17}$$

This type of coupling is likely to be most important on longer time scales. In each case, the mantle exerts an equal and opposite torque on the core. The response of the coupled core-mantle system to orbital forcing is given by (Goldreich and Peale, 1970; Ward and DeCampli, 1979; Bills, 1990b).

$$\begin{aligned} ds_m/dt &= \alpha_m(n \cdot s_m)(s_m \times n) - \beta_m(s_m - s_c) - \gamma_m(s_m \times s_c) \\ ds_c/dt &= \alpha_c(n \cdot s_c)(s_c \times n) + \beta_c(s_m - s_c) + \gamma_c(s_m \times s_c) \end{aligned} \tag{18}$$

where α_m is similar to α above, except that only mantle moments A_m and C_m are included, and

$$\begin{aligned} \beta_m &= k_d/C_m\, \upsilon \\ \gamma_m &= k_i/C_m\, \upsilon^2 \end{aligned} \tag{19}$$

where υ is the mean rotation rate.

Approach

The research design for this segment of the proposed investigation would consist of several parts. The objectives and methods are very similar to those described in the previous section. In this case, however, the intent would be to determine the precessional and paleoclimatic consequences of non-rigd core-mantle coupling, and to explore the possibility that useful constraints on the coupling parameters can be obtained from paleoclimatic proxy data.

A number of estimates already exist for the strengths of inertial and dissipative coupling torques (Toomre, 1966; Roberts, 1972; Rochester, 1976; Loper, 1975; Stix, 1982). By most accounts, the inertial torque is ~ 5 10^{20} N m, and the various viscous and magnetic dissipative torques are 102-104 times weaker. However, the inertial torque estimates are simply based on the premise that the core must coprecess with the mantle.

Solutions to the coupled precession problem can be found in a form analogous to Equation (11) for the rigid precession problem. The principle difference in the present situation is the increased richness of the free and forced oscillation spectra. There are modes in which the core and mantle precess together, and other modes which reflect differential precession. It is clear that the most climatically relevant behavior is the precessional motion of the mantle. Thus the chief interest, from that perspective, will be to explore the behavior of the mantle precession modes over plausible range of parameter values. Within the geophysically prescribed range of parameter space, are there any

climatically significant perturbations to obliquity or longitude of perihelion occasioned by partially decoupling the core from the mantle?

It is very clear that the mantle and core exhibit differential motions on nutational time scales (Mathews et al., 1991; Mathews and Shapiro, 1992). However, one of the difficulties in constructing a differential precession model which is truly useful for paleoclimatic studies is that the precise geodetic techniques, which are able to constrain nutation amplitudes within a few milliarcseconds, still have short enough time spans that most of the differential precession modes of interest are still indistinguishable from rigid rotation.

DEGLACIAL POLAR MOTION AND ABRUPT CLIMATE CHANGE

Statement of Problem

Recent models of the surficial mass transport associated with the last deglaciation (Tushingham and Peltier, 1991; Nakada and Lambeck, 1988) suggest that the magnitude of the flow and its departure from axial symmetry were both great enough that, if it were not closely balanced by internal flow and deformation, it would cause a shift in the body-fixed location of the axis of greatest inertia, by an amount of order 1o. If the pole were to move by a significant fraction of a degree, the resulting displacement of the geographic pattern of land and water relative to the incident radiation pattern would cause a climatic perturbation which could either augment or retard the progress of deglaciation, depending on the spatio-temporal pattern of the perturbation. The potential thus exists for a previously unexplored feed-back loop in the climate system.

During the peak of the last deglaciation, there was a brief but significant return to full glacial conditions. This Younger Dryas climatic event is perhaps best documented in the North Atlantic (Ruddiman and McIntyre, 1981; Broecker et al., 1988), but appears to have been global in scale (Currey, 1990; Engstrom et al., 1990; Gasse et al., 1991). Though the broad scale timing of the deglaciation is consistent with astronomical forcing, the Younger Dryas perturbation was too brief to be a linear response to the classical orbital or rotational variations. However, neither the magnitude nor duration is a priori inconsistent with a response to deglacial polar motion. The objective of this portion of the proposed investigation would be to examine the geodynamic and climatic consequences of deglacial mass flow.

Approach

The usual geodynamic modeling approach to deglacial polar motion is to use historical observations of the rate and direction of polar motion during this century, in conjunction with estimates of the surficial mass flow, to derive constraints on deep Earth structure models. However, these same models, once they have been calibrated, can be made to deliver estimates of the rates and directions of polar motion which occurred during the deglaciation. The magnitude of deglacial polar motion depends rather sensitively on the rate and spatial pattern of surficial mass transport and on the

internal structure of the Earth, as reflected in the spectrum of relaxation times for surficial loads and body forces (Sabadini et al., 1982; Wu and Peltier, 1984; Spada et al., 1992; Ivins et al., 1992).

A class of climate models which is very well suited to the proposed investigations incorporates spatial and temporal variations in a number of components of the global energy balance. The basic equation which governs the energy balance is (North et al., 1981)

$$A + B\,T + C\,\frac{\partial T}{\partial t} - \nabla \cdot (D\,\nabla T) = Q\,a\,F \tag{20}$$

The first two terms on the left parameterize outgoing radiation, the third term represents storage of heat and the fourth term represents divergence of the heat flux. The right hand side is the amount of incident radiation that gets absorbed.

Values for the outgoing radiation parameters (A = 210 W m^{-2}, B = 2.1 W m^{-2} K^{-1}; Short et al., 1984) can be estimated from satellite data. The heat capacity C is large over water and small over land (C_w/B = 4.6 years, C_l = C_w /60; North and Coakley, 1979). Though much of the lateral transport of heat is accomplished by winds and ocean currents, these effects can be modeled by a diffusive transport, with D/B = 0.310 (North, 1975; Wyant et al., 1988). For the incident radiation, Q = S/4 = 342 W m^{-2} (Schatten and Orosz, 1990), F is the spatial and temporal pattern of projected area, and a (0.75, Stephens et al., 1981) is the co-albedo.

Solutions to this equation with specified forcing can be readily obtained in the spectral domain, with spatial patterns represented by spherical harmonic series and temporal patterns represented by Fourier series. If A, B and D are assumed to be constants (no spatial or temporal variations), the base state solution to Equation (20) is simply

$$T_{nmp} = W^{-1}[Q\,G\,a_{nmp}\,F_{n0p}] \tag{21}$$

where G (whose 9 indices have been suppressed for typographical clarity) is a coupling constant for products of spherical harmonics (Rotenberg et al., 1959; Dill, 1991) and

$$W = [B + n(n+1)\,D + ipG\,C_{nmp}] \tag{22}$$

In the same notation, the temperature perturbation δT due to a small change in radiative forcing δF (associated with ϵ, e, or ϖ) is

$$\delta T_{nmp} = W^{-1}[Q\,G\,a_{nmp}\,\delta F_{n0p}] \tag{23}$$

Similarly, the temperature perturbation due to a change δC in the distribution of land and water

relative to the rotation axis (associated with deglacial polar motion) is

$$\delta T_{nmp} = W^{-1}[-i\,p\,G\,\delta C_{nmp}\,T_{nmp}] \tag{24}$$

Specific questions which should be addressed include:

- What is the likely history (magnitude and direction) of polar motion induced during deglaciation?
- How does the climatic impact of that polar motion compare in magnitude and spatio-temporal pattern with the impact of a 1° change in obliquity, or a 1% change in orbital eccentricity?
- Is the timing and magnitude of the climatic impact such that it would significantly perturb the deglaciation?
- Is this feed-back loop a viable contributor to the Younger Dryas climatic event?

FOURIER, LEGENDRE, AND MILANKOVITCH: ESTIMATING DIAGNOSTIC SEASONS AND LATITUDES FROM CLIMATE PROXY RECORDS

Statement of Problem

As was mentioned in the introduction, a weakness of previous paleoclimate models is the common practice of using an overly simplistic representation of the insolation forcing (values for July at 65° N are a particular favorite) when attempting to reconcile computed variations in orbital and rotational parameters with observed climate proxy records (Hays et al., 1976). An alternative approach, which shares many of the same problems is to use a linear combination of the orbital and rotational parameters as input to the models (Imbrie and Imbrie, 1980). A problem in using either a linear combination of orbital and rotational parameters, or a localized spatio-temporal measure of insolation, as a proxy input to climate models is the difficulty in choosing which single value to use (Broecker, 1966; Broecker and Van Donk, 1970). Furthermore, the two alternative formats for making the choice (time and location versus orbital and rotational parameter combination) are not equivalent. It is clear that choice of a specific latitude and time of year to represent the insolation pattern implies a unique (though non-linear) combination of orbital and rotational parameters. However, the converse is not necessarily true. For some combinations of (ϵ,e,ϖ) there is no corresponding location and time of year, at which the insolation pattern will be dominated by the selected combination of parameters.

In comparing calculated insolation pattern variations with an observed time series of some climate proxy (marine sediment oxygen isotope variations, for example), it is useful to have a simple physical model in mind. The observed isotopic anomalies are, to first order, due to two effects; global ice volume fluctuations and local to regional scale temperature variations (Emiliani and Shackleton, 1974; Kahn et al., 1981). These effects differ in two important ways. The ice volume effect is global in scale and its first time derivative should be proportional to insolation driven temperature changes. In contrast, the direct isotopic temperature effect is local to regional in scale, and is directly proportional to insolation driven temperature changes.

Approach

A modeling strategy which addresses several of these points involves estimating the linear combination of Fourier-Legendre coefficients of the insolation pattern which best reproduces the data records. This approach provides the opportunity to partition observed variations into global and regional effects. It also provides information on which aspects of the insolation pattern variations are most diagnostic of the observed proxy variations. If July insolation at 65° N is truly significant in a particular data record, the selected amplitudes for the Fourier-Legendre coefficients should clearly reflect that fact. Alternatively, if the amplitude of the seasonal cycle in the polar regions or tropics, or the annual mean equator to pole insolation contrast, or any other linear functional of the insolation pattern is most diagnostic, the analysis will indicate that fact.

As an example of a situation in which this approach could be used, Park and Maasch (1992) have recently compared the climate proxy record provided by $\delta^{18}O$ records from two long, high resolution cores (ODP 677 from the eastern equatorial Pacific (Shackleton et al., 1990) and DSDP 607 from the mid-latitude North Atlantic (Ruddiman et al., 1989; Raymo et al., 1989) with a new estimate of insolation at 65° N (Berger and Loutre, 1991). The three data records analyzed (benthic and planktonic records at ODP 677, benthic only at DSDP 607) have much in common, but there are also interesting, and possibly significant, differences. It is clear that variations which are common to several locations are more likely diagnostic of global climatic variations. Differences between locations, or differences between benthic and planktonic records at a single location provide a different and complementary view of the climatic response to insolation forcing. Figure (5) illustrates a 2 10^6 year history of variations in the amplitudes of the Fourier-Legendre coefficients and Figure (6) compares the DSDP 607 and ODP 677 data with a standard insolation curve.

Several specific questions should be addressed. The first category of questions relate to calibration and characterization of technique.

- Do the Fourier-Legendre coefficient time series form an orthogonal basis?
- What output time series would correspond to a spatio-temporal delta function (summer solstice at 65° N, for example)?
- What is the resolution ($\Delta\mu$,ΔM) versus data series length?
- How does the resolution depend on other factors besides the data string length?

- Are two short data strings from significantly different locations better than a single data string of equivalent aggregate length?

The next level of question pertains to the physical meaning or significance of a particular linear combination of Fourier-Legendre coefficients. Any such linear combination is equivalent to a spatio-temporal pattern of some sort. The result obtained with a finite resolution data structure will represent the convolution of the actual physical response with the data resolution kernel. How do errors in data chronologies map into errors in resolved spatio-temporal patterns of diagnostic insolation?

The final level of question relates to understanding the implications and significance of results obtained by this algorithm from actual data series.

- Using a variety of oceanic and continental paleoclimatic data series, what are the resolved patterns of climatically diagnostic insolation?
- What physical mechanisms are implicated?
- Are significantly different patterns obtained from data strings of different age?
- Is there a single pattern which duplicates the observed increase in amplitude of the 100 kyr signal after the Brunhes-Matuyama magnetic reversal?

REFERENCES

[1] Berger, A.L. (1976), Obliquity and precession for the last 5 million years, Astron. Astrophys. 51, 127-135.

[2] Berger, A.L. (1978), Long-term variations of caloric insolation resulting from the Earth's orbital elements, Quat. Res. 9, 139-167.

[3] Berger, A.L. and M.F. Loutre (1991), Insolation values for the climate of the last 10 million years, Quat. Sci. Rev. 10, 297-317.

[4] Berger, A.L., J. Imbrie, J.D. Hays, G.J. Kukla, and B. Saltzman (1984), Milankovitch and Climate, D. Reidel, Dordrecht, 895 pp.

[5] Berger, A.L., M.F. Loutre, and V. Dehant (1989), Influence of the changing lunar orbit on the astronomical frequencies of pre-Quaternary insolation patterns, Paleocean. 4, 555-564.

[6] Bills, B.G. (1990a), Rigid body obliquity history of Mars, J. Geophys. Res. 95, 14,137-14,153.

[7] Bills, B.G. (1990b), Obliquity histories of Earth and Mars: Influence of inertial and dissipative core-mantle coupling, Lunar Plan. Sci 21, 81-82.

[8] Bills, B.G. (1992), The influence of orbital and rotational variations on latitudinal and seasonal patterns of insolation, Clim. Dynam. (submitted),.

[9] Broecker, W.S. (1966), Absolute dating and the astronomical theory of glaciation, Science 151, 299-304.

[10] Broecker, W.S., and J. Van Donk (1970), Insolation changes, ice volumes, and the O^{18} record in deep-sea cores, Rev. Geophys. Space Phys. 8, 169-197.

[11] Broecker, W.S., M. Andree, W. Wolfi, H. Oeschger, G. Bonani, J. Kennett, and D. Peteet (1988), The chronology of the last deglaciation: Implications for the cause of the Younger Dryas event, Paleocean. 3, 1-19.

[12] Cazenave, A.., and S. Daillet (1981), Lunar tidal acceleration from Earth satellite orbit analysis, J. Geophys. Res. 86, 1659-1663.

[13] Christodoulidis, D.C., D.E. Smith, R.G. Williamson, and S.M. Klosko (1988), Observed tidal braking in the Earth/Moon/Sun system, J. Geophys. Res. 93, 6216-6236.

[14] Currey, D.L. (1990), Quaternary paleolakes in the evolution of semidesert basins, with special emphasis on Lake Bonneville and the Great Basin, Paleogeo. Paleoclim. Paleoecol. 76, 189-214.

[15] DeBlonde, G. and W.R. Peltier (1990), A model of late Pleistocene ice sheet growth with realistic geography and simplified cryodynamics and geodynamics, Clim. Dynam. 5, 103-110.

[16] Dickman, S.R., and J.R. Preisig (1986), Another look at the North Sea pole tide dynamics, Geophys. J. 87, 295-304.

[17] Dill, D. (1991), Implementing matrix mechanics in Mathematica: Determination of Clebsch-Gordan coefficients by matrix diagonalization, Compu. Phys. 6, 616-624.

[18] Emiliani, C., and N.J. Shackleton (1974), The Brunhes epoch: Isotopic paleotemperatures and geochronology, Science 183, 511-514.

[19] Engstrom, D.R., B.C.S. Hansen, and H.E. Wright (1990), A possible Younger Dryas record in Southeastern Alaska, Science 250, 1383-1385.

[20] Gasse, F., M. Arnold, J.C. Fontes, M. Fort, E. Gilbert and A. Huc (1991), A 13,000-year climate record from western Tibet, Nature 353, 742-745.

[21] Goldreich, P., and S.J. Peale (1970), The obliquity of Venus, Astron. J. 75, 273-284.

[22] Hansen, K.S. (1982), Secular effects of oceanic tidal dissipation on the Moon's orbit and the Earth's rotation, Rev. Geophys. Space Phys. 20, 457-480.

[23] Hargreaves, R. (1895), Distribution of solar radiation on the surface of the Earth and its dependence on astronomical elements, Trans. Camb. Phil. Soc. 16, 58-94.

[24] Hays, J.D., J. Imbrie, and N.J. Shackleton (1976), Variations in the Earth's orbit: Pacemaker of the ice ages, Science 194, 1121-1132.

[25] Herbert, T.D. and S.L. D'Hondt (1990), Precessional climate cyclicity in Late Cretaceous-Early Tertiary marine sediments: A high resolution chronometer of boundary events, Earth Plan. Sci. Lett. 99, 263-275.

[26] Hilgren, F.J. (1991) Extension of the astronomically calibrated time scale to the Miocene/Pliocene boundary, Earth Plan. Sci. Lett. 107, 349-368.

[27] Imbrie, J., and J.Z. Imbrie (1980), Modeling the climatic response to orbital variations, Science 207, 943-953.

[28] Ivins, E.R., C.G. Sammis, and C.F. Yoder (1992), Deep mantle viscous structure with prior estimate and satellite constraint, J. Geophys. Res. (submitted),.

[29] Kahn, M.I., T. Oba, and T.L. Ku, Paleotemperatures and glacially induced changes in oxygen-isotope composition of sea water during late Pleistocene and Holocene time, Geology 9, 485-490.

[30] Kinoshita, H. (1977), Theory of rotation of the rigid Earth, Celest. Mech. 15, 277-326.

[31] Kubo, Y. (1979), A core-mantle interaction in the rotation of the Earth, Celest. Mech. 19, 215-241.

[32] Laskar, J. (1986), Secular terms of classical planetary theories using the results of general theory, Astron. Astrophys. 157, 59-70.

[33] Laskar, J. (1988), Secular evolution of the solar system over 10 million years, Astron. Astrophys. 198, 341-362.

[34] Laskar, J. (1990), The chaotic motion of the solar system: A numerical estimate of the size of the chaotic zones, Icarus 88, 266-291.

[35] Laskar, J., T. Quinn, and S. Tremaine (1992), Confirmation of resonant structure in the solar system, Icarus 95, 148-152.

[36] Le Treut, H., and M. Ghil (1983), Orbital forcing, climate interactions, and glaciation cycles, J. Geophys. Res. 88, 5167-5190.

[37] Loper, D.E. (1975), Torque balance and energy budget for the precessionally driven dynamo, Phys. Earth Plan. Inter. 11, 43-60.

[38] Martinson, D.G., W. Menke, and P. Stoffa (1987), An inverse approach to signal correlation, J. Geophys. Res. 87, 4807-4818.

[39] Mathews, P.M. and I.I. Shapiro (1992), Nutations of the Earth, Ann. Rev. Earth Plan. Sci. 20, 469-500.

[40] Mathews, P.M., B.A. Buffet, T.A. Herring, and I.I Shapiro (1991), Forced nutations of the Earth: Influence of inner core dynamics, J. Geophys. Res. 96, 8219-8242.

[41] Merriam, J.B. (1988), Limits on lateral pressure gradients in the outer core from geodetic observations, Phys. Earth Plan. Inter. 50, 280-290.

[42] Milani, A.(1988), Secular perturbations of planetary orbits and their representation as series, in Long-term Dynamical Behavior of Natural and Artificial N-body Systems, A.E. Roy (ed), pp. 73-108, Reidel, Boston.

[43] Milankovitch, M. (1920), Theorie Mathematique des Phenomenes Thermiques Produits par la Radiation Solaire, Gauthier-Villars, Paris, 336 pp.

[44] Miskovic, V.V. (1931), Variations seculaires de elements astronomiques de l'orbite terrestre, Glas. Spr. Kral'yevske Akad. 143.

[45] Nakada, M., and K. Lambeck (1988), The melting history of the late Pleistocene Antarctic ice-sheet, Nature 333, 36-40.

[46] Nakiboglu, S.M. (1982), Hydrostatic theory of the Earth and its mechanical implications, Phys. Earth Plan. Inter. 28, 302-311.

[47] North, G.R. (1975), Theory of energy-balance climate models, J. Atmos. Sci. 32, 2033-2043.

[48] North, G.R. and J.A. Coakley (1979), Differences between seasonal and mean annual energy balance models, J. Atmos. Sci. 36, 1189-1204.

[49] North, G.R., R.F. Cahalan, and J.A. Coakley (1981), Energy balance climate models, Rev. Geophys. Space Phys. 19, 91-121.

[50] Olsen, P.E. (1986), A 40-million year lake record of Early Mesozoic orbital climatic forcing, Science 234, 842-848.

[51] Park, J., and K.A. Maasch (1992), Plio-Pleistocene time evolution of the 100-kyr cycle in marine paleoclimate records, J. Geophys. Res. (submitted).

[52] Peltier, W.R. (1982), Dynamics of the ice age Earth, Adv. Geophys. 24, 1-146.

[53] Platzman, G.W., G.A. Curtis, K.S. Hansen, and R.D. Slater (1981), Normal modes of the world ocean, J. Phys. Ocean. 11, 579-603.

[54] Poincare, H. (1910), Sur la precession des corps deformables, Bull. Astr. 27, 322-356.

[55] Quinn, T.R., S. Tremaine, and M. Duncan (1991), A three million year integration of the Earth's orbit, Astron. J. 101, 2287-2305.

[56] Raymo, M.E., W.F. Ruddiman, J. Backman, B.M. Clement, and D.G. Martinson (1989), Late Pliocene variation in northern hemisphere ice sheets and North Atlantic Deep Water circulation, Paleocean. 4, 413-446.

[57] Richardson, D.L., and C.F. Walker (1989), Numerical simulation of the nine-body planetary system spanning two million years, J. Astron. Sci. 37, 159-182.

[58] Roberts, P.H. (1972), Electromagnetic core-mantle coupling, J. Geomag. Geoelec. 24, 231-259.

[59] Rochester, M.G. (1962), Geomagnetic core-mantle coupling, J. Geophys. Res. 67, 4833-4836.

[60] Rochester, M.G. (1976), The secular decrease of obliquity due to dissipative core-mantle coupling, Geophys. J. 46, 109-126.

[61] Rotenberg, M., R. Bivins, N. Metropolis, and J.K. Wooten (1959), The 3-j and 6-j symbols, Technology Press, Cambridge.

[62] Ruddiman, W.F., and A. McIntyre (1981), The North Atlantic Ocean during the last deglaciation. Paleogeo. Paleoclim. Paleoecol. 35, 145-214.

[63] Ruddiman, W.F., M.E. Raymo, D.G. Martinson, B.M. Clement, and J. Backman (1989), Pleistocene evolution: Northern hemisphere ice sheets and the North Atlantic Ocean, Paleocean. 4, 353-412.

[64] Sabadini, R., D.A. Yuen, and P. Gasperini (1982), Polar wandering and the forced response of a rotating, multi-layered planet, J. Geophys. Res. 87, 2885-2903.

[65] Sasao, T., I. Okamoto, and S. Sakai (1977), Dissipative core-mantle coupling and nutational motion of the Earth, Publ. Astron. Soc. Japan 29, 83-105.

[66] Schatten, K.H., and J.A. Orosz (1990), Solar constant secular changes, Solar Phys. 125, 179-184.

[67] Shackleton, N.J., A. Berger, and R.W. Peltier (1990), An alternative astronomical calibration of the Lower Pleistocene timescale based on ODP Site 677, Trans. Roy. Soc. Edin. 81, 251-261.

[68] Sharaf, S.G., and N.A. Boudnikova (1967), Secular variations of elements of the Earth's orbit which influence climates of the geological past, Bull. Inst. Theor. Astron. 11, 231-261.

[69] Short, D.A., G.R. North, T.D. Bess, and G.L. Smith (1984), Infrared parameterization and simple climate models, J. Clim. Appl. Meteor. 23, 1222-1233.

[70] Short, D.A., J. G. Mengel, T.J. Crowley, W.T. Hyde, and G.R. North (1991), Filtering of Milankovitch cycles by Earth's geography, Quat. Res. 35, 157-173.

[71] Smith, M.L., and A.F.Dahlen (1981), The period and Q of the Chandler wobble, Geophys. J. 64, 223-281.

[72] Smylie, D.E., A.M.K. Szeto, and K. Sato (1990), Elastic boundary conditions in long period core oscillations, Geophys. J. Int. 100, 183-192.

[73] Spada, G., R. Sabadini, D.A. Yuen, and Y. Ricard (1992), Effects on post-glacial rebound from the hard rheology in the transition zone, Geophys. J. Int. 109, 683-700.

[74] Stacey, F.D. (1973), The coupling of the core to the precession of the Earth, Geophys. J. 33, 47-55.

[75] Stephens, G.L., G.G. Campbell, and T.H. Vonder Haar (1981), Earth radiation budgets, J. Geophys. Res. 86, 9739-9760.

[76] Stix, M. (1982), On electromagnetic core-mantle coupling, Geophys. Astrophys. Fluid Dynam. 21, 303-313.

[77] Taylor, K.E. (1984), Fourier representation of orbitally induced perturbations in seasonal insolation, in A.L. Berger et al. (eds) Milankovitch and Climate, 113-125, D. Reidel.

[78] Thomson, D.J. (1990), Quadratic inverse spectrum estimates: Applications to paleoclimatology, Phil. Trans. Roy. Soc. Lond. A332, 539-597.

[79] Toomre, A. (1966), On the coupling of the Earth's core and mantle during the 26,000-year precession, The Earth-Moon System, Plenum Press, pp. 33-45. Tushingham, A.M., and W.R. Peltier (1991), Ice-3G: A new model of late Pleistocene deglaciation based upon geophysical predictions of post-glacial relative sea-level change, J. Geophys. Res. 96, 4497-4523.

[80] Vernekar, A.D. (1972), Long period global variations of incoming solar radiation, Meteor. Mono. 12, 1-22.

[81] Vernekar, A.D. (1977), Variations in insolation caused by changes in orbital elements of the Earth, in The Solar Output and Its Variations, O.R. White (ed), pp. 117-130, Colo. Assoc. Univ. Press.

[82] Voorhies, C.V. (1991), Coupling an inviscid core to an electrically insulating mantle, J. Geomag. Geoelec. 43, 131-156.

[83] Ward, W.R. (1974), Climatic variations on Mars, 1. Astronomical theory of insolation, J. Geophys. Res. 79, 3375-3381.

[84] Ward, W.R. (1979), Present obliquity oscillations of Mars: Fourth-order accuracy in orbital e and I, J. Geophys. Res. 84, 237-241.

[85] Ward, W.R., and W.M. DeCampli (1979), Comments on the Venus rotation pole, Astrophys. J. Lett. 230, 117-121.

[86] Williams, G.E (1989a), Late Precambrian tidal rhythmites in South Australia and the history of the Earth's rotation, J. Geol. Soc. Lond. 146, 97-111.

[87] Williams, G.E. (1989b), Precambrian tidal sedimentary cycles and the Earth's paleorotation, Eos Trans. A.G.U. 70, 33-41.

[88] Williams, J.G., X X Newhall, and J.O. Dickey (1991), Luni-solar precession: Determination from lunar laser ranges, Astron. Astrophys. 241, L9-L12.

[89] Wu, P. (1990), Deformation of internal boundaries in a viscoelastic earth and topographic coupling between the mantle and core, Geophys. J. Int. 101, 213-231.

[90] Wu, P., and W.R. Peltier (1984), Pleistocene deglaciation and the Earth's rotation: A new analysis, Geophys. J. 76, 753-791.

[91] Wunsch, C. (1986), Dynamics of the North Sea pole tide reconsidered, Geophys. J. 87, 869-884.

[92] Wyant, P.H., A. Mongroo, and S. Hameed (1988), Determination of the heat transport coefficient in energy-balance climate models by extremization of entropy production, J. Atmos. Sci. 45, 189-193.

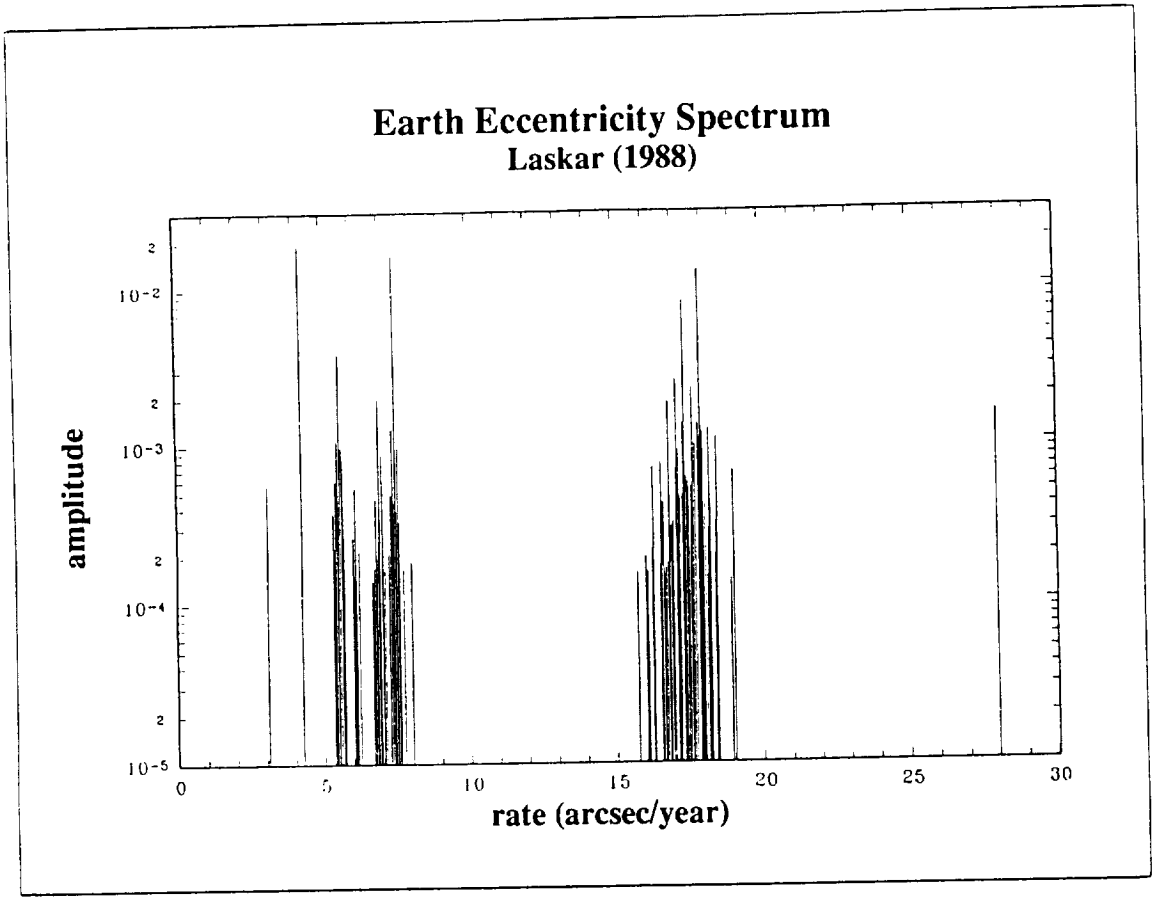

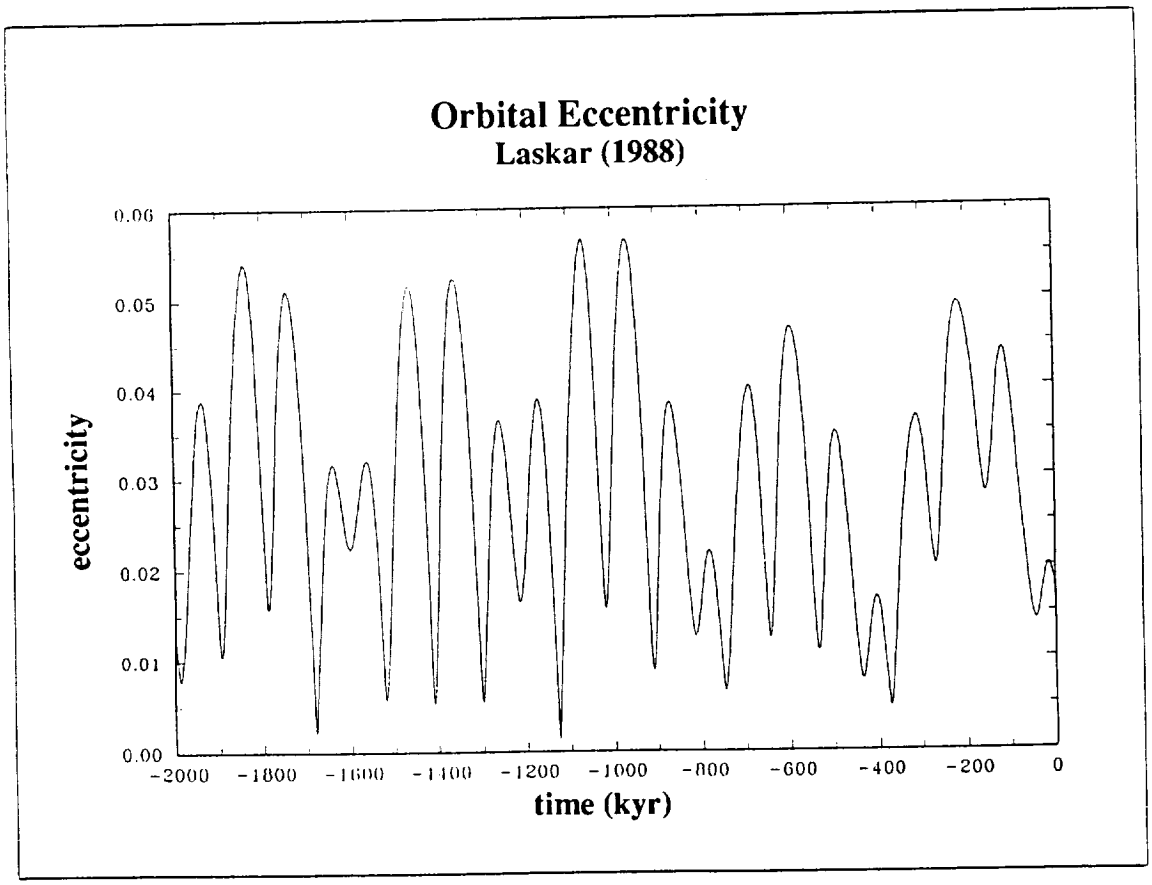

Figure 1
Orbital eccentricity spectrum and time series.
Both are based on the secular variation model of Laskar (1988).

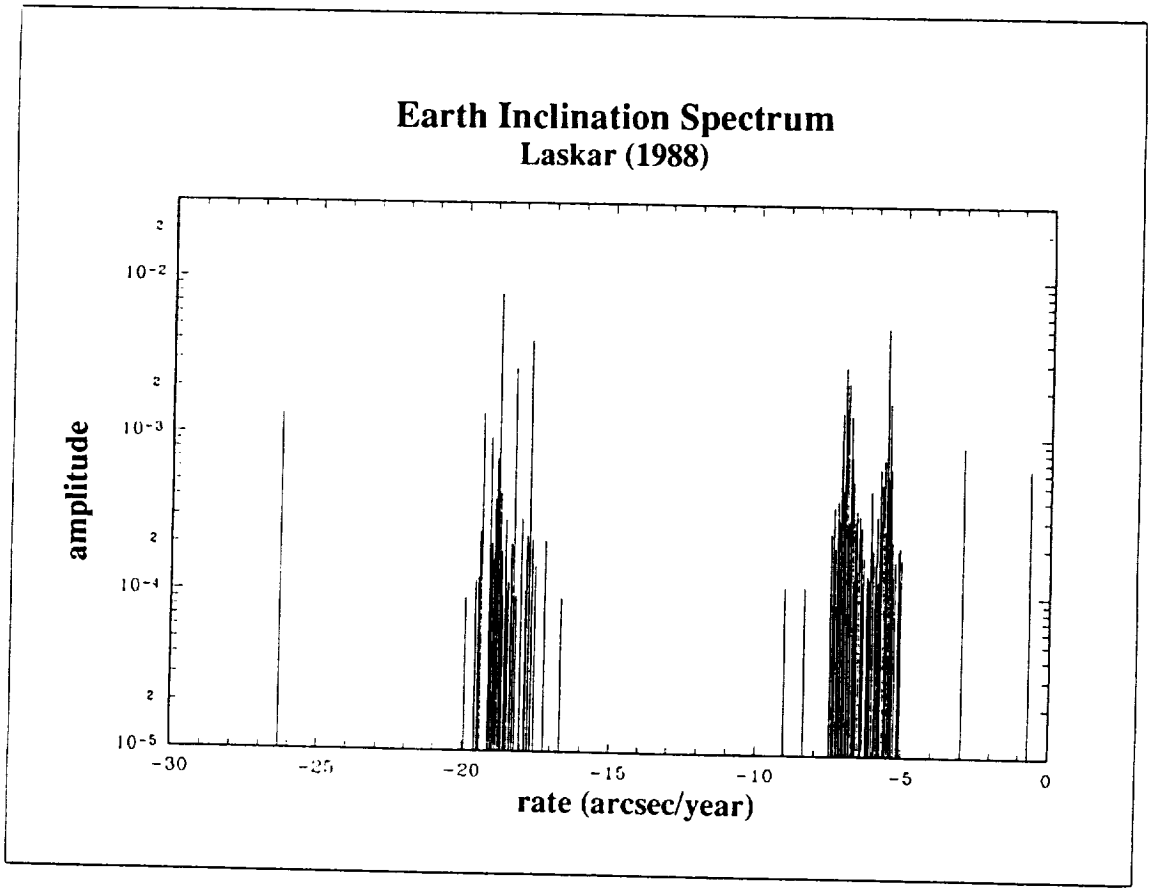

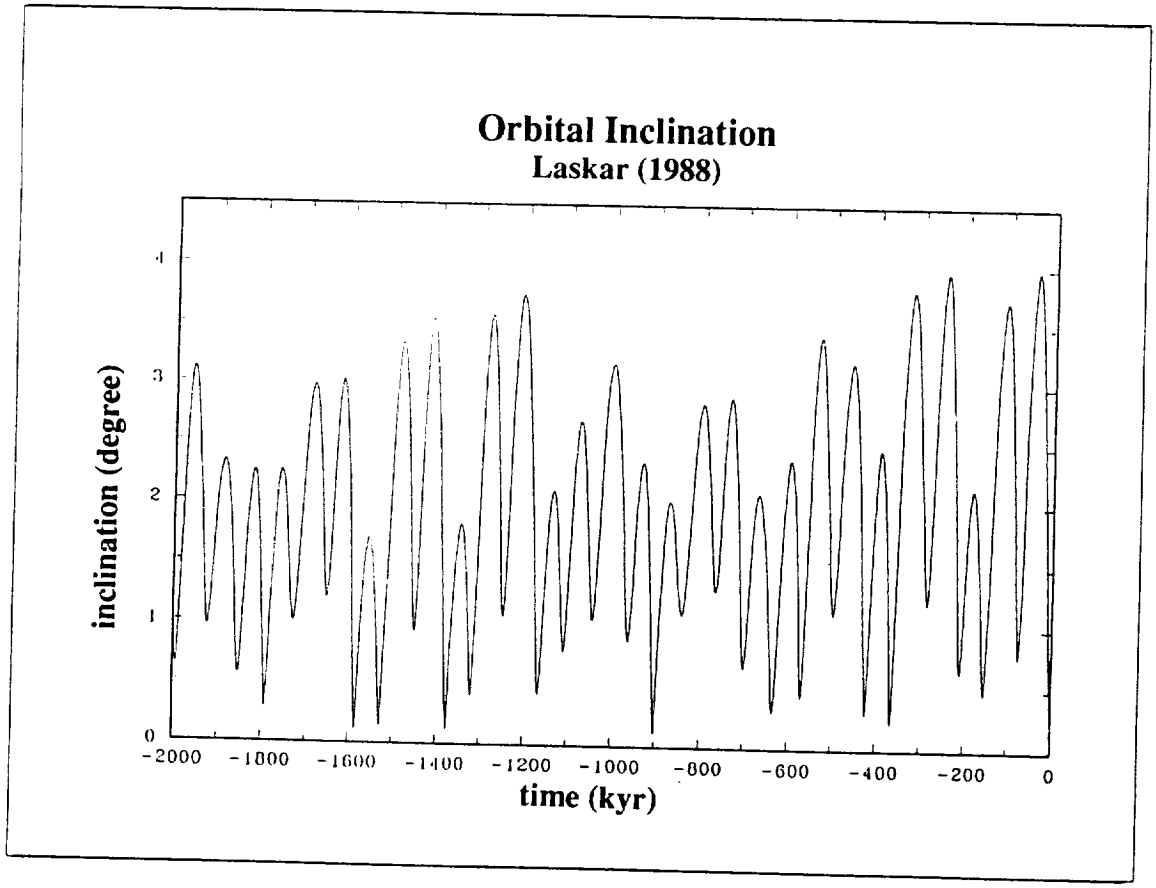

Figure 2
Orbital inclination spectrum and time series.
Both are based on the secular variation model of Laskar (1988).

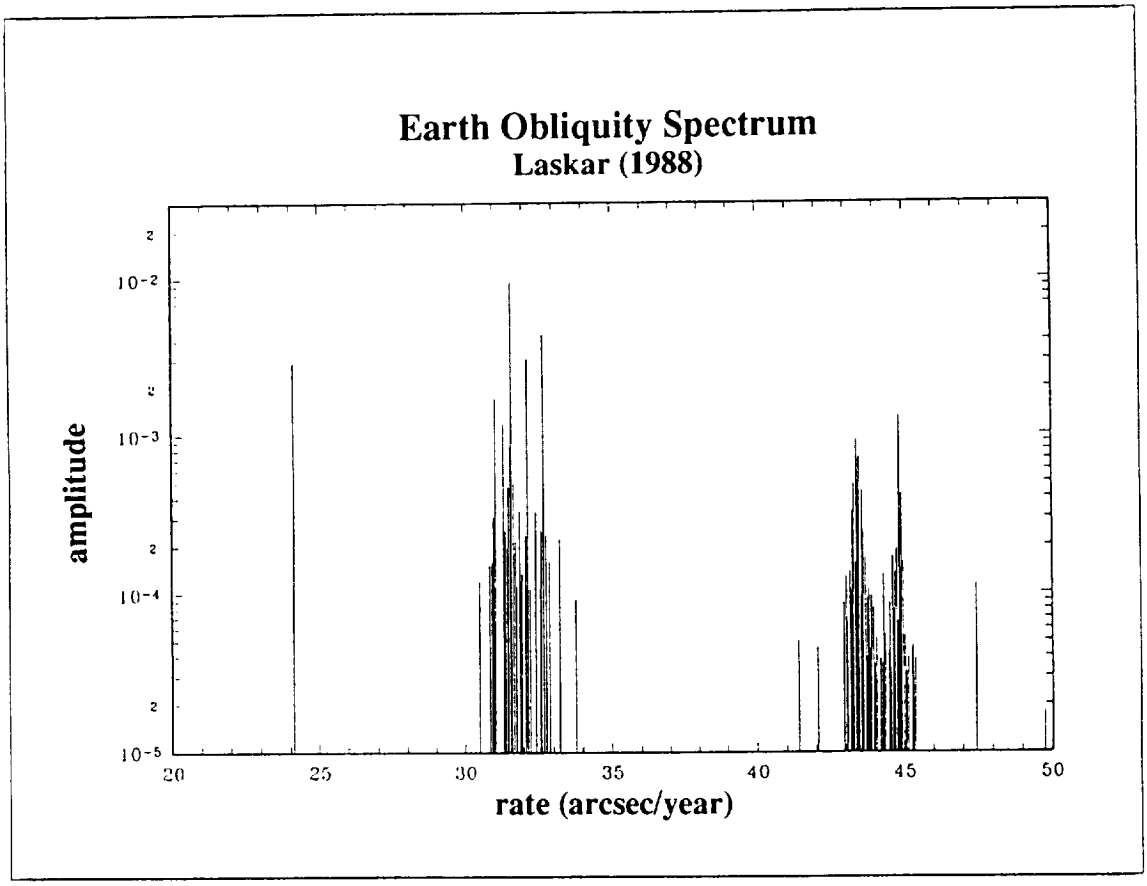

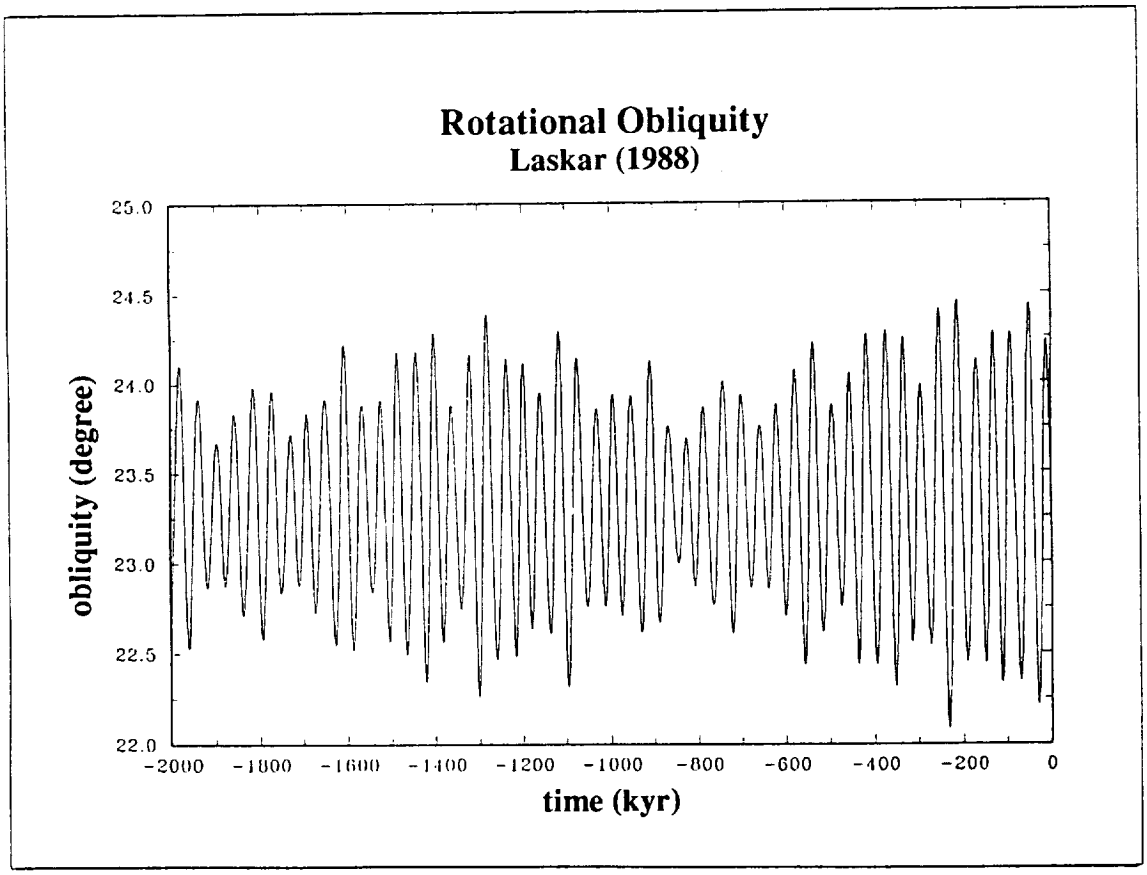

Figure 3

Rotational obliquity spectrum and time series.

Time series is based on rotational theory of Kinoshita (1977) and orbital model of Laskar (1988).

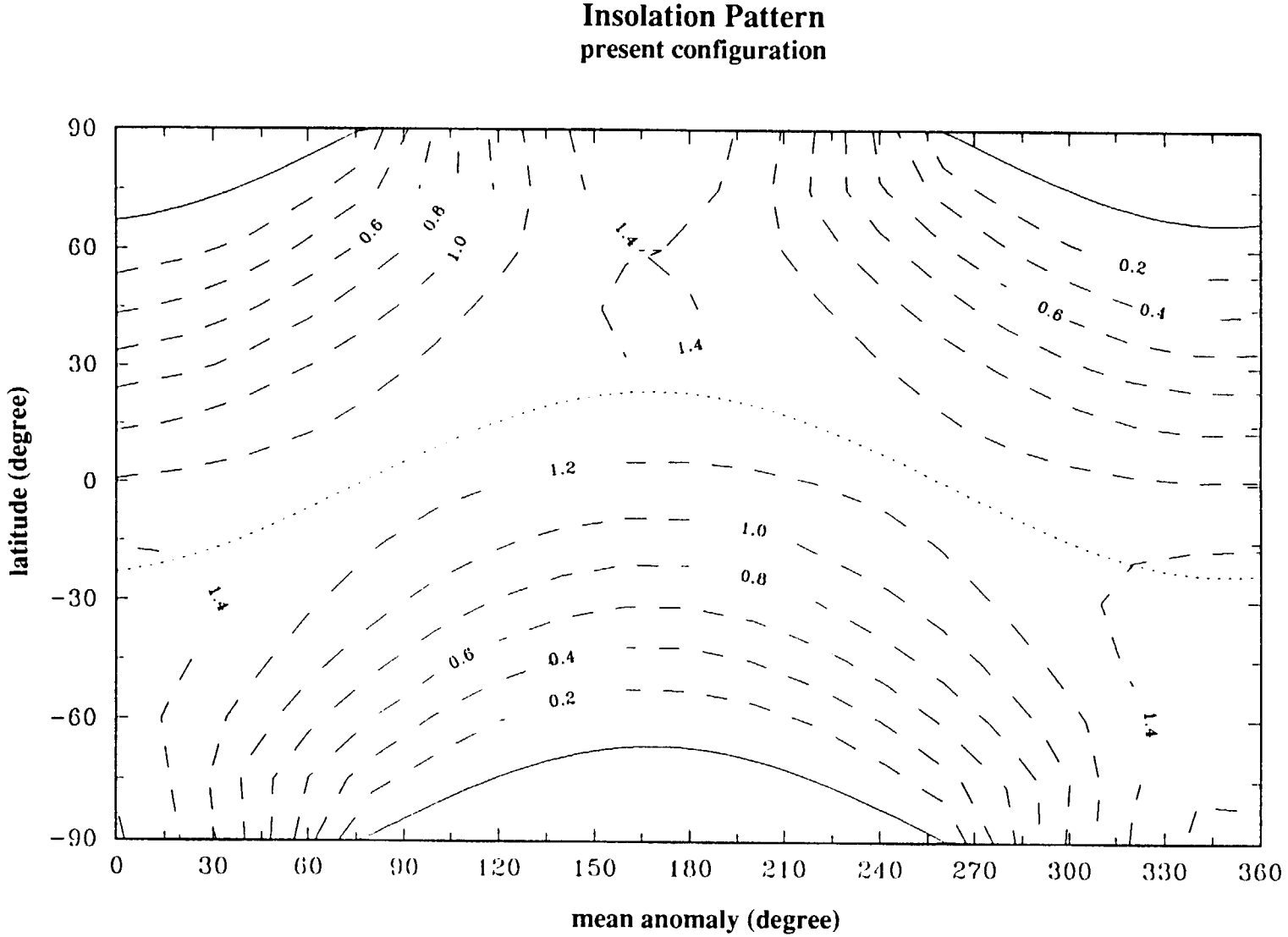

Figure 4
Latitudinal and Seasonal Insolation Pattern.

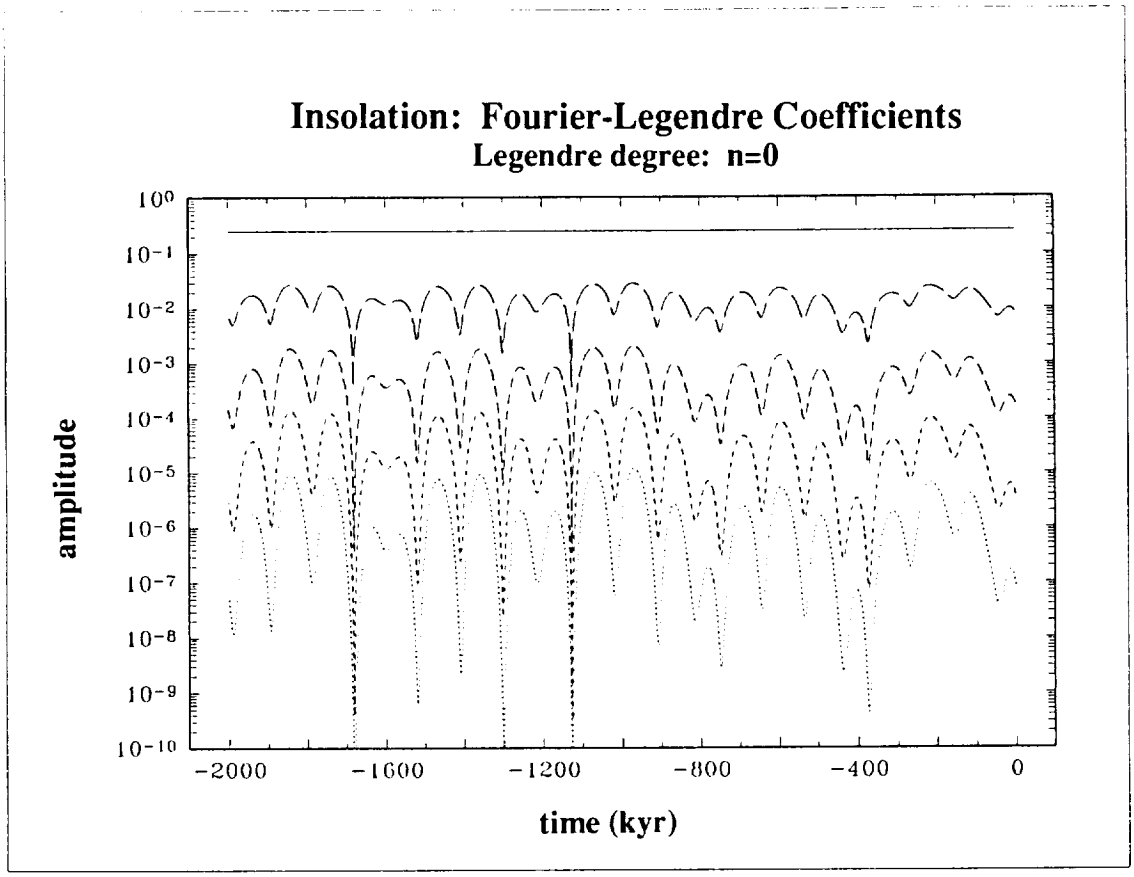

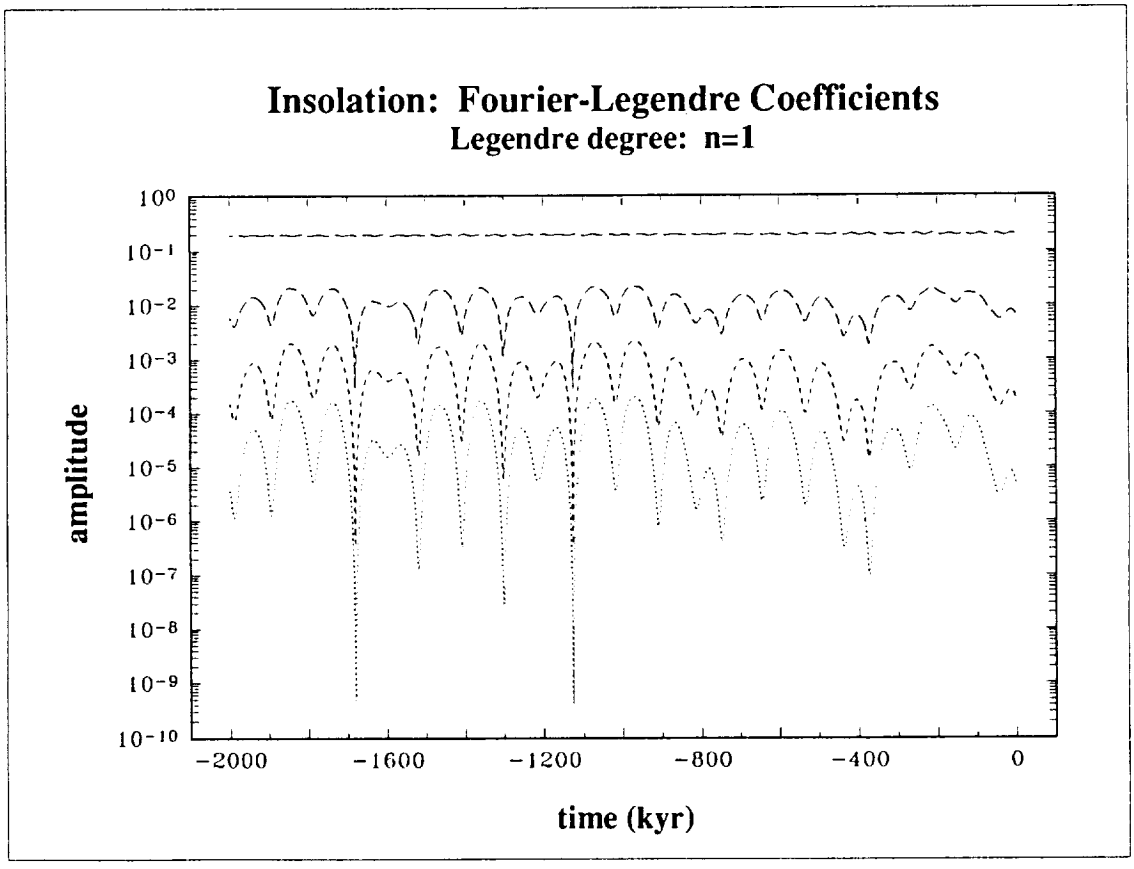

Figure 5a
Insolation Pattern Fourier-Legendre Coefficient Time Series.

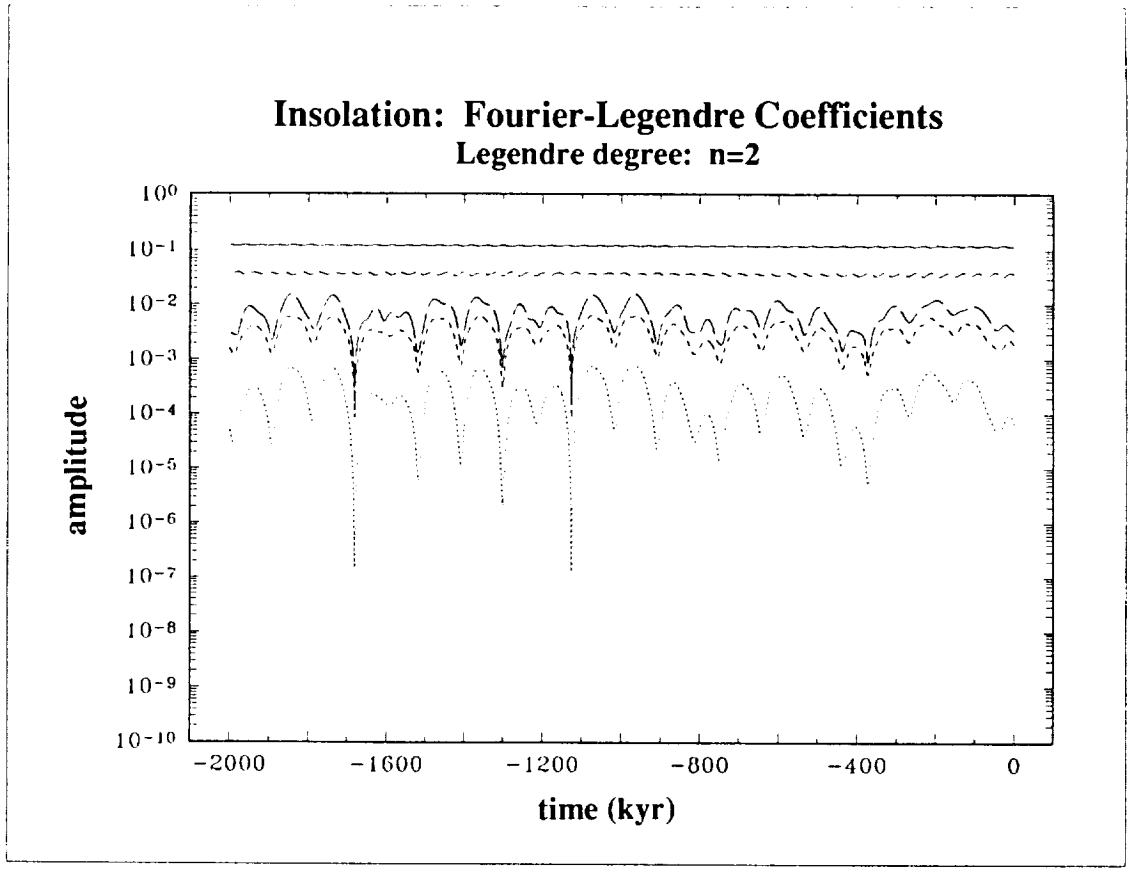

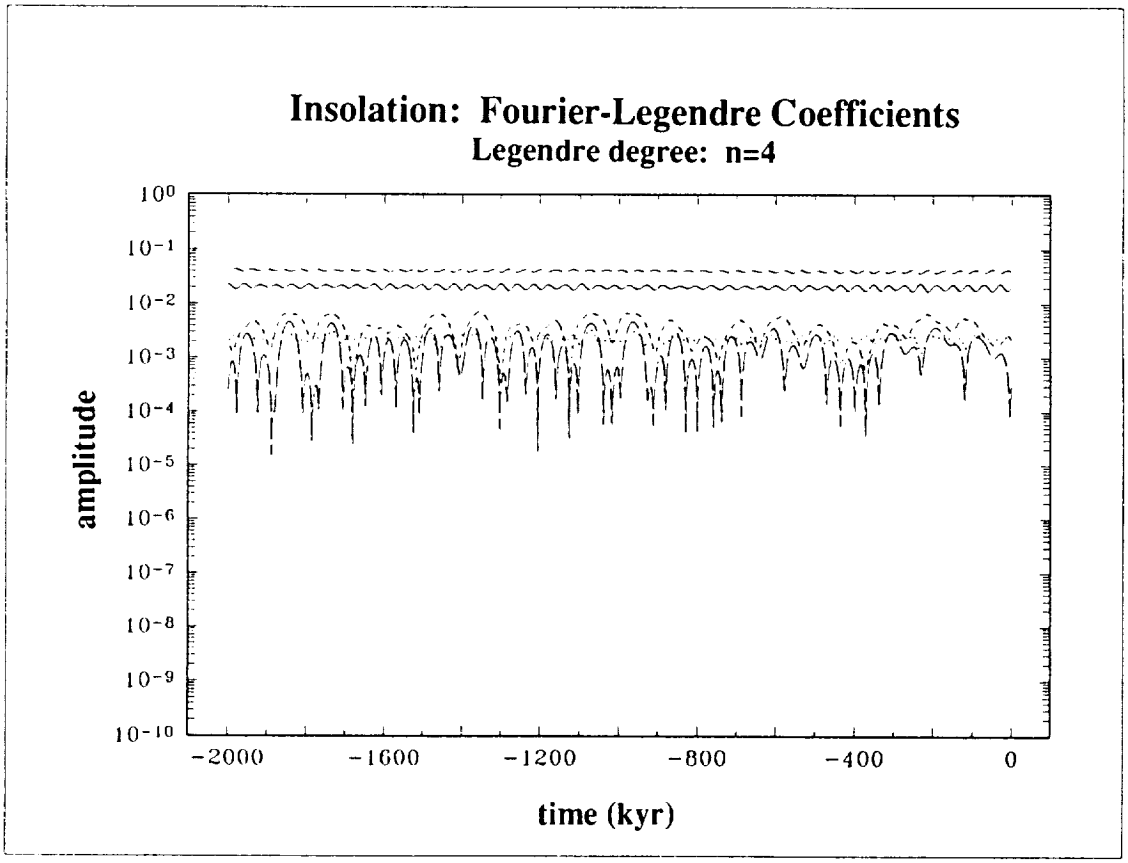

Figure 5b
Insolation Pattern Fourier-Legendre Coefficient Time Series.

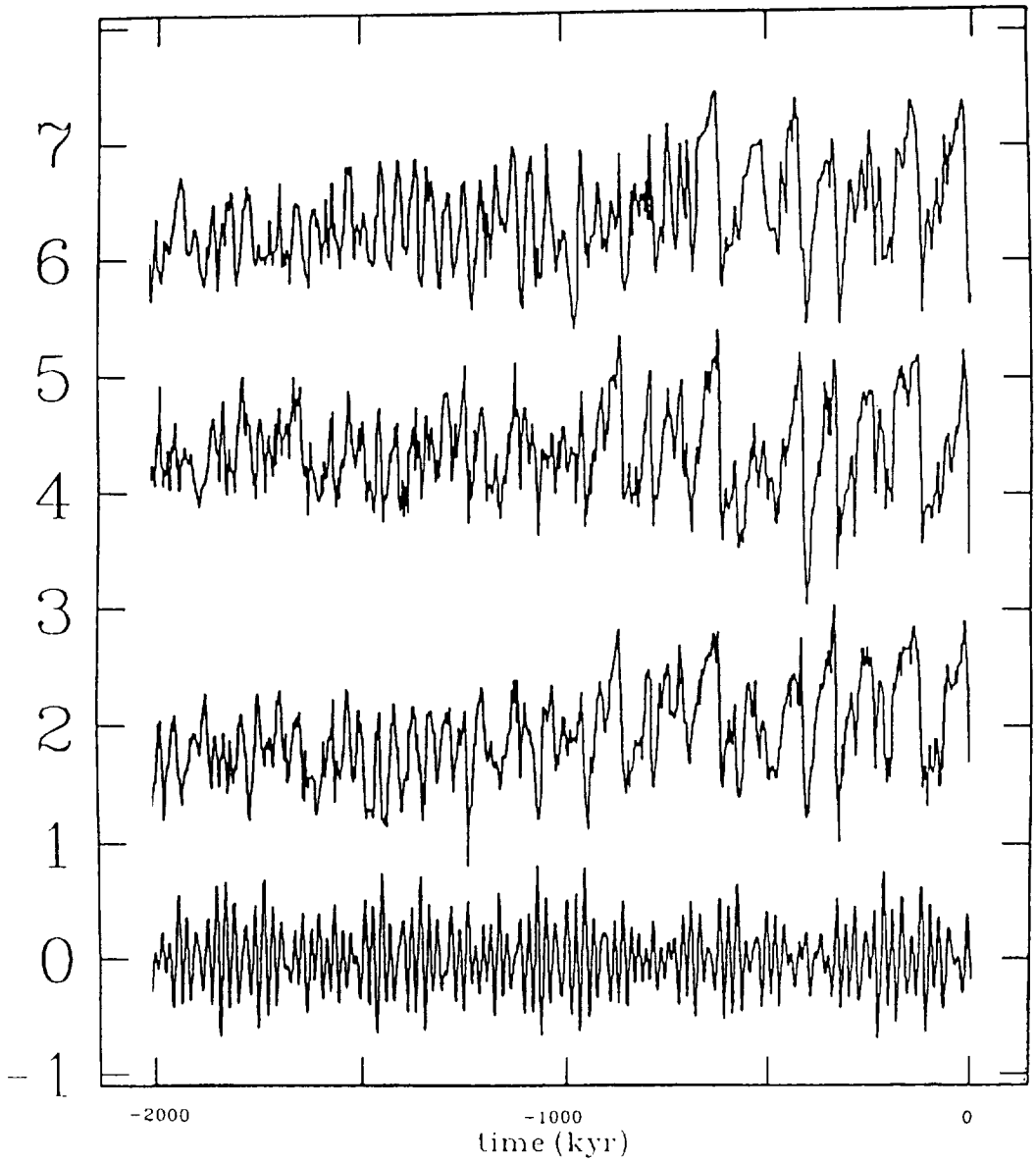

Figure 6
Paleoclimate Proxy Records and Insolation Time Series.
Curves are (top to bottom): DSDP 607 (benthic), ODP 677 (planktonic), ODP 677 (benthic), 65^{o} N insolation

Precessional quantities for the Earth over 10 Myr

Jacques LASKAR
Bureau des Longitudes,
URA CNRS 707,
77 Avenue Denfert-Rochereau
75014 Paris
France

Introduction

The insolation parameters of the Earth depend on its orbital parameters and of the precession and obliquity. Until 1988, the usually adopted solution for paleoclimate computation consisted in (Bretagnon, 1974) for the orbital elements of the Earth, which was completed by (Berger, 1976) for the computation of the precession and obliquity of the Earth. In 1988, I issued a solution for the orbital elements of the Earth, which was obtained in a new manner, gathering huge analytical computations and numerical integration (Laskar, 1988). In this solution, which will be denoted La88, the precession and obliquity quantities necessary for paleoclimate computations were integrated at the same time, which insure good consistancy of the solutions. Unfortunately, due to various factors, this latter solution for the precession and obliquity was not widely distributed (Berger, Loutre, Laskar, 1988). On the other side, the orbital part of the solution La88 for the Earth, was used in (Berger and Loutre, 1991) to derive an other solution for precession and obliquity, aimed to climate computations. I also issued a new solution (La90) which presents some slight improvements with respect to the previous one (Laskar, 1990). As previously, this solution contains orbital, precessional and obliquity variables. In order to make it widely available, it was distributed during this meeting on magnetic support and can also be obtain directly by request to the author at `laskar@friap51.bitnet`. In the present talk, I will discuss the main features of this new solution.

The orbital solution La90

The orbital solution is obtained by the numerical integration of an extended averaged system, which represents the mean evolution of the orbits of the planets. All the 8 main planets of the solar system are taken into account, as well as lunar and relativistic main perturbations. The use of numerical integration for the computation of the solution of the secular system is one of the reasons for the good quality of this solution, which can be checked by comparison with the available ephemeris over a short time scale (Laskar, 1985, 1986, 1988). In (Laskar, 1988), the solution La88 was represented in quasi-periodic form over 10 Myr, but these representations are slowly convergent, which prevents a good accuracy for the solution. Later on, I understood fully the reason of this slow convergence, which is due to the presence of multiple resonances in the secular system of the inner solar system. Due to these resonances, the motion of the solar system is chaotic, and not quasi-periodic, as was demonstrated by the computation of its Lyapunov exponents which reachs 1/(5 Myr) (Laskar, 1989). This implies that it is not possible to give any precise solution for the motion of the Earth over more than about 100 Myr, and most probably, ephemeris can only be given for about 10 Myr with good precision. Several integrations of the secular system of the solar system were made over 200 Myr and 400 Myr. The origin of the chaotic behaviour was identified, and is due to the presence of secular resonances in the inner solar system (Laskar, 1990). With a new numerical method, it was possible to show that the chaotic zones were the solar system belongs is large in the directions of the proper modes related to the inner planets. This is an indication that these results are stable against small changes of initial conditions or model.
One of the main consequence of interest for paleoclimate studies, is the fact that the main frequencies of the orbital motion of the planets can no longer be considered as constants, but are slowly evolving with time. The measured shift in frequency amount about 0.2 arcsec/year over 200 Myr for g_3 and g_4 while for g_5 it is of only 0.00002 arcsec/year. It should be stressed that, as the motion is chaotic, the computed solution cannot be considered as close to the real solution over more than a few 10 Myr, but it is reasonable to assume that the drift in frequency is of the same order of magnitude over the 200 Myr. One should nevertheless mention that over this time span, the change of the precession main frequency, due to tidal effects in the Earth-Moon system, are probably more important (Berger *et al.*, 1989).
Since, direct numerical integrations over 3Myr backward and forward were issued by (Quinn *et al.*, 1991), including also solutions for precession and obliquity (QTD6). The orbital solutions have been compared with La90. The two solutions present very small discrepancies over 3Myr, and the existence of the secular resonances in the inner solar system is confirmed (Laskar, Quinn, Tremaine, 1991). The very close agreement of the two orbital solutions over 3Myr gives the confirmation that the Earth parameters are now very well known over this time span, and insure that the orbital solution La90 can be used with confidence over 10 Myr for paleoclimate use. The precession and obliquity solutions present some small discrepancies which are probably due to the presence of the tidal effect in the Earth-Moon system in the QTD6 solution.

Precession and Obliquity in the La88 and La90 solutions

The precession quantities are completely determined by the two motions of the equatorial and ecliptic pole. The motion of the ecliptic is given by the secular theory La90 (Laskar 1990); the precession quantities are integrated at the same time, using the equations of the theory of the rigid Earth of Kinoshita (Kinoshita 1975, 1977, Laskar, 1986). The equations for the general precession in longitude p_A, and for the obliquity of the date ε are then

$$\begin{aligned}\frac{dp_A}{dt} &= R(\varepsilon) - \cot\varepsilon\big[\,\mathbf{A}(\mathbf{p},\mathbf{q})\sin p_A + \mathbf{B}(\mathbf{p},\mathbf{q})\cos p_A\big] - 2\,\mathbf{C}(\mathbf{p},\mathbf{q}) - p_g\\ \frac{d\varepsilon}{dt} &= -\qquad\qquad \mathbf{B}(\mathbf{p},\mathbf{q})\sin p_A + \mathbf{A}(\mathbf{p},\mathbf{q})\cos p_A\end{aligned}$$

with :

$$\begin{aligned}\mathbf{A}(\mathbf{p},\mathbf{q}) &= \frac{2}{\sqrt{1-\mathbf{p}^2-\mathbf{q}^2}}\,(\dot{\mathbf{q}} + \mathbf{p}(\mathbf{q}\dot{\mathbf{p}} - \mathbf{p}\dot{\mathbf{q}}))\\ \mathbf{B}(\mathbf{p},\mathbf{q}) &= \frac{2}{\sqrt{1-\mathbf{p}^2-\mathbf{q}^2}}\,(\dot{\mathbf{p}} - \mathbf{q}(\mathbf{q}\dot{\mathbf{p}} - \mathbf{p}\dot{\mathbf{q}}))\\ \mathbf{C}(\mathbf{p},\mathbf{q}) &= (\mathbf{q}\dot{\mathbf{p}} - \mathbf{p}\dot{\mathbf{q}})\end{aligned}$$

and :

$$\begin{aligned}R(\varepsilon) = \frac{3k^2 m_M}{a_M^3\omega}\frac{2C-A-B}{2C}\Bigg[&(\mathrm{M}_0 - \mathrm{M}_2/2)\cos\varepsilon + \mathrm{M}_1\frac{\cos 2\varepsilon}{\sin\varepsilon}\\ &-\mathrm{M}_3\frac{m_M}{m_E+m_M}\frac{n_M^2}{\omega n_\Omega}\frac{2C-A-B}{2C}(6\cos^2\varepsilon - 1)\Bigg]\\ +\frac{3k^2 m_\odot}{a_\odot^3\omega}\frac{2C-A-B}{2C}&\qquad[\mathrm{S}_0\cos\varepsilon]\end{aligned}$$

where $\mathbf{p} = \sin(i/2)\sin(\Omega)$, $\mathbf{q} = \sin(i/2)\cos(\Omega)$, ($i$ is the inclination of the Earth with respect to a fixed ecliptic, and Ω the longitude of the node). $R(\varepsilon)$ is the secular term due to the direct lunisolar perturbations. The quantities $\mathrm{M}_0, \mathrm{M}_1, \mathrm{M}_2, \mathrm{M}_3, \mathrm{S}_0$, and S_2 depend only on the orbital elements of the Moon and the Sun. The pincipal moments of inertia of the Earth are denoted by A, B, and C, and the angular velocity of the Earth is ω . The masses of the Sun, the Earth, and the Moon are denoted by $m_\odot$, m_E, and m_M; the sideral motion of the Sun and of the Moon by $n_\odot$ and n_M ; and the mean motion of the node of the Moon by n_Ω. The other terms present in equation (23) represent the effects of the secular variation of the ecliptic, caused by the secular planetary perturbations. The numerical values of $\mathrm{M}_0, \mathrm{M}_1, \mathrm{M}_2, \mathrm{M}_3$ are given in (Kinoshita, 1977):

$$\begin{aligned}\mathrm{M}_0 &= 496303.3 \times 10^{-6}\\ \mathrm{M}_1 &= -20.7 \times 10^{-6}\\ \mathrm{M}_2 &= -0.1 \times 10^{-6}\\ \mathrm{M}_3 &= 3020.2 \times 10^{-6}\end{aligned}$$

and from (Laskar, 1986),

$$S_0 = \frac{1}{2}(1-e^2)^{-3/2} - 0.422 \times 10^{-6}$$

The following numerical values, were also used (see Laskar, 1986 for complete references) :

ω	$= 474\,659\,981.597\,57\ ''/\mathrm{yr}$
n_M	$= 17\,325\,593.4318\ ''/\mathrm{yr}$
n_Ω	$= -69\,679.193\,6222\ ''/\mathrm{yr}$
a_M	$= 384\,747\,980.645$ m
k	$= 0.017\,202\,098\,95$
$m_\odot/(m_E+m_M)$	$= 328\,900.5$
$m_\odot/m_E$	$= 332\,946.0$

The quantity p_g is the geodesic precession due to the general relativity,

$$p_g = 0.019188''/\mathrm{yr}$$

The value of the dynamical ellipticity $E_D = (2C - A - B)/2C = 0.00328005$ is obtained by adjustment at the origine J2000 to the values of the speed of precession and obliquity give by the IAU (Grenoble, 1976) :

$$\begin{aligned} p &= 50.290966''/\mathrm{yr} \\ \epsilon_0 &= 23°26'21''448 \end{aligned}$$

For $t = 0$, we have $p_A = 0$,$\varepsilon = \epsilon_0$, $i = \Omega = 0$,and thus :

$$\left.\frac{dp_A}{dt}\right|_{t=0} = R(\epsilon_0) - 2\,\dot{\mathbf{p}}_{t=0} - p_g \cot \epsilon_0$$

These formula for precession gives a solution for precession and obliquity in agreement with the requirements of high accurate ephemeris (Laskar, 1986) and are thus best suited for paleoclimate computations.

Descripion of the files of the solution La90

The different files which are distributed are

`ear0m5.dat`	`orbital elements 0 to -5 Myr`
`pre0m5.dat`	`obliquity and precession 0 to -5 Myr`
`ear5m10.dat`	`orbital elements -5 to -10 Myr`
`pre5m10.dat`	`obliquity and precession -5 to -10 Myr`

All the elements are referred to the ecliptic and equinox J2000. The starting date is J2000. All angles are in radians

The `ear0m5.dat` and `ear5m10.dat` files contains $T, \mathbf{k}, \mathbf{h}, \mathbf{q}, \mathbf{p}$

T = time from J2000 in 1000yr
$\mathbf{k} = e\cos(\varpi)$
$\mathbf{h} = e\sin(\varpi)$
$\mathbf{q} = \sin(i/2)\cos(\Omega)$
$\mathbf{p} = \sin(i/2)\sin(\Omega)$

where e is the eccentricity of the Earth, i denotes the inclination of the Earth, ϖ the longitude of perihelion, and Ω the longitude of the node of the Earth with respect to the fixed ecliptic and equinox J2000.
The `pre0m5.dat` and `pre5m10.dat` files contains T, ε, p_A where
T is the time from J2000 in 1000yr, ε is the obliquity of the date (mean equator of date with respect to mean ecliptic of date), and p_A is the general precession in longitude.
All quantities generally used for climate studies are derived easily from these fundamental quatities. The eccentricity of the Earth is obtained by

$$e = \sqrt{k^2 + h^2}$$

And the longitude of perihelion from moving equinox is

$$\omega^\star = \varpi + p_A$$

The climatic precession $e\cos(\omega^\star)$ is thus equal to the real part of $z*\exp(ip_A)$, where $z = \mathbf{k}+i\mathbf{h}$.

Conclusions

The present solution La90 for orbital and precession elements for the Earth over can be used for as an ephemeris paleclimate computations over 10 Myr. On this time span, the fact that the motion of the solar system is chaotic is not perceptible on this level of precision. This new solution present some improvements from my previous solution La88 (Laskar 1988). The orbital solution is in very good agreement with the recent numerical integrations of (Quinn *et al.*, 1991) . Over the geological time scales exceeding 100 Myr, there is no hope to obtain such an ephemeris, due to the chaotic behaviour of the solar system, but one can assume that for a few 100 Myr, the slow diffusion of the astronomical frequencies observed during the 200 Myr integrations remains of about the same order. This should not be granted for billion years computations and more computations on the diffusion process in the solar system are clearly needed. More, due to the changes in frequencies, and presence of secular resonances in the orbital forcing, more extended studies of the resulting influence on the rotational evolution of the Earth should be done. Studies on the long term evolution of the Earth-Moon system are also needed in order to improve our knowledge of the rotational evolution of the Earth. The geological records, assuming that a good accuracy in the determination of the fundamental frequencies could be achieved, would then be the only possible observations for tracking the long term past evolution of the solar system for time span longer than 100 Myr.

References

Berger, A.: 1976, 'Obliquity and precession for the last 5 000000 years',*Astron. Astrophys.* **51,** 127–135.

Berger, A., Loutre, M.F., Laskar, J.: 1988, Une nouvelle solution astronomique pour les 10 derniers millions d'années. Sc. Report 1988/14. Institut d'Astronomie et de Géophysique G. Lemaitre, Université Catholique de Louvain, Louvain-la-Neuve

Berger,A., Loutre, M.F., Dehant, V.: 1989, The influence of the changing lunar orbit on the astronomical frequencies of the pre-Quaternary insolation patterns, *Paleoceanography*, **4(5)**, 555–564

Berger,A., Loutre, M.F.: 1991, Insolation values for the climate of the last 10 million years, *Quaternary Science Reviews*, **10**, 297–317

Bretagnon, P.: 1974, Termes à longue périodes dans le système solaire.*Astron. Astrophys.* **30,** 341–362.

Kinoshita, H.: 1975, *Smithsonian Astrophys. Obs. Special Report*, No. 364.

Kinoshita, H.: 1977, Theory of the rotation of the rigid Earth, *Celes. Mech.* **15,** 277–326.

Laskar, J.: 1985, Accurate methods in general planetary theory, *Astron. Astrophys.* **144,** 133–146.

Laskar, J.: 1986, Secular terms of classical planetary theories using the results of general theory,*Astron. Astrophys.* **157,** 59–70.

Laskar, J.: 1988, 'Secular evolution of the Solar System over 10 million years', *Astron. Astrophys.* **198,** 341–362.

Laskar, J.: 1989, A numerical experiment on the chaotic behaviour of the Solar System *Nature*, **338**, 237–238

Laskar, J.: 1990, The chaotic motion of the solar system. A numerical estimate of the size of the chaotic zones, *Icarus*, **88**,266–291

Laskar, J., Quinn, T., Tremaine, S.: 1991, Confirmation of Resonant Structure in the Solar System, *Icarus, in press*

Quinn, T.R., Tremaine, S., Duncan, M.: 1991, 'A three million year integration of the Earth's orbit', *Astron. J.* **101**, 2287–2305

NUMERICAL INVESTIGATION OF THE EARTH'S ROTATION DURING A COMPLETE PRECESSION CYCLE

David L. Richardson

Department of Aerospace Engineering
University of Cincinnati
Cincinnati, Ohio 45221

1 Overview

A theory for the long-term rotational motion of the quasi-rigid Earth has been constructed by numerical integration. The theory spans 72000 years centered about 1968 A.D., and provides accurate rotational and positional data for the Earth in the recent past and the near future. Details are provided in [6]. The physical model is termed *dynamically consistent* because developments for the active forces and torques are truncated based solely on their magnitudes regardless of their origin. The model includes all appropriate forces and torques due to the geopotential and tidal effects as well as lunisolar and planetary contributions. The elastic and inelastic deformations due to tidal action were too small to affect the mass properties of the Earth at the truncation level of the model. However, long-term dissipative effects of the tidal forces and torques were not negligible. These considerations gave the model its quasi-rigid characterization. The numerical output provided both rotational and orbital-element data. The data have been fitted throughout the 72000-year range using Chebyshev polynomial series. These series are quite portable and are available upon request.

The project was based on the desire to provide researchers with a data base of accurate orbital and rotational parameters which are needed as the astronomical input to (paleo)climatology theories. Current theories [2] use only a rigid-Earth model and are analytical in nature. In addition, they are not completely consistent in their physical models. To keep pace with the accuracy of current observational data, the numerical theory maintains an accuracy on the order of 0.01 mas. The physical model includes:

1. rigid-body torques produced by the Moon, Sun, Venus, Jupiter and Saturn
2. tidal torques due to the Moon and Sun
3. effects due to Earth rotation/lunar orbit coupling
4. point-mass effects arising from the orbital motion of a 10-body planetary system (counting the Sun and Moon with Pluto excluded)
5. a 4×4 geopotential field

The numerical integration was conducted using a 10^{th}-order Adams-Moulton predictor with an 11^{th}-order Adams-Bashforth corrector. This combination produced a local truncation error $E \approx h^{12}$. The stepsize h was set to 1/50 day. The selection of h was based on error comparisons with output generated by extended precision (32 place) integrations.

The major results are displayed graphically in [6]. The data give an average precession rate of $-50.45''$/year. The present adopted IAU value is $-50.29''$/year, and that of the best analytical theory ([2]) is $-50.41''$/year. The output for obliquity (relative to the invariable plane of the solar system) and the precession index[1] $e \sin\tilde{\omega}$ are shown on the following page.

2 Future Work

The data base is not nearly long enough to be of great use to paleoclimatologists. Part of what is needed as an accurate theory that extends backward approximately 1 million years. (The data would thus span at least two of the 400,000-year Milankovitch cycles). A hybrid numerical integration procedure would be required—one that effectively suppresses the growth of round-off error. Such a procedure has been developed by Panovsky and Richardson [4] and has been used successfully in a multi-million-year integration of the planetary system [5]. Data spanning a much longer time frame would allow the retrieval of an accurate (geologically-recent) history for the lunar retreat rate.

To produce a data base spanning a much greater time frame, the quasi-rigid model for the Earth in the present theory would have to be discarded in favor of some sort of radially-dependent viscoelastic model which includes core-mantle coupling (gravitational and pressure) and mass-property variations. The new model should include changes in continentality from plate motions as well as the long-term effects of the oceans and glaciation. It may be possible to devise a model that is accurate over the long-term by adjusting parameters so that the (concocted) tidal dissipation provides lunar retreat rates consistent with the various measurements that have been reported in the recent literature. The extremes of these measurements now span 650 million years (see [1] and [7]).

To push a numerically-integrated theory backwards through tens of millions of years would require the development and use of a semi-numerical theory applied to a much-improved physical model. Such a theory is based on the numerical integration of the equations of motion after they have been analytically averaged at least through second order. A similar process has been successfully implemented by Laskar [3] in his recent investigations of the long-term motion of the eight-body planetary system. The averaging process would remove all high-frequency effects and leave only the secular, long-period, and dominant non-linear effects. The numerical integration could then proceed with stepsizes on the order of weeks or months instead of hours.

[1] The parameters e and $\tilde{\omega}$ are respectively, the orbital eccentricity of the Earth and the Earth's argument of perihelion measured from the moving Vernal equinox.

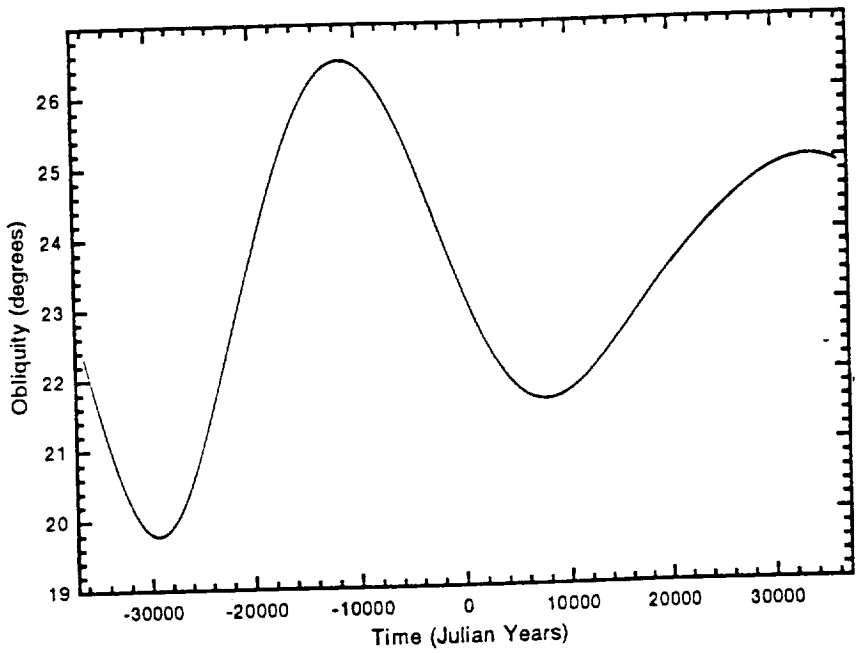

Obliquity for Full 72,000 Year Span.

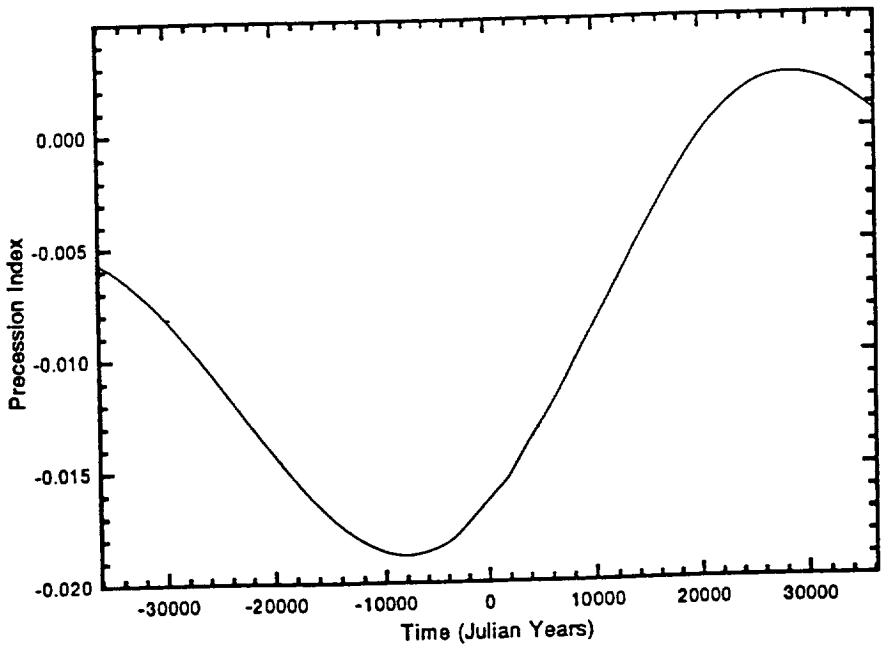

Precession Index $e \sin \tilde{\omega}$.

REFERENCES

[1] Dickey, J.O., Williams, J.G., and Newhall, X.X., "The impact of Lunar Laser Ranging on Geodynamics," *EOS. Trans. American Geophysical Union*, **71**, p. 475, 1990.

[2] Kinoshita, H. and Souchay. J., "The Theory of the Nutation of the Rigid Earth Model at Second Order," *Celestial Mechanics* **48**, 1990.

[3] Laskar, J., "Secular Evolution of the Solar System over 10 Million Years," *Astron. Astrophys.*, **198**, 1988.

[4] Panovsky, J. and Richardson, D.L., "A Method for the Numerical Integration of Ordinary Differential Equations Using Chebyshev Polynomials," AAS/AIAA Paper no. 85-405, 1985.

[5] Panovsky, J. and Richardson, D.L., "A Family of Implicit Chebyshev Methods for the Numerical Integration of Second-Order Ordinary Differential Equations," *J. of Computational and Applied Mathematics*, **23**, 1988.

[6] Walker, C.F. and Richardson, D.L., "A Self-Consistent Theory for the Earth's Rotational Motion," AAS/AIAA Paper no. 91-468, 1991.

[7] Williams, J.G., "Tidal Rhythmites: Key to the History of the Earth's Rotation and the Lunar Orbit," *J. Phys. Earth*, **38**, 1990.

Variations of the Milankovitch Frequencies in Time.

Loutre M.F. and Berger A.

1 Pre-Cenozoic Times

The sensitivity of the amplitudes and frequencies in the development of the Earth's orbital and rotational elements involved in the astronomical theory of paleoclimates (eccentricity, obliquity and climatic precession), to the Earth-Moon distance and consequently to the length of the day and to the dynamical ellipticity of the Earth has been discussed for the last billions of years (Berger et al., 1989a,b,c; Berger and Loutre, 1991).

The shortening of the Earth-Moon distance and of the length of the day, as well as the lengthening of the dynamical ellipticity of the Earth back in time induce a shortening of the fundamental astronomical periods for precession (the 19-kyr and 23-kyr quasi-periods becoming respectively 12.6 and 14.3-kyr at 2 10^9 yr BP) and obliquity (the 41-kyr and 54-kyr quasi-periods becoming respectively 19.6 and 22.1-kyr at 2 10^9 yr BP) (Figure 1). At the same time, the amplitudes of the different terms in the development of the obliquity are undergoing a relative enlargement of about 50% at 2 10^9 yr BP but the independent term is increasing very weakly (less than 0.1%). In other words, the value of the obliquity, which lies within a range of 21.°7 to 24.°9 over the Quaternary was restricted to a range of 22.°5 to 24.°1 at 2 10^9 yr BP. On the other hand, the amplitudes in the development of the climatic precession do not change. Moreover, these changes in the frequencies and amplitudes for both obliquity and climatic precession are larger for longer period terms. Finally, the periods in the eccentricity development are not influenced by the variation of the lunar distance.

But the motion of the solar system, especially of the inner planets, was shown to be chaotic (Laskar, 1990). It means that it is impossible to compute the exact motion of the planets over more than about 100 Myr, and the fundamental frequencies of the system are not fixed quantities, but are slowly varying with time. As long as we consider

the most important terms, the maximum deviation from the present-day value of the 19-kyr precessional period due to the chaotic motion of the solar system only does not reach more than a few tens of years around 80 Myr BP (Berger et al., 1991). Therefore the shortening of the obliquity and climatic precession periods is mostly driven by the change in the lunar distance and the consequent variations in the dynamical ellipticity of the Earth's angular speed.

At first sight, the deviation in the period for the eccentricity can be neglected, as the chaotic behaviour of the solar system implies a relative change of the main periods (404, 95 and 123 kyr-periods respectively) by less than 0.2%, 1.4% and 1.9% respectively, this maximum changes being achieved around 80 Myr BP. This implies, in particular, that the eccentricity periods used for Quaternary climate studies may be considered more or less constant for pre-Quaternay times and equal to their Quaternary values.

2 The Quaternary Period

The sensitivity of the frequencies of these astronomical elements to the dynamical ellipticity of the Earth has also been investigated for the Quaternary period (Dehant et al., 1990). According to the model used, the modification of the distribution of the masses on and inside the Earth during full glacial conditions has a weak influence on the moments of inertia of the Earth and consequently on the astronomical periods: more precisely the dynamical ellipticity of the Earth remains more or less constant for the isostatic equilibrium case (i.e. a subsidence of about 3/10 of the height of the ice sheet). For larger subsidences, the variation of the dynamical ellipticity of the Earth is positive and for smaller ones, it becomes negative, reaching 1.5% at the maximum. For a 1 % increase of the dynamical ellipticity of the Earth, the precessional quasi-periods (19 and 23 kyr) become 18.9 and 22.8 kyr while the quasi-periods of the obliquity (41 and 54 kyr) become 40.4 and 52.9 kyr.

3 Future research

- The determination of the Earth-Moon distance and/or the lunar recession rate for pre-Cenozoic times must be improved by taking into account the repartition and the displacement of the oceanic basins and of the continents in order to obtain a better time scale.
- A full model of the Earth interior would give more accurate values for the dynamical ellipticity of the Earth and the Earth's angular speed of rotation taking into account the repartition of the masses on and inside the Earth.
- The model used to compute the variation of the dynamical ellipticity of the Earth due to the waxing and waning of ice sheets could be improved by considering the

  - geographical location and height of the ice sheets
  - subsidence and rebound of the continents not covered by ice
  - subsidence and rebound of the marine lithospere

- A model accounting for the transient response to the ice sheet loading, instead of the snapshot reconstruction as used in the present study where we considered only full (maximum) glacial conditions and plain interglacials, would allow us to simulate the time evolution of the global effects of the ice sheets formation and melting, taking into account lagging subsidence and rebound of the lithosphere.

- Improvements in the interpretation of past proxy data and refinement of the time scale would allow to provide an independent determination of the astronomical frequencies found in pre-Cenozoic time series, allowing to validate and calibrate the astronomical models.

4 References

Berger A., Loutre M.F. and Dehant V. , 1989a, Astronomical frequencies for pre-Quaternary palaeoclimate studies. Terra Nova, 1, 474-479.

Berger A., Loutre M.F. and Dehant V., 1989b. Influence of the changing lunar orbit on the astronomical frequencies of pre-Quaternary insolation patterns. Paleoceanography, 4(5), 555-564.

Berger A., Loutre M.F. and Dehant V. , 1989c. Milankovitch frequencies for pre-Quaternary. Nature, 342, pp. 133.

Berger A. and Loutre M.F., 1991. Astronomical forcing through geological time. In: Orbital forcing and cyclic sedimentary sequences. (P.L. de Boer, ed), Utrecht.

Berger A., Loutre M.F. and Laskar J., 1991. Stability of the astronomical frequencies over the Earth's history for paleoclimate studies. Science (in preparation).

Dehant V., Loutre M.F. and Berger A., 1990. Potential impact of the northern hemisphere Quaternary ice sheets on the frequencies of the astroclimatic orbital parameters. J. Geophys. Res., 95 (D6), 7573-7578.

Laskar J., 1990, The chaotic motion of the solar system. A numerical estimate of the size of the chaotic zones. Icarus. 88, 266-291.

Walker J.C.G. and Zahnle K.J., 1986. Lunar nodal tide and distance to the Moon during the Precambrian. Nature, 320, 600–602.

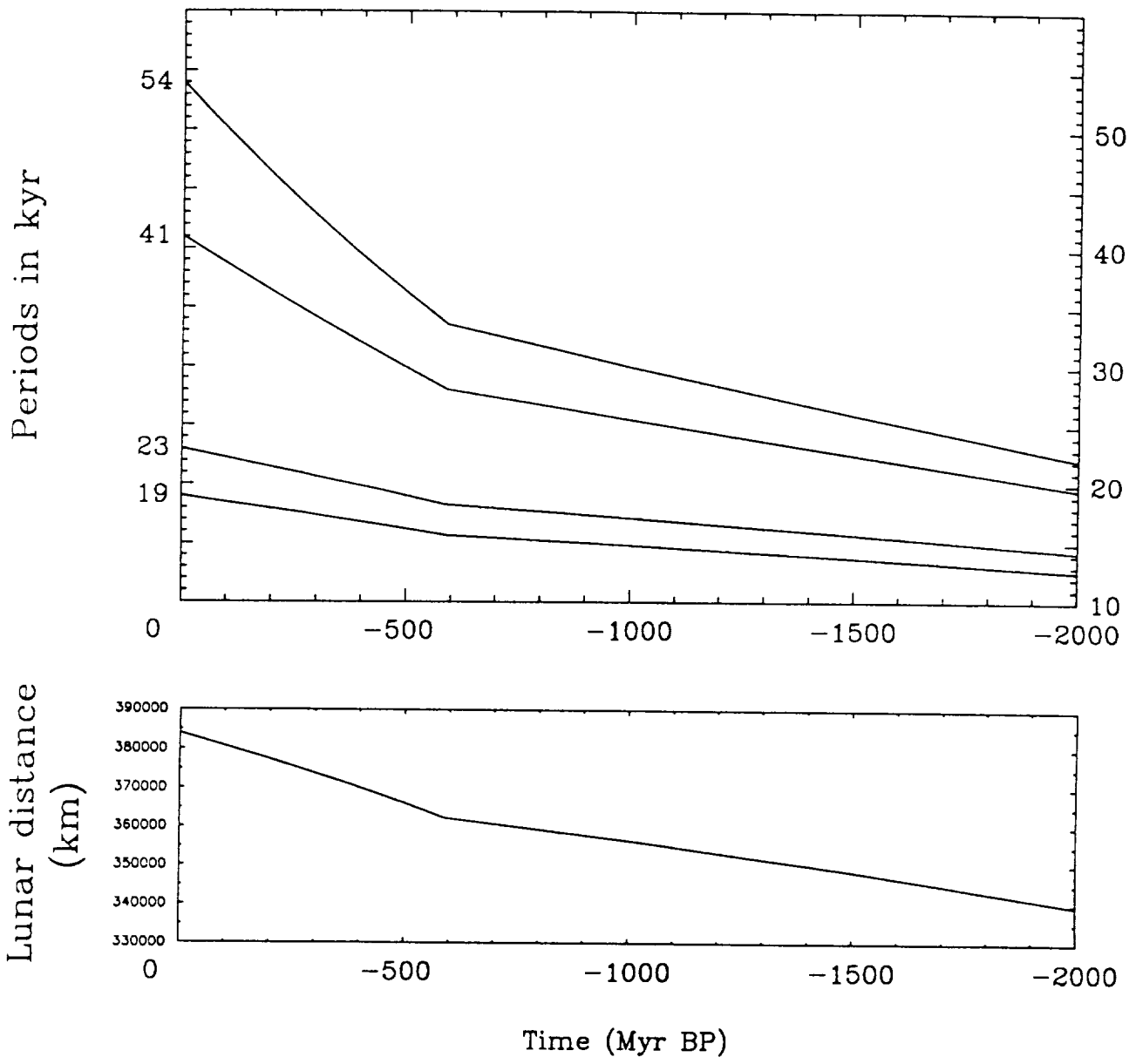

Figure 1: Estimated values of the periods of the orbital parameters (top) involved in the astronomical theory of paleoclimates considering the effect of the variations of the Earth-Moon distance (bottom) and of the Earth's figure and rotation (Berger and Loutre, 1991). It must be noted that the discontinuity in the rate of change of the astronomical periods reflects the artificial change in the value of the Earth-Moon recession rate taken to be 10^{-9} m s^{-1} for the last 590 Myr , and 0.43 10^{-9} m s^{-1} prior to 590 Myr BP (Walker and Zahnle, 1986; Berger and Loutre, 1991).

MAGNETIC SUSCEPTIBILITY VARIATIONS IN LOESS SEQUENCES AND THEIR RELATIONSHIP TO ASTRONOMICAL FORCING

Kenneth L. Verosub
Dept. of Geology
and
Michael J. Singer
Dept. of Land, Air and Water Resources
University of California-Davis
Davis, CA 95616

The long, well-exposed and often continuous sequences of loess found throughout the world are generally thought to provide an excellent opportunity for studying long-term, large-scale environmental change during the last few million years. In recent years, the most fruitful loess studies have been those involving the deposits of the loess in China. One of the most intriguing results of that work has been the discovery of an apparent correlation between variations in the magnetic susceptibility of the loess sequence and the oxygen isotope record of the deep sea. This correlation implies that magnetic susceptibility variations are being driven by astronomical parameters. However, the basic data have been interpreted in various ways by different authors, most of whom assumed that the magnetic minerals in the loess have not been affected by post-depositional processes. Using a chemical extraction procedure that allows us to separate the contribution of secondary pedogenic magnetic minerals from primary inherited magnetic minerals, we have found that the magnetic susceptibility of the Chinese paleosols is largely due to a pedogenic component which is present to a lesser degree in the loess. We have also found that the smaller inherited component of the magnetic susceptibility is about the same in the paleosols and the loess. These results demonstrate the need for additional study of the processes that create magnetic susceptibility variations in order to interpret properly the role of astronomical forcing in producing these variations.

The Chinese loess plateau stretches from 35°N to 40°N and from 100°E to 115°E and covers an area of 500,000 sq. km. The loess deposits are typically 150 m thick, and they appear to represent continuous deposition of wind-blown, silt-sized material during the past 2.4 million years. The source of this material is believed to be glacial outwash in the regions to the west and north of the plateau (Kukla and An, 1989). More importantly, the loess sequence contains many interbedded paleosols which attest to the existence of significant and cyclic climatic fluctuations. The most recent, comprehensive description of the units of the loess sequence is that of Kukla and An (1989), who recognized six stratigraphic units. From youngest to oldest, these are the Holocene

Black Loam Formation, the Malan Formation, the Upper Lishi Formation, the Lower Lishi Formation, the Wucheng Formation, and the Pliocene Red Clay.

On the basis of paleomagnetic studies (Heller and Liu, 1982; Kukla, 1987), the contact between the Wucheng Formation and the Red Clay layer has been dated at 2.4 million years, and the Brunhes/Matuyama, Olduvai event and Jaramillo event have each been identified in the sequence.

One of the primary parameters that has been used in the study of the loess/paleosol sequence has been magnetic susceptibility. Because the magnetic susceptibility of the loess is low while that of the paleosols is high, this parameter is considered an effective proxy for the quantitative study of the climatic fluctuations recorded by the loess/paleosol sequence (Heller and Liu, 1984; 1986).

The first comprehensive study of magnetic susceptibility variations in the loess/paleosol sequence was that of Heller and Liu (1984) who pointed out that there appeared to be a strong correlation between the magnetic susceptibility record and the oxygen isotope record of deep-sea cores from the equatorial Pacific Ocean. The relationship was further explored by Kukla *et al.* (1988) who published detailed magnetic susceptibility records from the loess/paleosol sections at Xifeng and Luochuan. These authors presented data to support their belief that the time required for the deposition of a particular loess unit was directly proportional to the product of the thickness of the unit and its magnetic susceptibility. They used this idea to construct a time scale that was independent of the oxygen isotope curve. On this time scale, the variations in magnetic susceptibility corresponded very closely to the variations in the oxygen isotope record from the deep sea, implying an interdependence among the rate of influx of loess, the volume of land-based ice, and the global climate. Additional evidence for astronomical forcing of the magnetic susceptibility record was provided by Wang *et al.* (1990).

A key component in the model used by Kukla *et al.* (1988; 1990) to account for the magnetic susceptibility variations was the assumption that the source of the magnetic susceptibility signal was a constant "rain" of ultrafine magnetic grains, carried into the upper atmosphere from volcanic eruptions and other unspecified processes. Kukla *et al.* further assumed that after these grains had been incorporated into the loess sequence during deposition, they remained inert and unaltered by post-depositional processes. The loess, on the other hand, was assumed to be essentially non-magnetic, and the modulation of the magnetic susceptibility signal was interpreted as a measure of the extent to which the magnetic "rain" had been diluted by loess. Thus, during glacial times, when the climate was cold and dry, the barren outwash plains could be easily eroded by aeolian processes, the rate of loess deposition would be at a maximum, and the magnetic susceptibility signal would be at a minimum. During interglacial times, when the climate was warm and humid, vegetation and soil moisture would tend to stabilize the outwash plains, loess deposition would be a minimum, and the magnetic susceptibility would be a maximum.

The model of Kukla *et al.* (1988; 1990) differs from that of Heller and Liu (1984) who suggested that the magnetic susceptibility values in the paleosols reflected a concentrating of the magnetic minerals by decalcification and soil compaction. Both models discounted any post-depositional alteration of the magnetic carriers. This fundamental assumption has been questioned by Zhou *et al.* (1990), Maher and Thompson (1991), and Zheng *et al.* (1991) who showed that there were significant differences between the rock magnetic properties of the magnetic minerals in the loess units and those in the paleosol units. These differences implied that there were differences in both the magnetic mineralogy and the grain size of the magnetic minerals in the two units. Maher and Thompson (1991) also raised questions about the methods that Kukla *et al.* used to demonstrate that the rate of accumulation of magnetic minerals had been constant. Zhou *et al.*, Zheng *et al.*, and Maher and Thompson all concluded that pedogenic processes had probably been important in the development of the magnetic susceptibility record of the paleosols.

We have obtained direct evidence that the magnetic susceptibility signal of *both* the loess units and the paleosols is due primarily to magnetic minerals formed by pedogenic processes. This conclusion is based on the studies of samples from ten loess/paleosol pairs from the classic section in Luochuan. The samples were provided to us by George Kukla of the Lamont-Doherty Geological Observatory, and they encompass the entire loess/paleosol sequence. Their designations, stratigraphic positions and approximate ages are shown in Table 1.

For each sample, we measured a variety of rock magnetic properties both before and after extraction with citrate-bicarbonate-dithionite (CBD). In this procedure, samples are subjected to sodium dithionite and bicarbonate, a strong buffered reductant, in the presence of sodium citrate, a chelating agent (Singer and Janitzky, 1986). The procedure was developed by Mehra and Jackson (1960) as a means of removing iron oxides from clay samples being prepared for X-ray diffraction analysis. The procedure was subsequently adopted by soil scientists as part of the standard chemical technique for characterizing the iron components of a soil. With that technique, extraction procedures involving pyrophosphate, oxalate and CBD are used to determine the amount of iron in organic, amorphous and crystalline phases, respectively. In recent years, we have used the CBD extraction technique in our studies of magnetic susceptibility enhancement in soil chronosequences in California (Singer and Fine, 1989; Fine *et al.*, 1989; Singer *et al.*, 1992). That work has shown that that CBD extraction is particularly effective in removing pedogenic magnetic grains (primarily maghemite) and that it leaves untouched essentially all of the magnetic grains that were inherited from the soil parent material (primarily magnetite and hematite). This selectivity has recently been confirmed by Mossbauer spectrometry (Singer *et al.*, 1991).

For untreated samples from the loess plateau, our rock magnetic measurements are fully consistent with those reported by Maher and Thompson (1991) and by Zhou *et al.* (1990). For example, the magnetic susceptibilities of the paleosols are as much as twenty times larger than

those of the corresponding loess samples (Table 1). Differences between loess and paleosol sample pairs are also noted in the frequency dependence of the magnetic susceptibility (which is a measure of the concentration of ultrafine grained, superparamagnetic particles), in the S-ratio (which is a parameter related to hematite concentration), in the ratio of saturation isothermal remanent magnetization to anhysteretic remanent magnetization (which is a measure of the relative abundance of single domain grains) and in the ratio of magnetic susceptibility to anhysteretic remanent susceptibility (which is related to mean magnetic grain size).

After CBD treatment, both the loess and the paleosol samples lose a significant percentage of their magnetic susceptibility (Table 1). These losses average 65% for the loess samples and 90% for the paleosol samples. Because the magnetic susceptibilities of the untreated paleosol samples are five to ten times greater than that of the untreated loess samples, the absolute decreases in magnetic susceptibility are much greater in the paleosols than in the loess units (Figure 1). Furthermore, after CBD treatment, the magnetic susceptibilities of the loess samples and the paleosol samples are about the same, regardless of the age of the samples (Figure 1). Several other rock magnetic properties also show decreases after CBD treatment with largest changes again occurring in samples from the paleosols (Figure 2). For a few rock magnetic properties, the values from the paleosol and loess samples move in opposite directions after CBD treatment. Furthermore, we have found a close relationship between magnetic susceptibility and dithionite-extractable iron (Figure 3), providing additional evidence of the importance of pedogenesis in determining the magnetic susceptibility of paleosols and loess.

Based on our work on the soil chronosequences in California, we interpret the CBD soluble fraction in the loess and paleosol samples as the pedogenic fraction, and the CBD insoluble fraction as the inherited fraction. This indicates that a significant portion of the magnetic susceptibility signal of both the loess samples and the paleosol samples is pedogenic in origin. The fact that pedogenesis is important in producing the magnetic susceptibility signal in the paleosols was suggested by Zhou *et al.* (1990), Maher and Thompson (1991) and Zheng *et al.* (1991). However, none of these groups postulated that pedogenesis could account for almost all of the magnetic susceptibility signal in the paleosols, and none of them proposed that pedogenesis would be important in the loess units as well. This latter observation gives us an entirely new perspective on the paleosol/loess sequences. In the conventional view, paleosol units are considered to have resulted from very different processes than those that produce the loess units. From our results, it seems that the same pedogenic processes might have been operating during times of loess deposition and paleosol formation but these processes were more intense during the former than during the latter.

Our results also show that other earlier inferences about the nature of the magnetic susceptibility signal were probably also wrong. For example, Maher and Thompson suggested

that the pedogenic component of the magnetic susceptibility was probably carried by magnetite while our data strongly support the conclusion that maghemite is the primary magnetic mineral. More importantly, our observations provide no support for the concept of an inert, ultrafine magnetic "rain" diluted to varying degrees by non-magnetic windblown silt, as proposed by Kukla *et al.* (1988; 1990). In fact, if the nearly constant residual magnetic susceptibility that we observe in both the paleosol and loess samples after CBD treatment is an exogenous magnetic component, it implies that the loess was accumulating at a same rate during glacial and interglacial stages and that the differences between paleosols and loess are due entirely to the degree of pedogenesis.

At present time, we are not prepared to argue the merits of this or any other explanation of our results. What we will argue is that we have shown that there is a clear need for a better understanding of the nature and origin of the magnetic susceptibility signal in the Chinese loess/paleosol sequence. This need is more than just a minor problem, of interest to a small group of rock magnetists. As noted above, the loess/paleosol sequences in general, and the Chinese sequences in particular, are considered the best recorders of terrestrial climate change during the last 2.4 million years. Almost exclusively, this change is being studied using magnetic susceptibility as a proxy indicator of paleoclimate. In fact, using assumptions about the magnetic susceptibility signal that our research has now shown to be incorrect, other workers have already developed an elaborate model for climate changes in Asia and the western Pacific. The model attributes these changes to astronomically-driven fluctuations in the summer monsoon that are modulated by uplift of the Tibetan plateau (Kukla, 1987; An *et al.*, 1991).

While certain aspects of this model may ultimately prove to be correct, the model itself cannot be validated until its underlying assumptions are based on the proper paleoclimate interpretation of the magnetic susceptibility record. Our work has shown that this interpretation must address the pedogenic nature of the magnetic susceptibility signal. This requirement also applies to loess/paleosol sequences elsewhere that are also being interpreted as records of terrestrial climate change.

REFERENCES

An, Z., G.J. Kukla, S.C. Porter, and J. Xiao, 1991, Magnetic susceptibility evidence of Monsoon variations on the Loess Plateau of central China during the last 130,000 years. *Quat. Res.*, v. 36, pp. 29-36.

Fine, P., M.J. Singer, R. La Ven, K. L. Verosub, and R.J. Southard., 1989, Role of pedogenesis in Distribution of Magnetic Susceptibility in Two California Chronosequences. *Geoderma*. v. 44, pp. 287-306.

Heller, F., and T.S. Liu, 1982, Magnetostratigraphical dating of loess deposits in China. *Nature*, v. 300, pp. 431-433.

Heller, F., and T.S. Liu, 1984, Magnetism of chinese loess deposits. J. Geophys. Res., v. 77, pp. 125-141.

Heller, F., and T.S. Liu, 1986, Palaeoclimatic and sedimentary history from magnetic susceptibility of loess in China. *Geophys. Res. Lett.*, v. 13, pp. 1169-1172.

Kukla, G., 1987, Loess stratigraphy in central China. Quat. Sci. Rev. v. 6, pp. 191-219.

Kukla, G., and Z.S. An, 1989, Loess stratigraphy in central China. *Palaeogeography, Palaeoclimatology, Palaeoecology*, v. 72, pp. 203-225 .

Kukla, G., F. Heller, Liu X. M., Xu T. C., Liu T. S., and An Z. S., 1988, Pleistocene climates in China dated by magnetic susceptibility. *Geology*, v. 16, pp. 811-814.

Kukla, G., Z.S. An, J.L. Melice, J. Gavin, and J.L. Xiao, 1990, Magnetic susceptibility record of Chinese Loess. *Trans. Roy. Soc. Edinburgh: Earth. Sci.*, v. 81, pp. 263-268.

Maher, B. A., and R. Thompson, 1991, Mineral magnetic record of the Chinese loess and paleosols. *Geology*, v.19, pp. 3-6.

Mehra, O.P., and M.L. Jackson, 1960, Iron oxide removal from soils and clays by dithionite-citrate system buffered with sodium bicarbonate. *Clays and Clay Min.*, v.5, pp. 317-327.

Singer, M.J. and P. Fine., 1989, Pedogenic Factors Affecting Magnetic Susceptibility of Northern California Soils. *Soil Sci. Soc. Am. J.* v. 53, pp. 1119-1127.

Singer, M.J. and P. Janitzky (Editors). 1986. Field and Laboratory Procedures Used in a Soil Chronosequence Study. U.S. Geological Survey Bulletin 1648. 50 pages.

Singer, M.J., L.H. Bowen, K.L. Verosub, and P. Fine, 1991, Characterization of magnetic carriers in soils using Mössbauer spectroscopy. *Eos. Trans A.G.U.*, v. 72 (supplement to no. 44) , p. 143.

Singer, M.J., P. Fine, K.L. Verosub, and O.A. Chadwick., 1992, Time dependence of magnetic susceptibility of soil chronosequences on the California coast. *Quat. Res.* (in press).

Wang, Y., and M. E. Evans, 1990, Magnetic susceptibility of Chinese loess and its bearing on paleoclimate. *Geophys. Res. Lett.*, v. 17, pp. 2449-2451.

Zheng, H., F. Oldfield, L. Yu, J. Shaw and Z. An, 1991, The magnetic properties of particle-sized samples from the Luo Chuan loess section: evidence for pedogenesis. *Phys. Earth Planet. Int.*, v. 68, pp. 250-258.

Zhou, L. P., F. Oldfield, A. G. Wintle, S. G. Robinson, and J. T. ,Wang, 1990, Partly pedogenic origin of magnetic variations in Chinese loess. *Nature* v. 346, pp. 737-379.

Table 1. Paleosol and Loess Samples from Luochuan, China. (Samples provided by George Kukla.)

Position	Depth	Age†	Magnetic susceptibility	
			Pre-CBD	Post-CBD
	m	ka	SI x 10^{-8} m^3 kg^{-1}	
S1	10.0	128	227.5	22.7
L2-LL1	12.5	174	11.4	8.1
S3	24.0	328	223.3	19.7
L4	26.0	357	57.2	18.6
S5	36.5	614	283.3	11.4
L6	42.0	652	59.7	13.7
S7	52.0	726	81.1	15.3
L8	52.5	?	58.5	15.0
S8	54.5	737	129.5	15.0
L9	57.5	834	26.9	15.3
L14	76.0	?	53.7	11.2
L15	78.5	1172	23.0	14.4
WS1WL1	86.0	1316	132.9	13.9
WS1SS1	86.5	?	86.2	14.3
WS1SS1	87.5	?	84.6	14.1
WS2SS2	99.0	1566	102.5	15.0
WL2LL2	101.0	1695	54.9	12.8
WS3LL1	107.5	1939	45.0	13.0
WS3LL1	109.0	1939	49.9	9.4
WL4LL3	134.0	2342	37.1	11.2
RsSS1	136.0	>2342	168.7	14.3

† Age from Kukla (1987) Table 5.

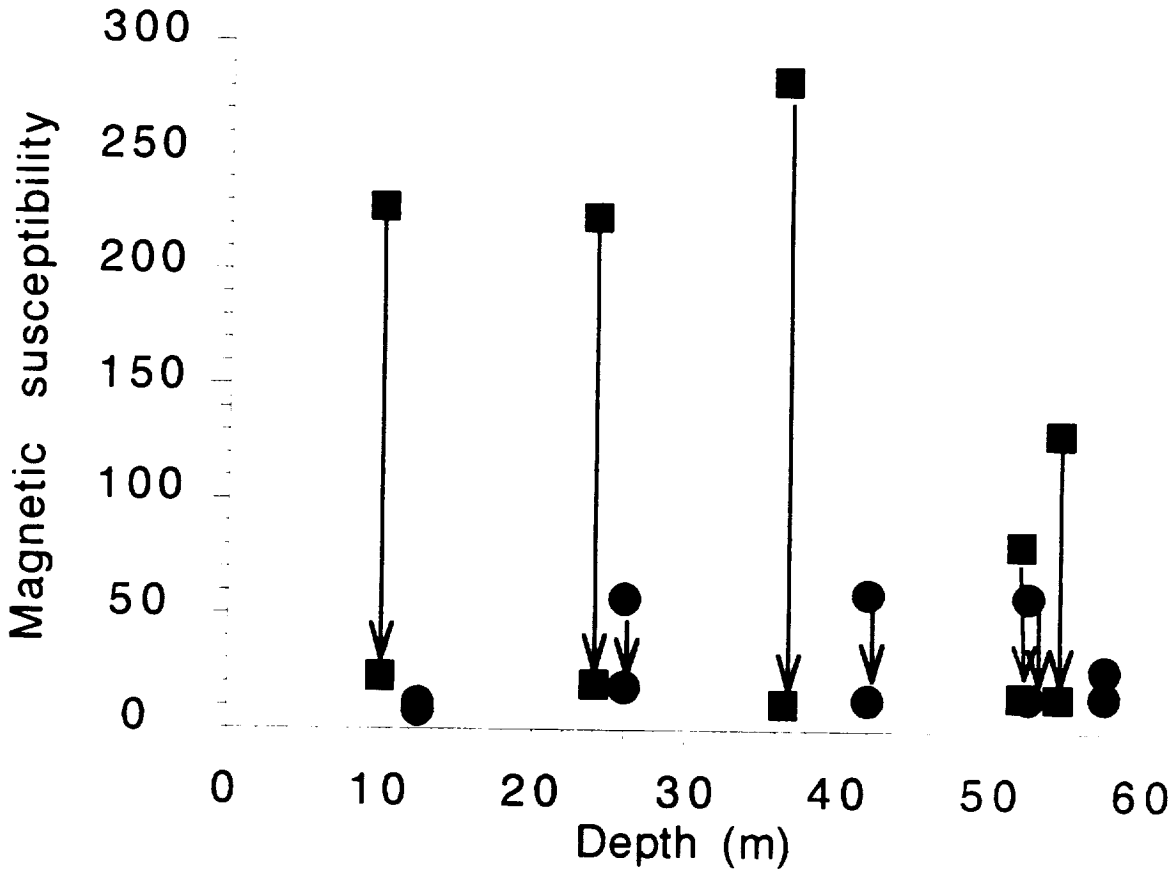

Figure 1. Effect of CBD treatment on magnetic susceptibility of some paleosol and loess units from the Lishi Formation, Luochuan, China. Squares are paleosol units; circles are loess units. Arrows indicate change upon CBD treatment. The post-CBD values for both paleosols and loess units are about the same.

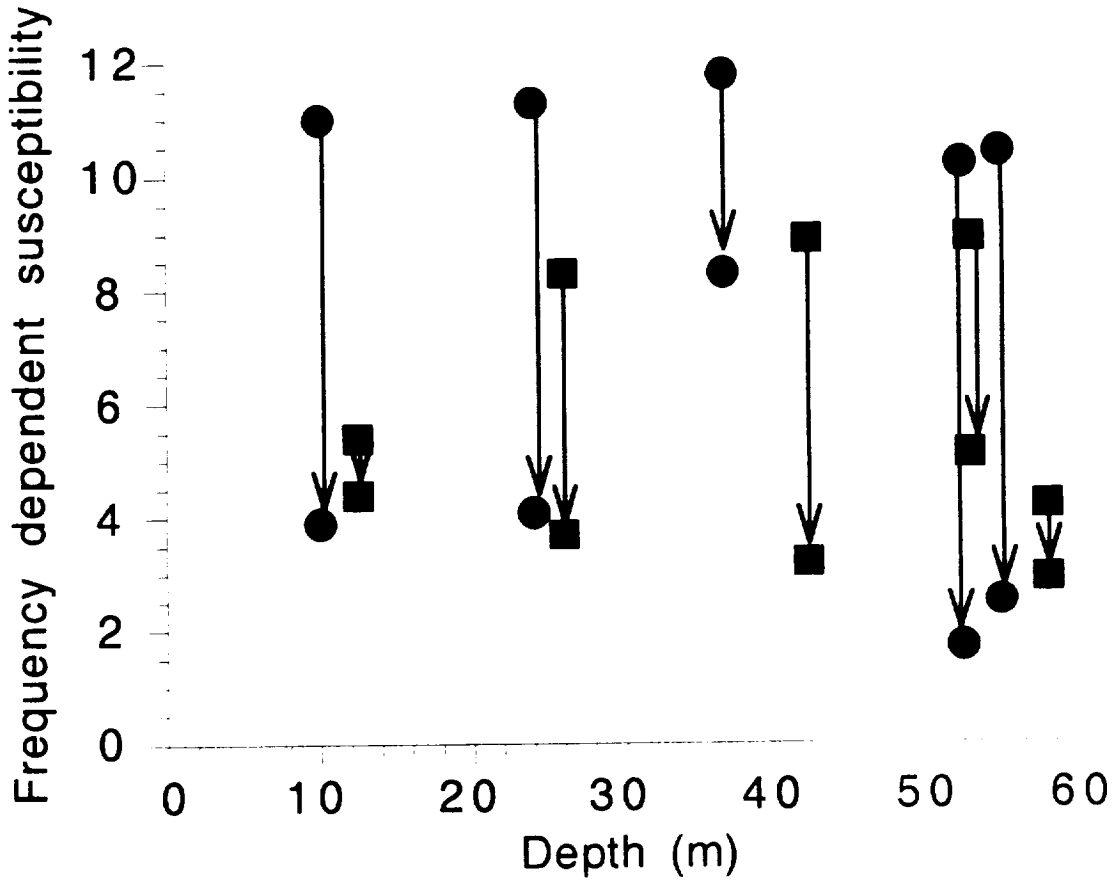

Figure 2. Effect of CBD treatment on the frequency dependence of the magnetic susceptibility of some paleosol and loess units from the Lishi Formation, Luochuan, China. Squares are paleosol units; circles are loess units. Arrows indicate change upon CBD treatment. The post-CBD values for both paleosols and loess units are about the same.

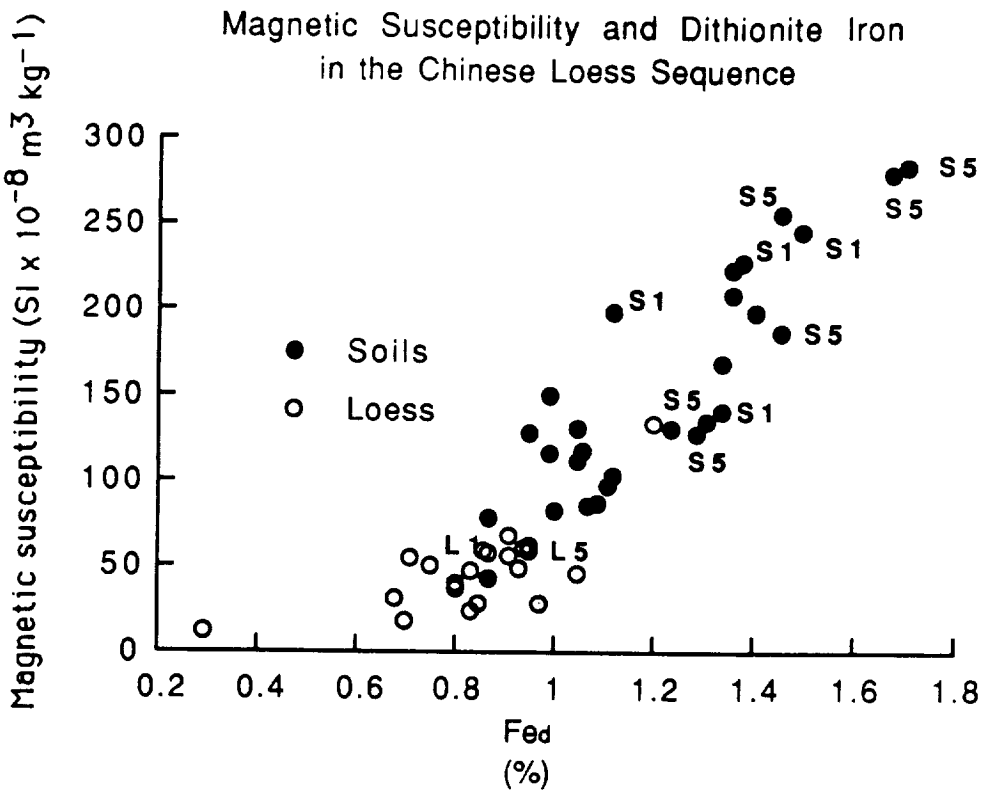

Figure 3. Relationship between dithionite extractable iron and magnetic susceptibility of some paleosol and loess units.

Ice Ages and Geomagnetic Reversals

Patrick Wu
Dept. of Geology & Geophysics, University of Calgary
2500 University Dr.N.W., Calgary, Alberta
CANADA

1. Climatic Cooling related to Geomagnetic Reversals?

There have been speculations on the relationship between climatic cooling and polarity reversals of the earth's magnetic field during the Pleistocene (Kawai et al. 1975, Rampino 1981, Krishnamurthy et al 1986, and Jacobs 1984 for a review). Two of the common criticisms on this relationship have been the reality of these short duration geomagnetic events and the accuracy of their dates. Champion et al. (1988) have reviewed recent progress in this area. They identified a total of 10 short-duration polarity events in the last 1 Ma and 6 of these events have been found in volcanic rocks, which also have K-Ar dates. The nomenclature and the estimated ages for these events are shown on the top of Fig.1a. Events with age dated from volcanic rocks are shown as solid bars, those from sedimentary rocks as stippled bars. Also, typeface and size of the names represent the degree of confidence in the exact age or existence of that polarity event. Following Rampino (1981), the eccentricity of the earth's orbit over the past 1.2 Ma is also calculated (Berger 1977) and plotted with the stacked oxygen isotope data (with the SPECMAP time scale, Imrie et al 1984) at the bottom of Fig.1a.

An inspection of Fig.1a shows that during the last 600 ka, where the 100 ka cycle (due to eccentricity) was the dominant signal in the oxygen isotope data, magnetic polarity events seem to occur near times of maximum eccentricity and rapid glaciation, thus giving some support to a possible climate-magnetic reversal connection. For $t > 600$ ka, the correlation is not as good - although there is an apparent correlation between times of maximum eccentricity and the Kamikatsura event, the end of the Jaramillo and the Cobb Mountain event. If the ages of these older events are revised according to Shackleton et al. (1990), then all of these older events, except the Kamikatsura, appear to occur near eccentricity maxima (Fig.1b).

Anyhow, Champion et al. (1988) found that the mean of the polarity interval lengths (in Fig.1a) to be close to the 100 ka main orbital eccentricity period of the earth, they therefore suggested that linkage between geomagnetic, paleoclimatic and possible underlying earth orbital parameters should be further studied.

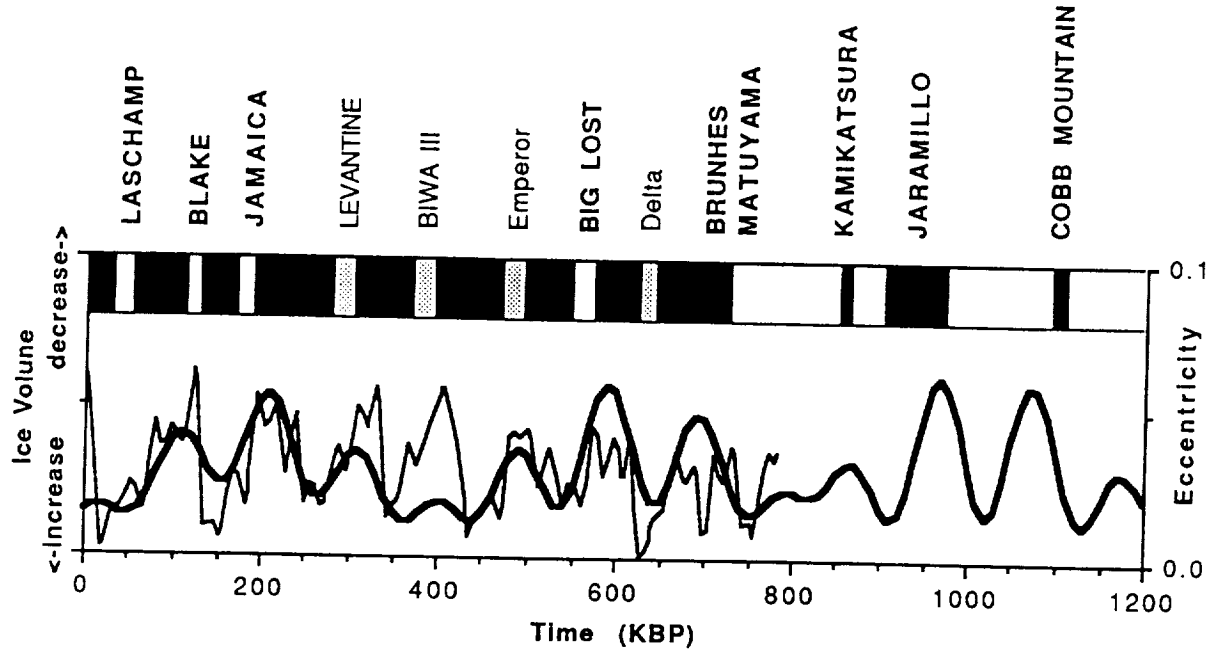

Fig.1a Correlation of the polarity events with the eccentricity of the Earth's orbit, and δO^{18} (ice volume) variation over the past 1.2 Ma.

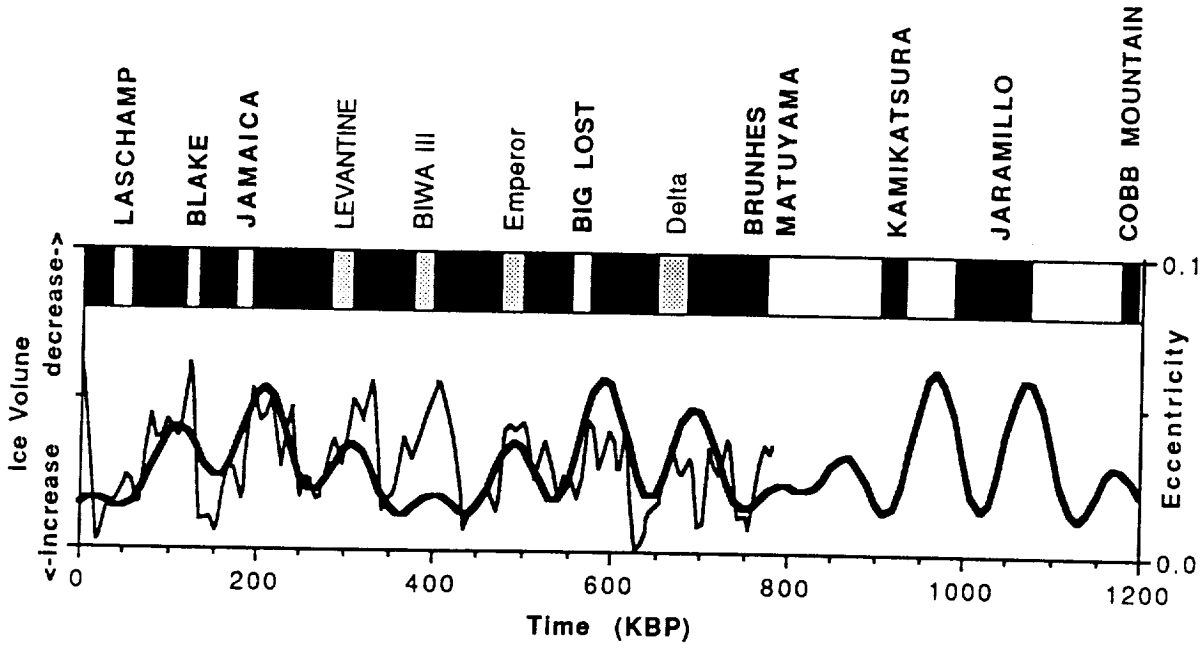

Fig.1b Same as Fig.1a, except ages greater than 600 ka are modified according to Shackleton et. al (1990)

2. Mechanisms that relate climatic cooling & Geomagnetic Reversals

Supposing that the speculated relationship between climatic cooling and geomagnetic reversals actually exist, two mechanisms that assume climatic cooling causes short period magnetic reversals will be investigated. It should be noted that this is NOT an attempt to explain the occurrence of ALL the magnetic polarity events in terms of glacial advances, for it is obvious that magnetic reversals has occurred throughout the history of the earth - even during times when there is no glaciation. Therefore, the mechanisms that we investigate operates only within the Pleistocene and it should be clear that other mechanisms, with different time scales, may be operative at the same time and they may be responsible for the reversals outside this epoch.

2.a Core-Mantle Boundary Topography

A possible mechanism results from the variation of topographic interaction across the core-mantle boundary (CMB). For example, the formation of large bumps or depressions at the CMB will set up Taylor columns in the core (Hide, 1969), disrupt the flow which drives the geodynamo and possibly change the geomagnetic field. The critical height for topographic coupling to be effective has been estimated to be around 1 km .

Gubbins and Richards (1986) have investigated the effect of thermal and subduction-induced topography and have concluded that both have the right magnitude to cause coupling. However, the thermal time scale is of the order of 100 Ma whereas changes in topography due to subduction is about 10 Ma. Since polarity reversals can occur several times in 1 Ma, there must be other phenomena which cause the short time scale variations in topographic coupling during the Pleistocene. Now, the period of a glacial cycle is about 100 ka and for a 3 km thick ice sheet, the depression at the earth's surface is about 1 km. Thus, depending on how rapid this deformation attenuates with depth, glacial induced topography at the CMB, if suitably located, may be able to enhance (or diminish) the coupling due to thermal and subduction-induced topography such that the total coupling can exceed (or fall below) the threshold value required to disrupt core flow.

The topography of the CMB due to glacial loads at the earth's surface has been calculated for 3 different earth models L1, L2 & L3 which has lower mantle viscosities of 10^{21}, $3x10^{21}$ and 10^{22} Pa-s respectively. The ice model consists of 3 centers of glaciation corresponding to the Laurentide, FennoScandian and Antarctic ice masses which has total mass equivalent to a sea level drop of 100 meters and whose glacial history consists of 30 cycles of glaciation, the last of which is plotted in Fig.2a. The result of this calculation is described in Wu (1990) which shows that the maximum topography occurs underneath the Laurentide ice center and the time variation of this maxima is shown in

Fig.2c. In view of its smallness in height and its location relative to other topographic highs as deduced from seismic tomography, glacial induced CMB topography is not expected to be able to significantly modulate total coupling and modify core flow today.

2.b Transfer of Rotational Energy to the core

An alternate mechanism is the transfer of rotational energy into the fluid core: the redistribution of water masses during glaciation and deglaciation will cause the moment of inertia of the earth to change - for example, when water is taken from the ocean basins and is locked in the ice sheets near the pole, the moment of inertia will decrease. By the conservation of angular momentum, the decrease in the moment of inertia must be accompanied by an increase in the angular velocity of the mantle. If the increase in velocity at the bottom of the mantle exceeds the 0.03 cm/sec flow velocity in the fluid core (estimated from the westward drift of the non-dipole component), then the transfer of angular momentum into the core would disrupt the convective heat engine inside and possibly result in a change in magnetic polarity (Doake 1977, Muller & Morris 1986).

The change in velocity at the bottom of the mantle due to the simple glaciation/deglaciation model described earlier is plotted in Fig.2b. The solid line, the dotted line and the dashed line correspond to earth models L1, L2 and L3 respectively. The stripped area in the middle indicates that the velocity at the bottom of the mantle is below the preexisting flow velocity in the fluid core. From Fig.2b it can be seen that model L1 (and possibly L3 near glacial minimum) can produce velocity changes comparable to the existing flow in the core.

Given that a 100m change in sea levels can produce velocity changes at the bottom of the mantle to be comparable to the existing flow in the core, the next question concerns how energy is transferred from the mantle to the core. The mantle and the core can interact by electromagnetic coupling, viscous coupling and topographic coupling. If the roughness of the CMB exceeds the thickness of the viscous hydromagnetic boundary layer, then topographic coupling becomes the dominant mechanism . Although the topography induced by glacial loads has been shown to be too small to cause coupling, the topography due to density loads in the mantle exceeds the critical value and possibly provides the coupling mechanism to transfer rotational energy into the core to cause geomagnetic reversals.

3. Conclusion

In conclusion, the variation in CMB topography induced by the surface glacial loads has the correct time scale but not the amplitude, unless the maxima are suitably located, to significantly modify the total coupling mechanism and disrupt the flow pattern in the core resulting in geomagnetic field reversals. The transfer of rotational energy from the mantle to

the core via topographic coupling is a more likely candidate, provided that the change in sea level is of the order of 100 meters and the coupling is via thermal and subduction induced topography.

4. Questions and Future Work

More precise dates and the establishment of the reality of some polarity events (eg. the Emperor & Delta events) are required to establish/disprove the controversial relationship between climatic cooling and geomagnetic reversals. In the compilation of Champion et al (1988), some of the events have rather large uncertainties in their age, and, as shown in Fig.1, the correlation of some of the older events with eccentricity maxima depends critically on their age.

Opponents to a climate-magnetic reversal relationship often question whether polarity events observed in different parts of the world but with approximately the same age can be correlated and whether they correspond to the same global events. Another question is whether there are only 8 polarity events in the Brunhes, for, if more events are discovered, then there may be no correlation between polarity events and eccentricity maxima. Clearly, cores in different parts of the earth, with more complete record and dates are needed to answer these questions.

Even when the relationship between climate and magnetic reversals is established, the next question is which is the cause and which is the effect? If magnetic field is the cause, then the question is why they do not always cause climatic cooling (eg. during the Cretaceous)? If climatic cooling is the cause, then, are there other mechanisms?

A better seismic tomographic map of the CMB would confirm whether glacial induced topography can modulate total coupling and modify core flow. Glacial induced topography is rejected because, in seismic tomographic maps of the CMB (Morelli & Dziewonski 1987, Creager & Jordan 1986), no topographic hills/troughs seem to exist underneath Laurentia. These seismic tomographic maps are, however, not consistent with each other and therefore have some degrees of uncertainty in them.

More work is needed to understand the details of the core-mantle coupling mechanisms and how energy and angular momentum can be transferred from the mantle to the core.

Finally, even after this is achieved, questions still remain as to how this energy and momentum are going to disturb the flow field and the convective engine of the core? how a polarity reversal comes about ? and why the reversals are often so brief?

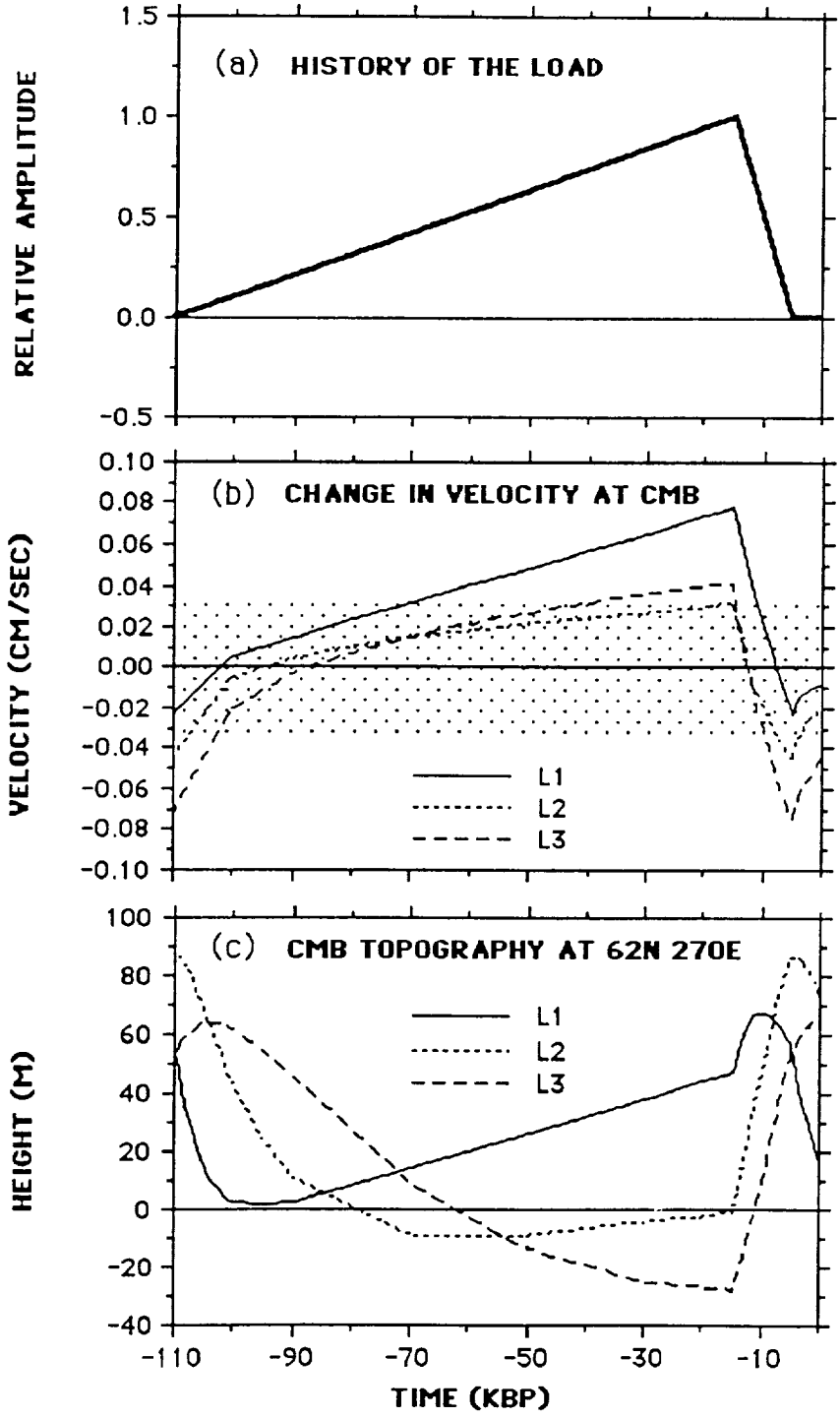

Fig.2 (a) The last cycle of the saw-tooth load history. (b) The time history of the change in velocity at the bottom of the mantle due to increased spin rate of the mantle. (c) The time evolution of the CMB topography under the Laurentide ice center for the 3 earth models.

References

Berger, A., 1977. Support for the astronomical theory of climatic change.*Nature*, **269**,44.

Champion, D.E., Lanphere,M.A. & Kuntz,M.A., 1988. Evidence for a new geomagnetic reversal from lava flows in Idaho: discussion of short polarity reversals in the Brunhes and Late Matuyama polarity chrons. *J.Geophy.Res.*,**93**,11667-11680.

Creager, K.C. & Jordan, T.H., 1986. Aspherical structure of the core-mantle boundary from PKP travel times, *Geophys. Res.Lett.*,**13**,1497-1500.

Doake, C.S.M., 1977. A possible effect of ice ages on the Earth's magnetic field, *Nature*,**267**,415-417.

Gubbins, D. & Richards M., 1986. Coupling of the core dynamo and mantle: thermal or topographic? *Geophys.Res.Lett.*, **13**,1521-1524.

Hide, R., 1969. Interaction between the Earth's liquid core and the solid mantle. *Nature*,**222**,1055.

Imbrie, J., Hays,J.D., Martinson,D.G., McIntyre,A., Mix,A.C., Morley,J.J., Pisias,N.G., Prell,W.L. & Shackleton,N.J., 1984. The orbital theory of Pleistocene climate: support from a revised chronology of the marine δO^{18} record. In Berger,A., Imbrie,J., Hays,J.D., Kukla,G. & Saltzman,B. Milankovitch and Climate, pp.269-305. Hingham, Mass.: D. Reidel.

Jacobs, J.A., 1984. *Reversals of the Earth's magnetic field.* Adam Hilger Ltd, Bristol.

Kawai, N., Yaskawa, K., Nakajima, T., Torii, M & Natsuhara, N., 1975. Voices of geomagnetism from Lake Biwa, *Paleolimnology of Lake Biwa and the Japanese Pleistocene, vol 3*, ed. S.Horie (Otsu:Kyoto University) p.143.

Krishnamurthy, R.V., Bhattacharya, S.K. & Sheela Kusumgar, 1986. Palaeoclimatic changes deduced from $^{13}C/^{12}C$ and C/N ratios of Karewa lake sediments,India, *Nature*,**323**,150.

Morelli, A. & Dziewonski, A.M., 1987. Topography of the core-mantle boundary and lateral homogeneity of the liquid core, *Nature*,**325**,678-683.

Muller, R.A. & Morris, D.E., 1986. Geomagnetic reversals from impacts on the earth, *Geophys.Res.Lett.*,**13**,1177-1180.

Rampino, M.R., 1981. Revised age estimates of Brunhes palaeomagnetic events: support for a link between geomagnetism and eccentricity. *Geophy.Res.Lett.*, **8**,1047-50.

Shackleton, N.J., Berger A. & Peltier, W.R., 1990. An alternative astronomical calibration of the lower Pleistocene timescale based on ODP Site 677. *Trans.Roy. Soc.Edinburg: Earth Sciences*, **81**,251-261.

Wu, P., 1990. Deformation of internal boundaries in a viscoelastic earth and topographic coupling between the mantle and core, *Geophys.J.Int.*, **101**,213-231.

Late Quaternary Time Series of Arabian Sea Productivity: Global and Regional Signals

S.C. Clemens W.L. Prell D.W. Murray

Brown University
Providence, RI

Modern annual floral and faunal production in the northwest Arabian Sea derives primarily from upwelling induced by strong southwest monsoon winds during June, July, and August. Indian Ocean summer monsoon winds are, in turn, driven by differential heating between the Asian continent and the Indian Ocean to the south. This differential heating produces a strong pressure gradient resulting in southwest monsoon winds and both coastal and divergent upwelling off the Arabian Peninsula (Figure 1). Over geologic time scales (10^4 to 10^6 years), monsoon wind strength is sensitive to changes in boundary conditions which influence this pressure gradient. Important boundary conditions include the seasonal distribution of solar radiation, global ice volume, Indian Ocean sea surface temperature, and the elevation and albedo of the Asian continent. To the extent that these factors influence monsoon wind strength, they also influence upwelling and productivity. In addition, however, productivity associated with upwelling can be decoupled from the strength of the summer monsoon winds via oceanic mechanisms which serve to inhibit or enhance the nutrient supply in the intermediate waters of the Indian Ocean, the source for upwelled waters in the Arabian Sea (Prell, 1990).

To differentiate productivity associated with wind-induced upwelling from that associated with other components of the system such as nutrient sequestering in glacial-age deep waters (i.e. Boyle, 1988) we employ a strategy which monitors independent components (Figure 2) of the oceanic and atmospheric subsystems. Using sediment records from the Owen Ridge, northwest Arabian Sea, we monitor the strength of upwelling and productivity using two independent indicators, % G. bulloides

(Prell, 1984, 1990) and opal accumulation (Murray, 1990). We monitor the strength of southwest monsoon winds by measuring the grain-size of lithogenic dust particles blown into the Arabian Sea from the surrounding deserts of the Somali and Arabian Peninsulas (Clemens and Prell, 1990a).

The planktonic foraminifer G. bulloides is typically a subpolar species found in the Southern ocean between the Subtropical Convergence and the Antarctic Convergence. However, G.bulloides is also found in high abundance in tropical upwelling areas such as the northern Arabian Sea of the coast of Arabia (Hutson and Prell, 1980; Cullen and Prell, 1984) and Cariaco Trench, located off Venezuela (Overpeck et al., 1989). G. bulloides abundance in the Arabian Sea is negatively correlated to summer sea surface temperature (Prell and Curry, 1981) which, in turn, is negatively correlated with wind-induced upwelling during the summer monsoon (Prell and Streeter, 1982). Similarly, opal accumulation is positively correlated with nutrient distribution associated with upwelling but less influenced by regional sea surface temperatures (Murray, in preparation).

The Owen Ridge lies beneath the axis of the strong summer monsoon winds. These winds can transport lithogenic dust particles such as those found on the Owen Ridge (mean diameter of 14.4 μm) for thousands of kilometers given mean velocities of 15 m/s and values for the coefficient of turbulent exchange found in typical cyclonic storms and frontal systems (Tsoar and Pye, 1987). The largest particles (40 to 50 μm) can also be transported up to ~ 1000 km in more extreme dust storm events. These estimates of transport distances are consistent with studies which identify the Somali and Arabian Peninsulas as primary source areas for dust found in Arabian Sea sediments (Middleton, 1986; Sirocko and Samthein, 1989). Over geologic time scales, increases in the strength of monsoon winds result in the transport of larger lithogenic particles to the Arabian Sea, thus increasing the median grain size of the lithogenic component (Clemens and Prell, 1990a).

Spectral analyses of these records allow us to examine concentrations of variance held in common between these independent abiotic and biotic records of wind strength and productivity. Our results unambiguously demonstrate that all three independent records are linearly related and in phase with one another over the Earth's orbital precession cycles (23 kyr cycles; Figure 3). We interpret these relationships as indicating that: (1) to first order, all three indicators are linked by a common response to monsoon wind strength and upwelling, and (2) precessional insolation is the primary external forcing mechanism for the late Quaternary monsoon and the associated upwelling induced productivity. However, variance associated with precession accounts for only ~ 25% of the total variance in any given record. A large portion of the total variance in the biotic records is concentrated at the 41 kyr period associated with the obliquity of the Earth's orbit (Figure 4; Prell, 1990). The

grain-size record, on the other hand, contains large amounts of variance at the 29, 35, and 54-kyr periods which represent heterodyne periods of the primary orbital periods (100, 41, and 23 kyr periods; Clemens and Prell, 1990b). It is the dissimilarities between these records that contains the information possibly allowing differentiation of productivity associated with monsoon-induced upwelling from that associated with other mechanisms.

Our current hypothesis is that the variability associated with the 41 kyr power in the G. bulloides and opal accumulation records derive from nutrient availability in the intermediate waters which are upwelled via monsoon winds. This hypothesis is testable by comparison with Cd records of intermediate and deep waters of the Atlantic and Indian Ocean (e.g. Boyle, 1988).

The 35 and 54 kyr heterodyne periods in the grain-size record are positively correlated with large amplitude insolation events at 30°south in the Indian Ocean, the latitude of the subtropical high pressure cells from which the Indian Ocean monsoon winds initiate. The 29 kyr variability is linearly related to sea surface temperature records from the southern subtropical Indian Ocean. Both associations can be explained via the relationship between latent heat (a function of ocean-atmosphere temperature gradients) and monsoon strength as follows (Clemens and Prell, 1990b). Latent heat collected overt the southern subtropic Indian Ocean is transported across the equator and released in the mid-troposphere about the Tibetan Plateau. This increases the strength of the monsoon low, resulting in increased wind strength and transport of larger lithic particles to the Arabian Sea. This hypothesis is currently being tested by development of late Quaternary sea surface temperature records from ~ 30° south. Concentrations of variance at the 35, and 54 kyr periods in these records would support the latent heat link between the insolation record and the grain size record of monsoon strength.

Confirmation of the hypotheses described above will eventually enable us to quantitatively partition variance within these records into that attributed to monsoon-induced upwelling (regional) and oceanic mechanisms of nutrient distribution (global). Identification of a global signal in regional upwelling productivity would then provide a framework for comparison of productivity records from upwelling regions throughout the world ocean.

REFERENCES CITED

Boyle, E. A., 1988. Cadmium: Chemical tracer of deep water paleoceanography. *Paleoceanography*, 3:471-489.

Clemens, S. C. and W. L. Prell, 1990a. Late Pleistocene variability of Arabian Sea summer-monsoon winds: An eolian record from the lithogenic component of deep-sea sediments. *Paleoceanography,* 5:109-145.

Clemens, S. C., and Prell, W. L., 1990b. A Fourier model for paleomonsoon wind strength in the Arabian Sea: Northern Hemisphere response to Southern Hemisphere ocean-atmosphere interaction: *Trans. American Geophysical Union*, 71:1367.

Cullen, J. L., and W. L. Prell, 1980. Planktonic foraminifera of the northern Indian Ocean: Distribution and preservation in surface sediments, *Mar. Micropaleonto.*, 9:1-52, 1984.

Hutson, W. H., and W. L. Prell, A paleoecological transfer function, FI-2, for Indian Ocean planktonic foraminifera, *Paleontology*, 54:381-399.

Middleton, N. J., 1986. Dust Storms in the Middle East, *J. Arid Environ.*, 10:83-96.

Murray, D. W., and Prell, W. L., 1990. Biogenic sedimentation on the Owen Ridge, northwestern Arabian Sea during the past one million years: Evidence for changes in monsoon-induced upwelling:*Trans. American Geophysical Union*, 71:1397.

Overpeck, J. T., L. C. Peterson, N. Kipp, J. Imbrie, and D. Rind, 1989. Climate change in the circum-North Atlantic region during the last deglaciation, *Nature*, 338:553-557.

Prell, W. L., 1990. The amplitude and phase of monsoonal upwelling indices: A key to the identification of atmospheric and oceanic mechanisms in the paleoceanographic record: *Trans. American Geophysical Union*, 71:1367.

Prell, W. L., 1984. Monsoonal climate of the Arabian Sea during the late Quaternary: A response to changing solar radiation. *Milankovitch and Climate, Part 1* A. Berger, J. Imbrie, J. Hays, G. Kukla and B. Saltzman (Eds.), p. 349-366. Hingham (D. Reidel).

Prell, W. L., and H. F. Streeter, 1982. Temporal and spatial patterns of monsoonal upwelling along Arabia: A modern analogue for the interpretation of Quaternary SST anomalies, *J. of Mar. Res.*, 40:143-155.

Prell, W. L., and W. B. Curry, 1981. Faunal and isotopic indices of monsoonal upwelling: Western Arabian Sea, *Oceanol. Acta*, 4:91-98.

Sirocko, F. and M. Sarnthein, 1989. Wind-borne deposits in the northwestern Indian Ocean: a record of Holocene sediments versus modern satellite data. *Palaeoclimatology and Palaeometerology: Modern and Past Patterns of Global Atmospheric Transport,* M Leinen, and M. Sarnthein (Eds.) 282:401-433. Boston (Kluwer).

Tsoar, H., and K. Pye, 1987. Dust transport and the question of desert loess formation, *Sedimentology*, 34:139-153.

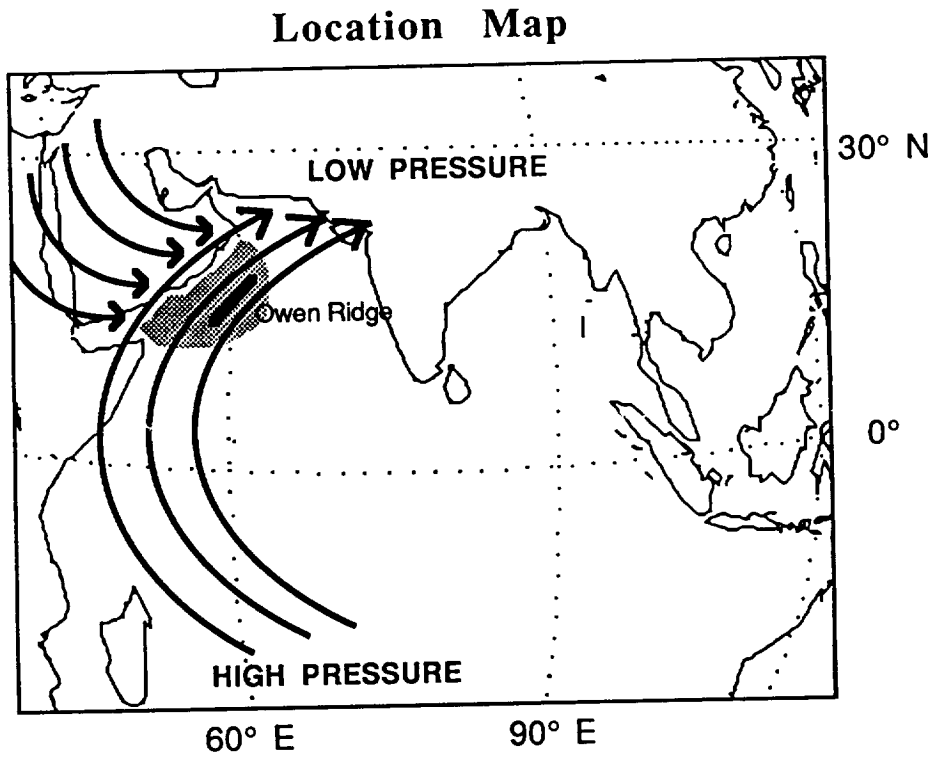

Figure 1. The lithogenic and biogenic components of Owen Ridge sediments record late Quaternary climatic changes associated with the Indian Ocean monsoon system. Strong southwest winds (arrows) flow from high pressure to low pressure inducing coastal and divergent upwelling (shaded) off the Arabian Peninsula. Upwelling productivity is recorded in the geological record of fossil planktonic foraminifera (carbonate) and radiolaria (opal) preserved in Owen Ridge sediments. Both southwest and northwest summer winds transport terrigenous dust to the Owen Ridge from deserts of Somali and Arabia. The grain size of the lithogenic component varies as a function of the strength of the transporting winds.

Time Domain

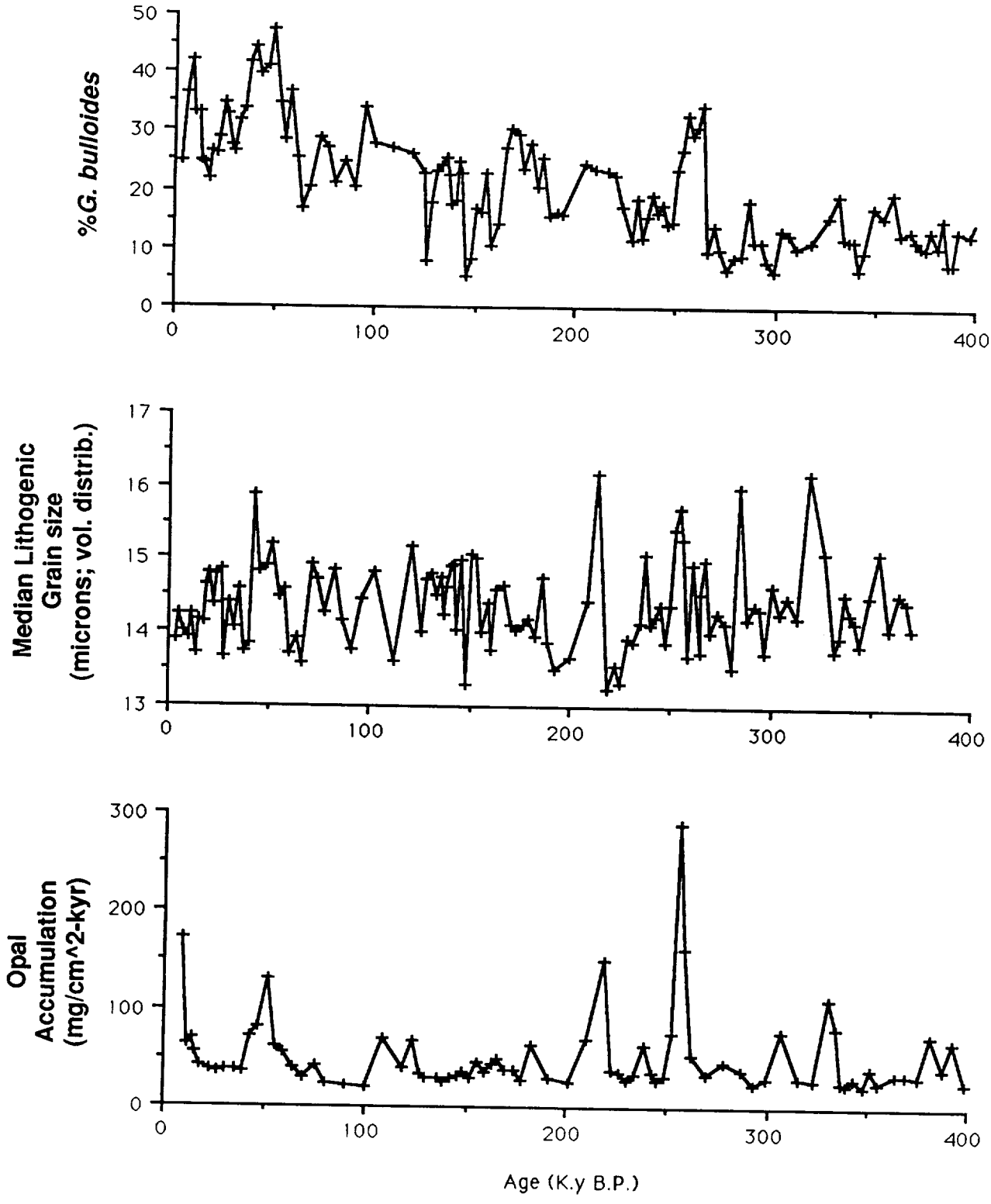

Figure 2. Lithogenic and biogenic indicators of monsoon wind strength and upwelling-induced productivity. Increased *% G. bulloides* and opal accumulation record changes in productivity associated with nutrient content of the intermediate waters upwelled during the summer monsoon. Increased grain size of the lithogenic component varies as a function of the strength of summer winds.

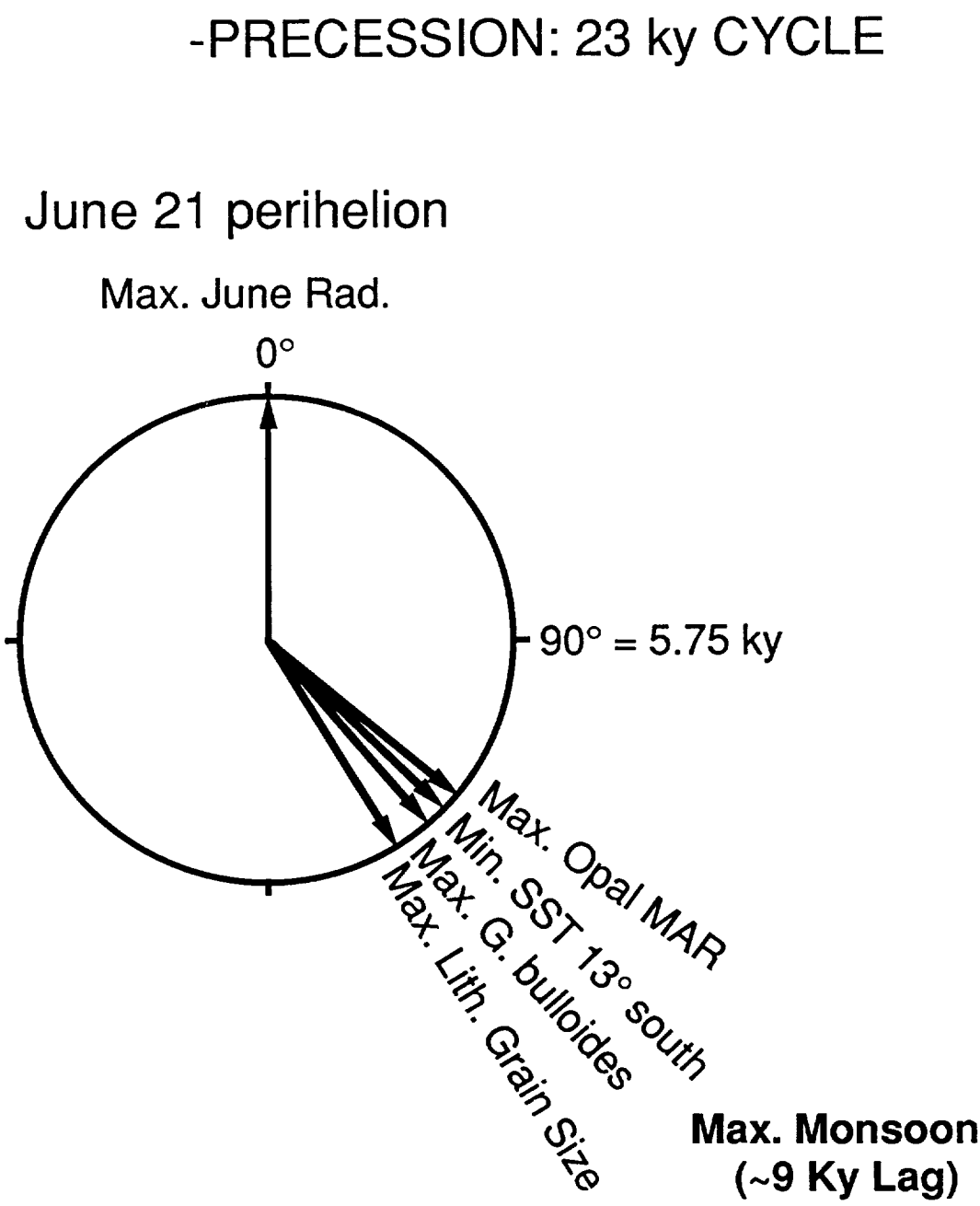

Figure 3. Precessional phase wheel summarizing the coherency and phase relationships between several monsoon indices and the Earth's orbital precession. All parameters shown are coherent (at or above the 80% confidence level) with insolation patterns driven by the precession of the Earth's orbit. The phasing indicates that all the monsoon records attain maxima ~9 kyrs after maxima in precessional insolation but simultaneously with minima in sea surface temperatures (SST) at 13° south in the Indian Ocean. This, similar to modern monsoon dynamics, indicates that latent heat availability in the southern subtropic Indian Ocean exerts a strong influence on the timing of strong monsoons and upwelling in the Arabian Sea over the past 400 kyrs.

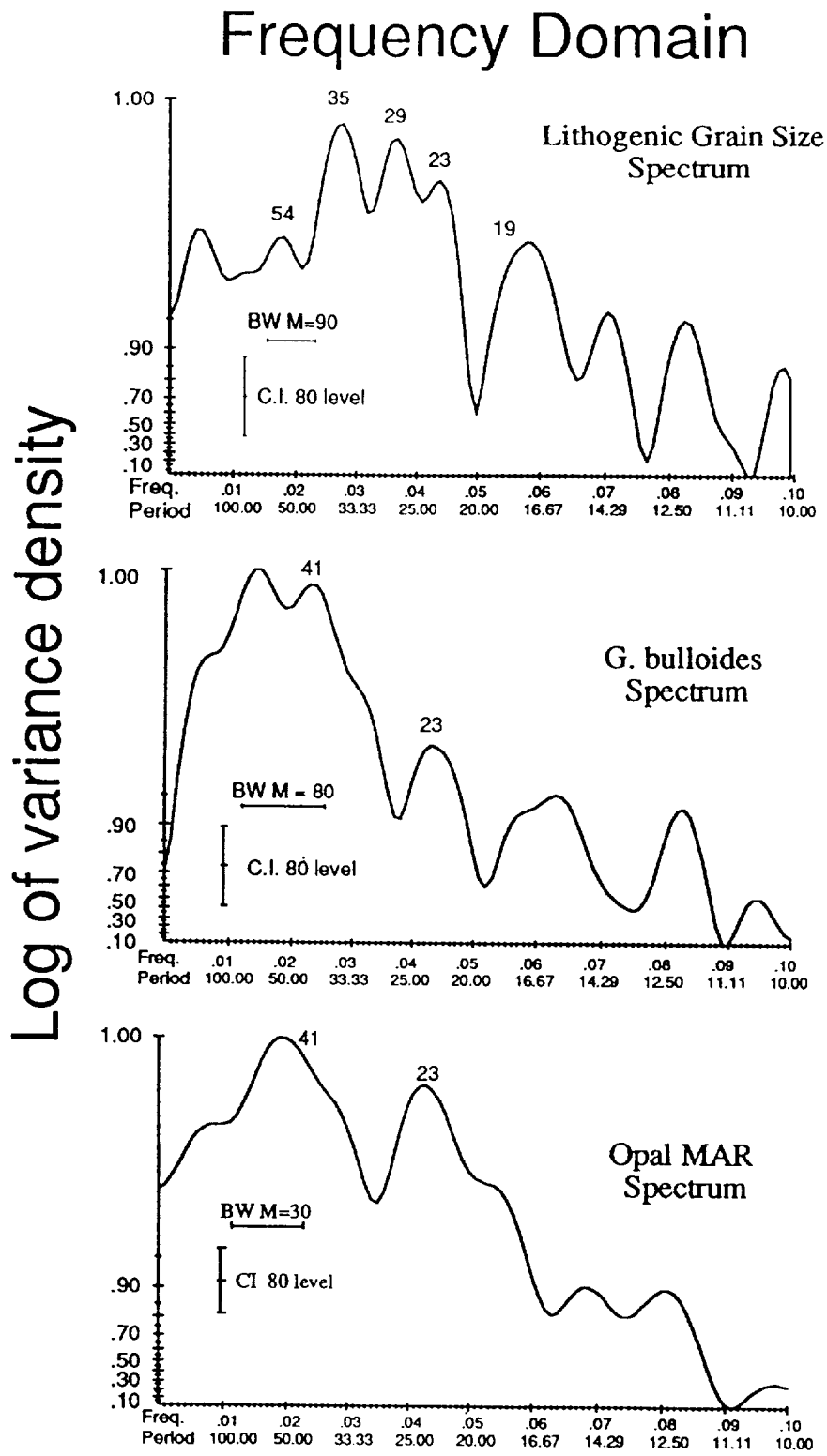

Figure 4. Spectra of the biogenic and abiogenic indicators of monsoon wind strength and the associated upwelling-induced productivity. The 41 kyr (orbital obliquity) variance in the *G. bulloides* and opal records is absent from the lithogenic (abiotic) record indicating that variance in this frequency band may not be driven by productivity due to monsoon-induced upwelling. This variance may be associated with more global oceanic mechanisms which enhance or reduce the nutrient content of the intermediate waters of the Indian Ocean. The 29, 35, and 54 kyr spectral peaks in the grain size record are linearly related to SST and insolation patterns in the southern subtropic Indian Ocean indicating a link between latent heat flux and monsoon strength as is observed in modern monsoon dynamics.

Annual, Orbital, and Enigmatic Variations in Tropical Oceanography Recorded by the Equatorial Atlantic Amplifier

Andrew McIntyre
Lamont-Doherty Geological Observatory
Palisades, NY 10964
and
Department of Geology
Queens College of CUNY
Flushing, NY 11357

Equatorial Atlantic surface waters respond directly to cahnges in zonal and meridional lower tropospheric winds forced by annual insolation. This mechanism has its maximum effect along the equatorial wave guide centered on $10°W$. The result is to amplify even subtle tropical climate changes such that they are recorded by marked amplitude changes in the proxy signals. Model realizations, NCAR AGCM and OGCM for 0 Ka and 126 Ka (January and July), and paleoceanographic proxy data show that these winds are also forced by insolation changes at the orbital periods of Precession and Obliquity.

Perhelion in boreal summer produces a strengthened monsoon, e.g. increased meridional and decrease zonal wind stress. This reduces oceanic Ekman divergence and thermocline/nutricline shallowing. The result, in the equatorial Atlantic, is reduced primary productivity and higher euphotic zone temperatures; vice versa for perihelion in boreal winter. Perihelion is controlled by precession. Thus, the dominant period in spectra from a stacked SST record (0-252 Ka BP) at the site of the equatorial Atlantic amplifier is 23 Ky (53% of the total variance). This precessional period is coherent (k=0.920) and in phase with boreal summer insolation.

Oscillations of shorter period are present in records from cores sited beneath the amplifier region. These occur between 12.5 and 74.5 Ka BP, when eccentricity modulation of precession is at a minimum. Within this time interval there are 21 cycles with mean periods of (3.0±0.5)Ky. Similar periods have been documented from high latitude regions, e.g. Greenland ice cores from Camp Century. The Camp Century signal in this same time interval contains 21 cycles. A subjective correlation was made between the Camp Century and the equatorial records; the signals were statistically similar, (r=0.722) and (k=0.960).

Modeling Orbital Changes on Tectonic Time Scales

Thomas J. Crowley
ARC Technologies
305 Arguello Drive
College Station, TX 77840

Geologic time series indicate significant 100 ka and 400 ka pre-Pleistocene climate fluctuations, prior to the time of such fluctuations in Pleistocene ice sheets. The origin of these fluctuations must therefore depend on phenomena other than the ice sheets. In a previous set of experiments (Short et al., Quat. Res. 35, 157-173, 1991) we tested the sensitivity of an energy balance model to orbital insolation forcing, specifically focusing on the filtering effect of the Earth's geography. We found that in equatorial areas, the twice-yearly passage of the sun across the equator interacts with the precession index to generate 100 ka and 400 ka power in our modeled time series. The effect is proportional to the magnitude of land in equatorial regions. We suggest that such changes may reflect monsoonal variations in the real climate system, and that subsequent wind and weathering changes may transfer some of this signal to the marine record. A comparison with observed fluctuations of Triassic lake levels is quite favorable.

A number of problems remain to be studied or clarified:

- the EBM experiments need to be followed up by a limited number of GCM experiments;
- the sensitivity to secular changes in orbital forcing needs to be examined;
- the possible modifying role of sedimentary processes on geologic time series warrants considerably more study;
- the effect of tectonic changes on Earth's rotation rate needs to be studied;
- astronomers need to make explicit which of their predictions are robust and geologists and astronomers have to agree on which of the predictions are most testable in the geologic record.

Plio–Pleistocene time evolution of the 100-ky cycle in marine paleoclimate records

Jeffrey Park and Kirk A. Maasch*
Department of Geology and Geophysics
Box 6666, Yale University
New Haven, CT 06511

To constrain theories for the dynamical evolution of global ice mass through the late Neogene, it is important to determine whether major changes in the record were gradual or rapid. Of particular interest is the evolution of the near 100-ky ice age cycle in the middle Pleistocene. We have applied a new technique based on multiple taper spectrum analysis which allows us to model the time evolution of quasi-periodic signals [Park and Maasch, 1992]. This technique uses both phase and amplitude information, and enables us to address the question of abrupt versus gradual onset of the 100-ky periodicity in the middle Pleistocene.

The variation of climate proxy variables at a given frequency f_o (with associated period $T_o = 1/f_o$) can be parameterized by $\Re\{A(t)e^{-2\pi i f_o t}\}$, a sinusoid with a slowly-varying amplitude $A(t)$. The function $A(t)$ is complex-valued, allowing slow variations in phase as well as magnitude. We define $A(t)$ as the 'envelope' of the signal at 'carrier frequency' f_o. If $A(t) = A_o$ is a constant, the signal is termed 'periodic' or 'a phase-coherent sinusoid.' If $A(t)$ varies, the signal is termed 'quasi-periodic.' All methods of determining the envelope of a quasi-periodic signal have shortcomings. Bandpass filters, such as those used by Ruddiman et al [1989], cannot model discontinuities in the envelope of a quasi-periodic signal, and thus, are of little help in discriminating between a sudden and a gradual onset for the 100-ky ice age cycle. Moreover, a narrow bandpass in the frequency domain requires a long time-domain filter, so that a significant number of data points at the ends of the series must be discarded. Similarly, the choice of length for the overlapping data segments in the Ruddiman et al [1986b] analysis involves a tradeoff between frequency and time resolution.

We apply instead a more flexible approach based on multiple-taper spectrum analysis [Thomson 1982; 1990; Park et al. 1987, Berger et al 1991]. The multitaper

*Current Address: Institute for Quaternary Studies, 320 Boardman Hall, University of Maine, Orono, ME 04468

approach allows the analyst to model the envelope function $A(t)$ using the tools of linear inverse theory, solving for the envelope function that fits the time series data while optimizing some property of the envelope. Inversion algorithms can be derived that find the 'smallest' and 'smoothest' envelopes that fit spectral 'data' from a given time series [Park 1990; Park 1992]. Special cases of these the algorithms can be derived to model sudden changes in the envelope. This allows us to examine the abruptness of the onset of the 100-ky periodicity as well as the evolution of the obliquity and precession signals. The estimation procedure relates spectral estimates at f_o, using a set of orthogonal Slepian data tapers, as linear functionals of an unknown envelope $A(t)$, so that the envelope is constructed from a linear combination of the Slepian tapers. Since the Slepian tapers are optimally bandlimited, multitaper envelope estimation can be thought of as an extremely sharp narrow-band filter valid for the entire duration of the series.

The shortcomings of the algorithm we use are similar to those of other linear inverse problems. For instance, the multitaper envelope estimation procedure can model envelope discontinuities, but the technique cannot by itself discriminate between continuous and discontinuous models for the 100-ky cycle, since envelopes of both types can be constructed that fit the spectral 'data' exactly. The analyst must use other, perhaps subjective, criteria for choosing among models that fit the data. This nonuniqueness is a common problem in linear inverse theory; in principle an infinite number of envelopes can fit a finite number of spectral data exactly. In most cases, the *a priori* constraint that the signal at a carrier frequency f_o have a 'slowly-varying' envelope, except at one or more specified time points, reduces greatly the number of acceptable models for the envelope, and motivates the solution of a 'smoothest' envelope that fits the spectral data.

We investigated the time-evolution of the 100-ky cycle in δ^{18}O data, thought to reflect global ice-volume variations. We analyzed δ^{18}O data from DSDP Site 607 and ODP Site 677, from which three long (> 2.6 My) time series have been published [Shackleton and Hall, 1989; Ruddiman et al 1986ab; 1989; Raymo et al 1989]. We find evidence for a coherent δ^{18}O signal for both cores in the eccentricity and obliquity frequency bands, consistent with variations in global ice volume as the causative factor. However, the nature of the earth system response to orbital insolation cycles depends on the time scale adopted in the spectral analysis. If the Ruddiman/Raymo time scale for DSDP Site 607 is accepted, the δ^{18}O obliquity cycle has enhanced amplitude between 1.0 and 1.5 Ma, relative to the late Pleistocene ($t < 1.0$ Ma), and a nonlinear response of the earth system to orbital obliquity is inferred (Figure 1). If the Shackleton et al [1990] time scale for ODP Site 677 is accepted, the amplitude match between the δ^{18}O obliquity cycle and the 65°N insolation derived by Berger

and Loutre [1991] from the recent astronomical solution of Laskar [1988; 1990] is very good for times $t \lesssim 2.3$ Ma (Figure 2). (The phase match for obliquity is enhanced by the fact that the data series were tuned to the astronomical time series, so that the observed phase agreement is not surprising.) The veracity of the ODP 677 time scale therefore correlates with a linear earth-system response to orbital obliquity.

Based on our analysis of data from these two deep-sea cores, we do not find compelling evidence for an abrupt change in the 100-ky $\delta^{18}O$ signal. Rather, envelope inversions in the eccentricity band suggest that the 100-ky $\delta^{18}O$ cycle is phase-locked with the 124-ky eccentricity cycle some 300-400 ky prior to its late-Pleistocene growth in amplitude and phase-lock with the 95-ky eccentricity cycle (Figure 3). An abrupt change in the 95-ky envelope near 0.85 Ma is consistent with DSDP 607 data on the Ruddiman/Raymo time scale, but such a transition would occur while leaving the 124-ky envelope largely unchanged. If the Shackleton et al [1990] time scale for ODP 677 is accepted, our three $\delta^{18}O$ records are consistent with a low-amplitude 100-ky cycle between 1.2 and 2.6 Ma, whose local period of oscillation alternates between the two major eccentricity periods at 95 and 124 ky. The phase of these 100-ky oscillations prior to 1.2 Ma is related to the phase of the astronomical eccentricity cycles where the cycles have significant amplitude. The match between the precessional envelopes of Sites 607 and 677 is poor, when both are expressed in terms of the Shackleton et al [1990] time scale. Climate simulation studies suggest that cyclic salinity changes in equatorial surface waters are a plausible contributor to the ODP 677 $\delta^{18}O$ data in the precessional band, and could explain this discrepancy. However, our time-rescaling of data from DSDP 607, using visual isotope-stage matching, may not be precise enough to transform the short-period precession cycles with sufficient accuracy.

Further study of more paleoclimate records will be necessary in order to address more fully the time-evolution of the 100 kyr cycle. For instance, the correlation of $\delta^{18}O$ signals from Sites 677 and 607 is intriguing, but comprehensive tests for the global coherence of $\delta^{18}O$ signals should use data from more than two sites. The phase information contained in the paleoclimate records may reaffirm the notion that external earth-orbital forcing could be the pacemaker of the ice age cycles. However, the mid-Pleistocene amplitude increase of the quasi-periodic 100-ky $\delta^{18}O$ signal awaits a complete explanation, which appears to depend on factors other than orbital insolation changes.

Future Tasks:

1) Collection of climate proxy data series, with good time control, from both deep-sea, lake-bed, and land-based sedimentary sequences. Much data probably lies dormant in the older cores stored by the Ocean Drilling Program, but only the older

cores often suffer from coring gaps that impede detailed time series analysis. Newer core data are spliced from parallel-paired drill cores at a single location.

2) careful cross-spectral analysis of different data series to investigate how the earth climate system, as a whole, responded to orbital insolation cycles over the past 2–3 My, the period of Earth history most relevant to current global change problems. The techniques developed for the above project can be extended to cross-series studies. The buzzword for this kind of study is 'global teleconnections,' the manner in which climate at different parts of the globe interacts. The response of climate to modest changes in its boundary conditions can (in principle) be tracked by its response over individual Milankovitch cycles.

3) similar analysis of data series from earlier periods of Earth history e.g. the Cretaceous and the Eocene. Data is accumulating for a significant response to orbital cycles, but a global synthesis has only been attempted so far with numerical climate models. The Earth's climate was warmer in these two periods, but our understanding of how the Earth sustained such temperature is, at best, incomplete. Many studies point towards higher carbon dioxide levels as a causative factor, and the ubiquitous Milankovich-driven limestone/black-shale sequences suggest big changes in ocean circulation. Are the Cretaceous and Eocene global climates a picture of what awaits us in a greenhouse future?

4) Despite a decade of global-warming predictions based on numerical climate models, it must be admitted that these models (global circulation, energy balance, etc) can represent the earth's climate dynamics only in a crude manner. The features of the climate system that are critical to its longer-term variation (decades and centuries) may not be apparent with the current generation of numerical climate models. Improving the global circulation models is a high priority. This includes atmospheric, ocean and coupled atmosphere-ocean models.

5) Collection of a long-term global climate database to 'validate' the output of global circulation models. Such data are essential to check if the numerical climate models are working. Comparisons of atmospheric GCM results with satellite data have begun, but I am not aware of a global data-validation of oceanic GCMs.

References

Berger, A., A simple algorithm to compute long-term variations of daily or monthly insolation, *Inst. Astron. Geophys. G. Lemaitre* Contrib. 18, 17 pp, 1978.

Berger, A., and M. F. Loutre, L., 1991. Insolation values for the climate of the last 10 million years, *Quaternary Science Reviews, 10*, 297–317.

Berger, A., J. L. Melice and L. Hinnov, 1991. A strategy for frequency spectra of Quaternary climate records, *Climate Dynamics, 5*, 227–240.

Laskar, J., 1988. Secular evolution of the solar system over 10 million years, *Astron. Astophys., 198*, 341–362.

Laskar, J., 1990. The chaotic motion of the solar system: A numerical estimate of the size of the chaotic zones, *Icarus, 88*, 266–291.

Park, J., C. R. Lindberg and F. L. Vernon III, 1987. Multiple-taper spectral analysis of high frequency seismograms, *J. Geophys. Res., 92*, 12675–12684.

Park, J, 1990. Observed envelopes of seismic free oscillations, *Geophys. Res. Letts., 17*, 1489–1492.

Park, J, 1992. Envelope estimation for quasi-periodic geophysical signals in noise: A multitaper approach, In: Walden A., Guttorp, P., (eds), *Statistics in the Environmental Earth Sciences*, in press.

Park, J., and K. A. Maasch, 1992. Plio–Pleistocene time evolution of the 100-ky cycle in marine paleoclimate records, submitted to *J. Geophys. Res.*.

Raymo, M. E., Ruddiman, W. F., Backman, J., Clement, B. M., and D. G. Martinson, 1989. Late Pliocene variation in northern hemisphere ice sheets and North Atlantic Deep Water circulation, *Paleoceanography, 4*, 413–446.

Ruddiman W. F., A. McIntyre, and M. Raymo, 1986a. Paleoenvironmental results from North Atlantic Sites 607 and 609, In: Ruddiman W. F., Kidd R. B., E. Thomas, et al. (eds), *Init. Repts. DSDP, 94*, U.S. Govt. Printing Office, Washington, pp. 855–878.

Ruddiman W. F., M. Raymo, and A. McIntyre, 1986b. Matuyama 41,000–year cycles: North Atlantic ocean and northern hemisphere ice sheets, *Earth Planet. Sci. Lett., 80*, 117–129.

Ruddiman, W. F., Raymo, M. E., Martinson, D. G., Clement, B. M., and J. Backman, 1989. Pleistocene evolution: Northern hemisphere ice sheets and the North Atlantic Ocean, *Paleoceanography, 4*, 353–412.

Shackleton, N. J., A. Berger, and W. R. Peltier, 1990. An alternative astronomical calibration of the lower Pleistocene timescale based on ODP Site 677, *Trans. Roy. Soc. Edinburgh, 81*, 251-261.

Shackleton, N. J., and M. A. Hall, 1989. Stable isotope history of the Pleistocene at ODP Site 677. In: Becker, K., Sakai, H. et al (eds) *Proc. ODP, Sci. Results, 111*, College Station, TX, 295–316.

Thomson, D. J., 1982. Spectrum estimation and harmonic analysis, *IEEE Proc., 70*, 1055–1096.

Thomson, D. J., 1990. Quadratic-inverse spectrum estimates; applications to paleoclimatology, *Philos. Trans. R. Soc. London, 332*, 539–597.

Figure Captions

Figure 1. Envelope inversions for the time-evolution of the 41-ky signal in the benthic $\delta^{18}O$ series from DSDP Site 607 and ODP Site 677, plotted against similar analyses for the astronomical insolation series derived from Berger [1978] ('65° old') and Berger and Loutre [1991] ('65°N new'). Seven 4π-prolate Slepian eigentapers are used to constrain the estimates, using 'smoothness' penalty function (10). The amplitude units in this and succeeding plots are parts-per-thousand $\delta^{18}O$. Note the phase correlation (with a constant shift) between the older astronomical series and data from DSDP Site 607, and the correlation between the newer astronomical series and data from ODP Site 677. This arises from the orbital tuning performed on the data series. Orbital tuning does not enforce correlations between envelope amplitudes, as is evident from the upper panel.

Figure 2. Similar to Figure 1, but with the envelope of the Berger [1978] series omitted and benthic $\delta^{18}O$ data from DSDP Site 607 expressed in terms of the Shackleton et al [1990] time scale. Seven 4π-prolate Slepian eigentapers are used to constrain the estimates, using a 'smoothness' penalty function. Note the phase correlation (with a constant shift) between the data series. Note the improved correlations between envelope amplitudes in the upper panel.

Figure 3. Test for the abrupt onset of the 100-ky signal. Double-line envelope inversion for the benthic $\delta^{18}O$ series from DSDP Site 607 on its published time scale, at the two major eccentricity quasi-periods of 95 and 124 ky. Seven 4π-prolate Slepian eigentapers are used to constrain the envelopes, which are constrained to be smooth everywhere except at t_o =0.85 Ma.

Figure 1

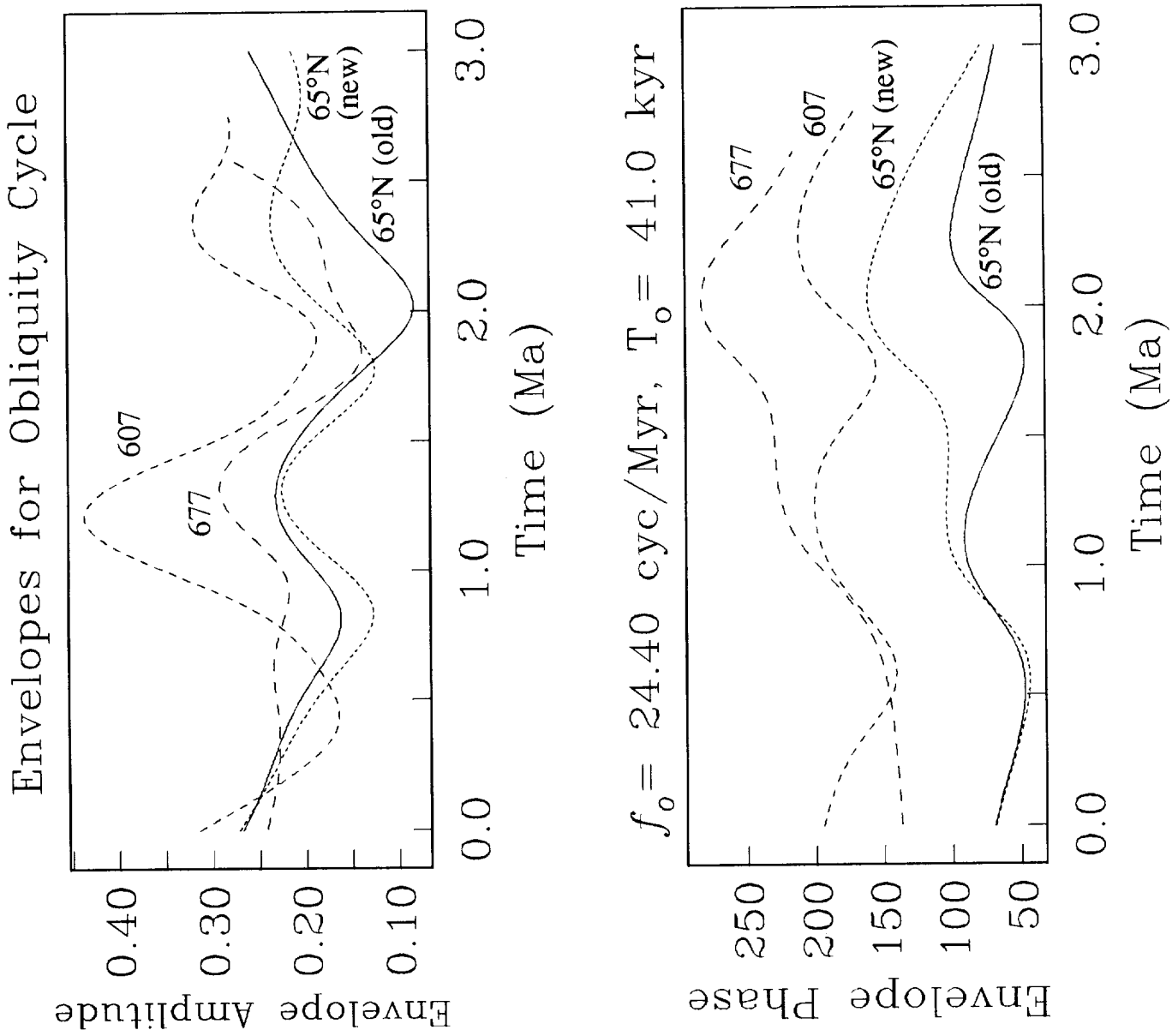
Envelopes for Obliquity Cycle
Envelope Amplitude
0.40
0.30
0.20
0.10
607
677
65°N (new)
65°N (old)
0.0
1.0
2.0
3.0
Time (Ma)
f_o = 24.40 cyc/Myr, T_o = 41.0 kyr
Envelope Phase
250
200
150
100
50
677
607
65°N (new)
65°N (old)
0.0
1.0
2.0
3.0
Time (Ma)

Figure 2

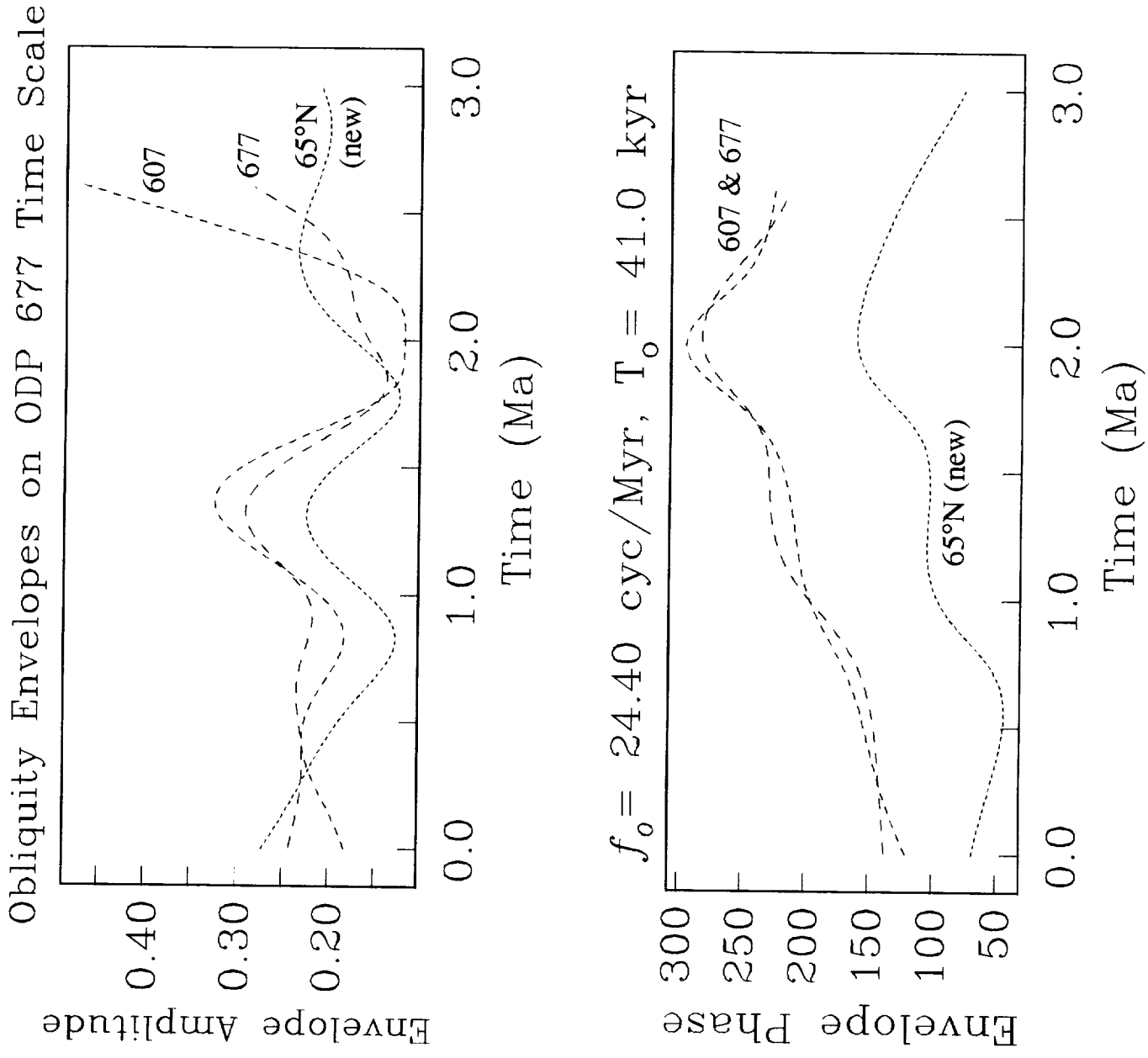
Obliquity Envelopes on ODP 677 Time Scale
Envelope Amplitude
0.40
0.30
0.20
607
677
65°N
(new)
0.0
1.0
2.0
3.0
Time (Ma)
f_o= 24.40 cyc/Myr, T_o= 41.0 kyr
Envelope Phase
300
250
200
150
100
50
607 & 677
65°N (new)
0.0
1.0
2.0
3.0
Time (Ma)

Figure 3

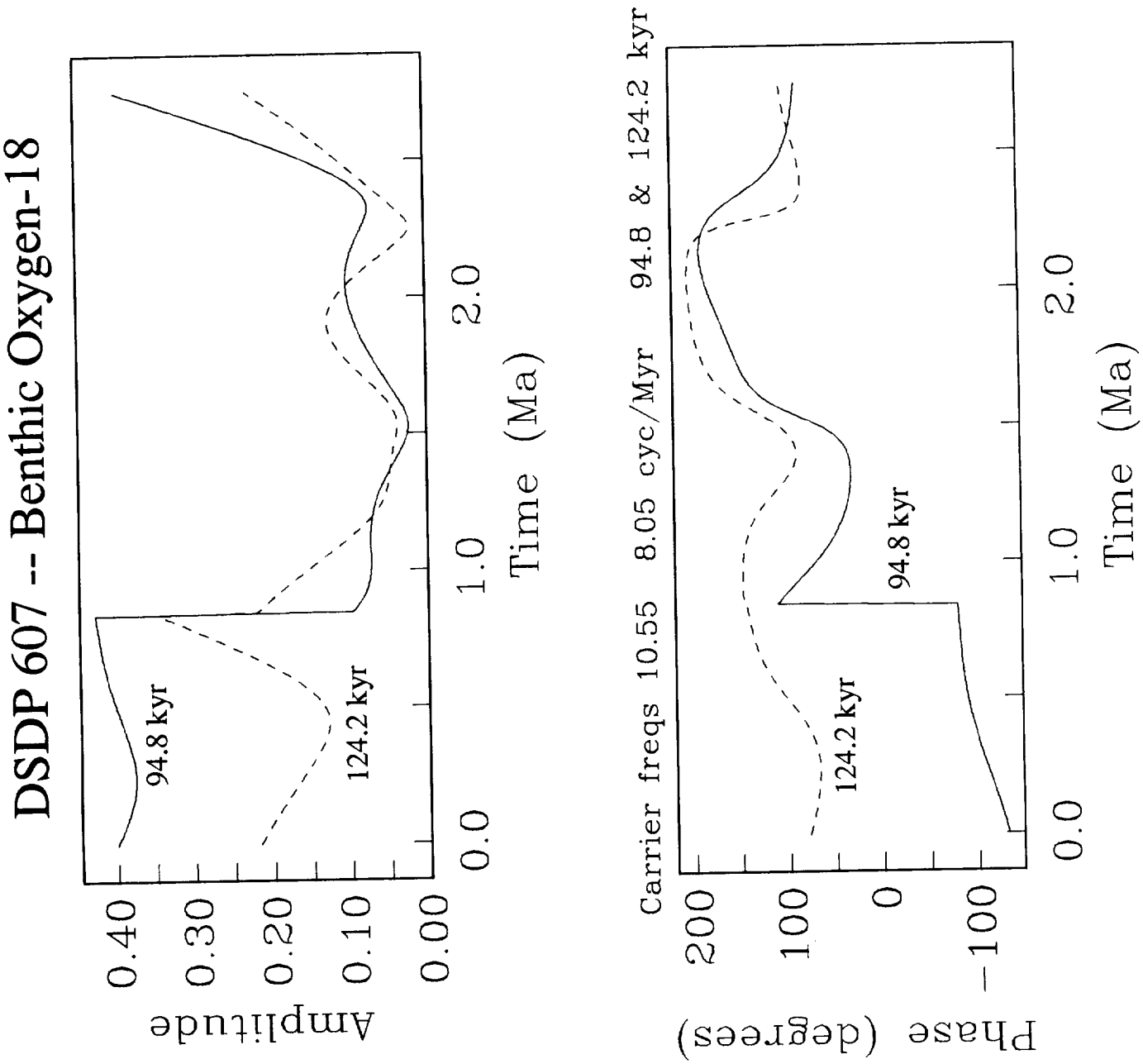
DSDP 607 -- Benthic Oxygen-18
Amplitude
0.40
0.30
0.20
0.10
0.00
94.8 kyr
124.2 kyr
0.0
1.0
2.0
Time (Ma)
Carrier freqs 10.55 8.05 cyc/Myr 94.8 & 124.2 kyr
Phase (degrees)
200
100
0
−100
94.8 kyr
124.2 kyr
0.0
1.0
2.0
Time (Ma)

A First-Order Global Model of Late Cenozoic Climatic Change: Orbital Forcing as a "Pacemaker" of the Ice Ages

Barry Saltzman
Department of Geology and Geophysics, Yale University
New Haven, CT 06511

The development of a theory of the evolution of the climate of the earth over millions of years can be subdivided into three fundamental, nested, problems:

(I) to establish by equilibrium climate models (e.g., general circulation models) the diagnostic relations, valid at any time, between the fast-response climate variables (i.e., the "weather statistics") and both the prescribed external radiative forcing and the prescribed distribution of the slow response variables (e.g., the ice sheets and shelves, the deep ocean state, and the atmospheric CO_2 concentration),

(II) to construct, by an essentially inductive process, a model of the time-dependent evolution of the slow-response climatic variables over time scales longer than the damping times of these variables but shorter than the time scale of tectonic changes in the boundary conditions (e.g, altered geography and elevation of the continents, slow outgassing and weathering) and ultra-slow astronomical changes such as in the solar radiative output, and

(III) to determine the nature of these ultra-slow processes and their effects on the evolution of the equilibrium state of the climatic system about which the above time-dependent variations occur.

In this discussion we touch upon all three problems in the context of the theory of the Quaternary climate, which will be incomplete unless it is embedded in a more general theory for the fuller Cenozoic that can accommodate the onset of the ice-age fluctuations. We construct

a simple mathematical model for the Late Cenozoic climatic changes based on the hypothesis that forced and free variations of the concentration of atmospheric greenhouse gases (notably CO_2), coupled with changes in the deep ocean state and ice mass, under the additional "pacemaking" influence of earth-orbital forcing, are primary determinants of the climatic state over this period. Our goal is to illustrate how a single model governing both very long term variations and higher frequency oscillatory variations in the Pleistocene can be formulated with relatively few adjustable parameters. Although the details of these models are speculative, and other factors neglected here are undoubtedly of importance, it is hoped that the "dynamical systems" formalism described can provide a basis for developing a comprehensive theory and systematically extending and improving it.

The equations for the variations of global ice mass (I), carbon dioxide (μ) and ocean temperature (Θ), as presented by Saltzman and Maasch (1991) for our model system are:

$$\frac{dI}{dt} = \alpha_1 - \alpha_2 \tanh(c\mu) - \alpha_3 I - \alpha_2 k_\theta \theta - \alpha_2 k_R [R(t) - R^*] + W_I \tag{4}$$

$$\frac{d\mu}{dt} = \beta_1 - \beta_2 \mu + \beta_3 \mu^2 - \beta_4 \mu^3 - \beta_5 \theta + F_\mu(t) + W_\mu \tag{5}$$

$$\frac{d\theta}{dt} = \gamma_1 - \gamma_2 I - \gamma_3 \theta + F_\theta(t) + W_\theta \tag{6}$$

where c, k_Θ, and k_R are constants determined from equilibrium climate model (e.g., GCM) experiments relating summer surface temperature at high latitudes to atmospheric CO_2 content, to deep ocean temperature, and to the departure of incoming solar radiation at high latitudes, R(t), from the present value R^*. α_3 and γ_3 are inverse time constants for the response of glacial

ice and deep ocean temperature assumed to be $(10ky)^{-1}$ and $(4\ ky)^{-1}$, respectively. α_1, β_1, and γ_1 are the rates at which global ice mass, CO_2, and mean ocean temperature would tend to increase, respectively, if there were no CO_2 in the atmosphere (μ = O), no ice on the planet (I = O), no random forcing (W = O), mean ocean temperature was at O°C, and R at its present value R^*; these coefficients determine the equilibrium values of I, μ, and Θ for any level of forcing F and are to be evaluated from the observed late Pleistocene state as an initial condition (in a hindcast sense). The remaining six coefficients α_2, β_2, β_3, β_4, β_5, and γ_2 are considered to be the adjustable parameters of our model that can be tuned to account for as much of the observed variability and covariability of I, μ, and Θ as possible.

In Fig 1 we depict in a highly simplified schematic form the interactions implied by our model between the three slow-response variables, I, μ, and Θ, and between these variables and both the fast response climatic variables, e.g., surface temperature τ, and external forcing due to both insolation changes and tectonic variations. A heavy dashed arrow denotes an essentially simultaneous, quasi-static (or equilibrated) response of the sign indicated, while a heavy solid arrow denotes an inertial time lag in the response. Because cryospheric bedrock depression, D, forms the basis of many other models we also include possible interactions of ice load with this variable in this diagram. The influence of the slow-response variables on the sign and magnitude of fast response climate can be estimated by GCM sensitivity studies and many useful results have been obtained; the sign shown on the heavy dashed arrows refers to the influence of the slow variables on one particular fast variable, surface temperature τ. Although it is difficult to calculate the relevant fluxes that determine the slow-response changes, we indicate by the signs on the heavy arrows our assumption regarding the signs of the first order effects.

In the lower part of the figure we depict by the thinner lines the Berner-Lasaga-Garrels (1983)-type model for the equilibrated response of atmospheric CO_2 to fundamental tectonic and weathering processes.

By assuming plausible time constants for the glacial ice mass and global mean ocean temperature, and setting the values of six adjustable parameters (rate constants), a solution for the last 5 My is obtained displaying many of the features observed over this time period including the transition to the near-100 ky major ice age oscillations of the late Pleistocene (see Fig 2). In obtaining this solution it is also assumed that variations in tectonic forcing lead to a reduction of the equilibrium CO_2 concentration (perhaps due to increased weathering of rapidly uplifted mountain ranges over this period). As a consequence of this CO_2 reduction the model dynamical system can become unstable, bifurcating to a free oscillatory ice-age regime that is under the "pacemaker" influence of earth-orbital (Milankovitch) forcing.

We view this model as an illustration of the potential of a "dynamical systems" approach to the formulation of a theory of long term climatic change occurring under the constraints of prescribed radiative and tectonic forcing.

References

Saltzman, B. 1990: Three basic problems of paleoclimatic modeling: a personal perspective and review. Climate Dynamics, 5, 67-78.

Saltzman, B. and K. A. Maasch, 1991: A first-order global model of late Cenozoic climatic change II. A simplification of CO_2 dynamics. Climate Dynamics, 5, 201-210.

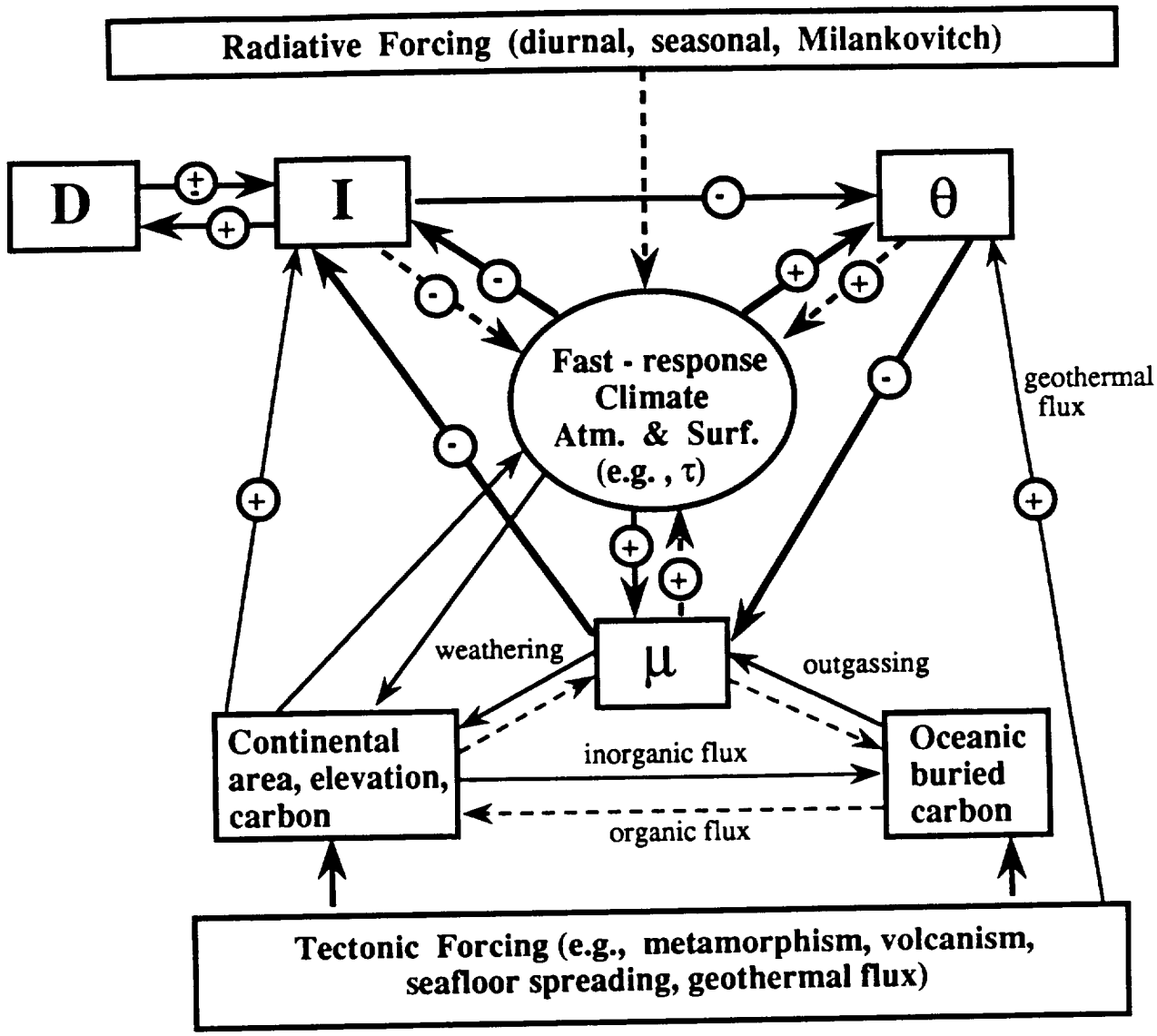

Fig. 1 Schematic diagram showing the interactions implied by the model between the three slow-response variables I, μ, and Θ, the fast-response "climate" variables, such as τ (inner circle), and external forcing due to insolation changes (upper box) and tectonic variations (lower box). The effects of bedrock depression, not included in this model, are represented by D.

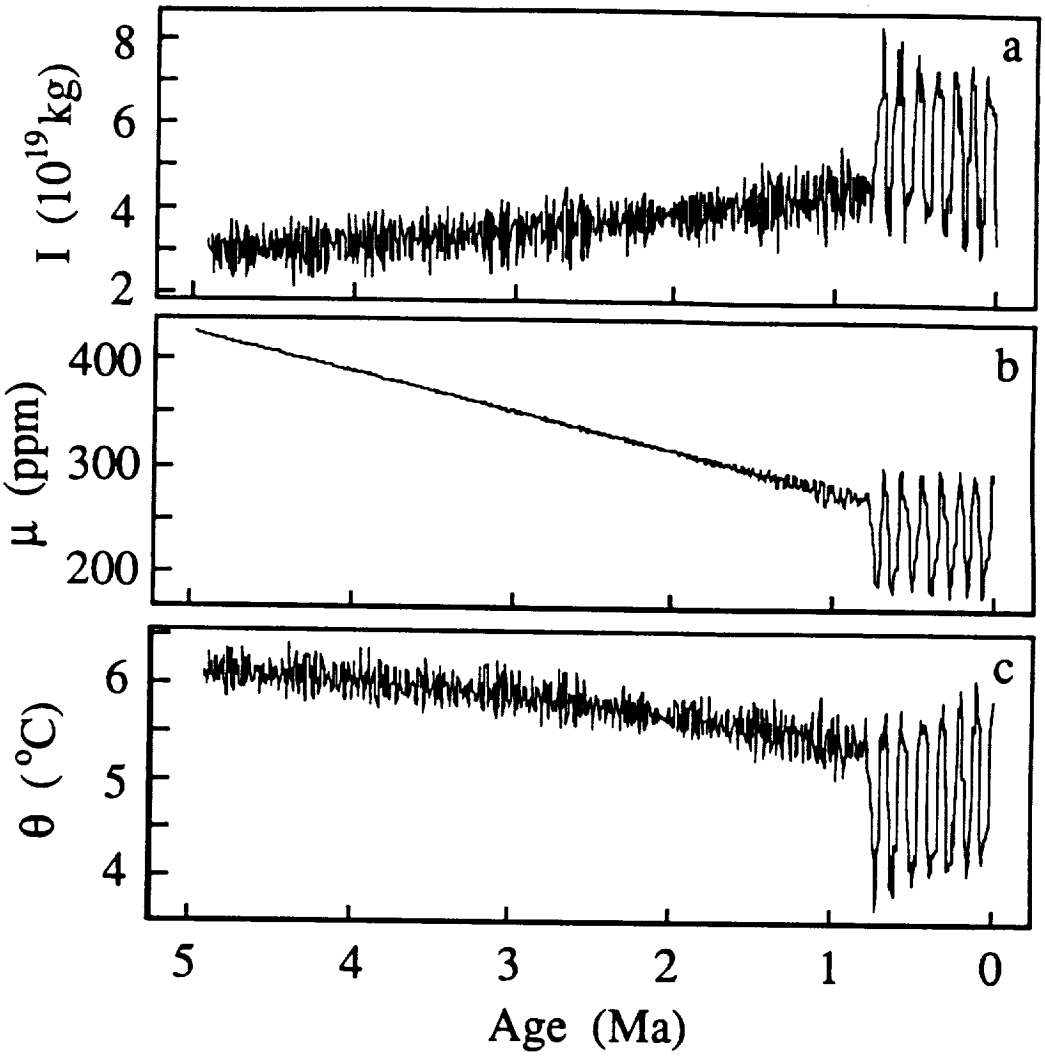

Fig. 2 Orbitally forced solution ($R(t) \neq 0$) for the past 5 My, for ice mass (I), atmospheric carbon dioxide (μ), and ocean temperature (Θ), all in dimensional units.

The Orbital Record in Stratigraphy

Alfred G. Fischer
Department of Geological Sciences
University of Southern California
Los Angeles, CA 90089-0740

Abstract

Orbital signals are being discovered in pre-Pleistocene sediments. Due to their hierarchical nature these cycle patterns are complex, and the imprecision of geochronology generally makes the assignment of stratigraphic cycles to specific orbital cycles uncertain, but in sequences such as the limnic Newark Group under study by Olsen and pelagic Cretaceous sequence worked on by our Italo-American group the relative frequencies yield a definitive match to the Milankovitch hierarchy.Due to the multiple ways in which climate impinges on depositional systems, the orbital signals are recorded in a multiplicity of parameters, and affect different sedimentary facies in different ways. In platform carbonates, for example, the chief effect is via sea-level variations (possibly tied to fluctuating ice volume), resulting in cycles of emergence and submergence. In limnic systems it finds its most dramatic expression in alternations of lake and playa conditions. Biogenic pelagic oozes such as chalks and the limestones derived from them display variations in the carbonate supplied by planktonic organisms such as coccolithophores and foraminifera, and also record variations in the aeration of bottom waters.Whereas early studies of stratigraphic cyclicity relied mainly on bedding variations visible in the field, present studies are supplementing these with instrumental scans of geochemical, paleontological and geophysical parameters which yield quantitative curves amenable to time- series analysis; such analysis is, however, limited by problems of distorted time-scales. My own work has been largely concentrated on pelagic systems. In these, the sensitivity of pelagic organisms to climatic-oceanic changes, combined with the sensitivity of bottom life to changes in oxygen availability (commonly much more restricted in the Past than now) has left cyclic patterns related to orbital forcing. These systems are further attractive because (1) they tend to offer depositional continuity, and (2) presence of abundant microfossils yields close ties to geochronology. A tantalizing possibility that stratigraphy may yield a record of orbital signals unrelated to climate has turned up in magnetic studies of our Cretaceous core. Magnetic secular

variations here carry a strong 39 ka periodicity, corresponding to the theoretical obliquity period of that time - Does the obliquity cycle perhaps have some direct influence on the magnetic field?

I consider the following lines of research to be particularly important:

- (1) Studies of stratigraphic sequences in which Milankovitch cyclicity is particularly apparent, and in which the record appears to be unbroken and extends for time spans in the 10^6 - 10^7 Ma range. This includes such sequences as the Newark Series (Olsen), the pelagic Cretaceous of Italy which we have been studying, and the Eocene of Angola (Fig. 5).
- (2) Extending such studies to the tracking of magnetic secular variation, which may turn out to provide a record of orbital variations independent of climate.
- (3) Exploring the geographic dimension, by global mapping of the distribution of cycle styles for given time-slices. How do cycle patterns change with latitude, from hemisphere to hemisphere, from ocean to ocean? Only such studies will bring cyclostratigraphic studies to bear on the problems of climatic change. ALBICORE is a start in that direction.
- (4) Extending cyclostratigraphic research into the Paleozoic. Milankovitch patterns, in particular the 1;5;20 ratio of precession to the eccentricity cycles, have now been established back to the Triassic Period, but Paleozoic stratigraphic patterns do not seem to fit this scheme. Were the orbital periods, or the Earth's response to them, different in Paleozoic times?

1 Orbital Variations

Quasi-rhythmical orbital variations have affected the Earth since its inception. The current patterns of such rhythms with periods of up to 400,000 years, are well defined from astronomical observations. Not so clear is how the major orbital parameters and their minor variations have changed through time. The length of the day, for example, is lengthening with transfer of angular momentum to the moon, and the current rate of change has been well established, but it seems highly unlikely that the change has been linear, and the existing data on this from historical geology are unsatisfactory. Other orbital variations such as the obliquity cycle and the precession are linked to the rotation rate, so that they too have changed with time, in ways that remain undefined.Astronomers are interested in the patterns of change for obvious reasons, but so are geologists and climatologists. If the orbital variations of the past have left a record in the rocks - specifically, in the sequentially accumulated layers of sedimentary and volcanic rocks that form an incomplete envelope of the crust - they may provide a geochronology (Gilbert, 1895) and a means for refining the crude time scale provided by radiochemistry. But furthermore, the orbital variations influence

the latitudinal and seasonal distribution of insolation, and thereby atmospheric climate and oceanic dynamics, and thus come to be agents in "Global Change." While the major Icehouse and Greenhouse modes of the outer Earth have probably been driven by internal cycles (mantle convection - Wilson cycle of plate tectonics: Fischer, 1984). The orbital variations have modulated oceanic an climatic behavior within these major modes. Such modulations may be thought of as experiments, and if they can be reconstructed from the historical record they will bring light to the range of climatic-oceanic behavior that lies beyond the realm of human experience.

2 The Quaternary Record

The case for such orbital forcing has now been compellingly made for the Pleistocene. It was first suggested nearly 150 years ago by Adhemar, and the theory was further developed and improved by Croll (for a summary, see Imbrie & Imbrie, 1979), but its quantitative footing - that the orbital variations vary insolation substantially - was the life-work of M. Milankovitch (1941), subsequently improved by Berger (1980, 1988) and others. The tie of the glacial record to orbital variations did not become definitive until Imbrie and others discovered that the isotopic record in the foraminifera of Pleistocene stratigraphic sequences retrieved from the ocean floor provided a proxy of ice volume, and found that the fluctuations in ice volume not only showed the same hierarchical frequencies of the orbital variations, but also historical coherence between these different phenomena (Imbrie, 1982).

3 Pre-Quaternary Record of Orbital Variations

But many climatologists and geologists remained dubious about the existence of an orbital record during non-glacial times. Duff, Hallam and Walton (1967) suggested that whereas the relatively small changes in insolation values during glacial times became greatly amplified by the positive feedback of a greatly increased Earth albedo due to the spread of glaciers and pack ice, the absence of such feed-back during non-glacial times made a record of orbital variations unlikely. Stratigraphers working in the gap- riddled record of the epicontinental regions saw little hope of recovering a record of persistent rhythmicity.Yet, some stratigraphers found rhythmic patterns in the stratigraphic record that seemed best explained as products of orbital forcing. Thus G.K. Gilbert (1895) interpreted the rhythmic spacing of limestones in the Late Cretaceous of Colorado as the expression of the precessional cycle, W. Bradley (1929) viewed the rhythmical alternations of oil shales and dolomite beds in the lacustrine Green River Formation (Eocene) of the Rocky Mountain region in the same manner, and W. Schwarzacher (1947) viewed the alternations of massive and laminated

carbonates in the Late Triassic Dachstein platform of the Alps as precessional, and their grouping into bundles of 5 as an expression of the 100 ka eccentricity cycle. As geological attention has shifted from purely local or regional concerns to global patterns, the number of these stratigraphers has grown (e.g., ROCC group, 1986; Fischer, 1986; Fischer et al., 1990; Fischer, 1991; Fischer and Bottjer, 1991).

4 Oscillations Recorded in Older Stratigraphy

The pragmatic facts are that the stratigraphic record is replete with repetitive features - some visible to the eye, (Fig. 5), others (such as the Pleistocene isotope curve) only retrievable by instrumental studies. Some reflect only the stochastically recurring alternations between the several modes of a depositional system, such as the alternation of channel and overbank deposits in alluvial systems, and were designated as "autocyclic." But others seem to have been "allocyclic," driven by forces outside the regional setting, and candidates for the rhythmic climatic- oceanographic changes to be expected from global forcing. These oscillations are of many sorts, of which the following have been recognized to date:

- 1. Cryogenic cycles. Changes in global ice volume, reflected in
  - (a) variations in the isotopic composition of sea water. Best recorded in foraminiferal tests of pelagic sediments retrieved from the deep-sea floor (isotopic cycles) (Imbrie, 1982)
  - (b) oscillations in sea level, on the scale of 10^{-1}- 10^{2} m, best recorded in subtidal-intertidal alternations and emergence cycles of carbonate platforms (emergence cycles), (e.g. Schwarzacher 1947, Fischer 1964, Goldhammer et al. 1987, Hinnov and Goldhammer 1991), (Fig. 1).
- 2. Carbonate production cycles. Oscillations in productivity of pelagic carbonate producing organisms (mainly coccolithophorids) are best recorded in pelagic chalk and marl sequences (Herbert and Fischer, 1987; Herbert and d'Hondt, 1990; Fischer et al. 1991) (Figs. 2, 5).
- 3. Dilution cycles. Oscillations in the flux of detrital mud are best recorded in hemipelagic sediments of continental margins (Roof et al., 1991).
- 4. Dissolution cycles. Oscillations in the depth and intensity of the lysocline - the level at which oceanic carbonate accumulation gives way to carbonate dissolution, best recorded in relatively deep (2-5 km) pelagic sequences.
- 5. Desiccation cycles. Oscillations in the regional precipitation-evaporation ratio are best recorded in

- (a) marginal marine evaporite sequences, where annual varving permits an approach to net evaporation as recorded in annual sulfate precipitation (Anderson, 1982, 1984).
- (b) alternations of lake and playa conditions in lacustrine systems (Fig. 1) (Olsen 1987, Fischer and Roberts 1991).

- 6. Redox cycles. Oscillations in the aeration of bottom waters best recorded in pelagic systems by
  - (a) retention of organic carbon (Figs. 2, 5), and
  - (b) shifts in the spectrum of bottom-dwelling animals, best reflected in their burrowing patterns (ichnofabric) (Fischer et al., 1991).

- 7. Magnetic cycles. Oscillations in magnetic parameters may be significant in sediments which acquired a remnant magnetism during or soon after deposition, and in which this signature has not been irretrievably lost by subsequent/magnetic overprints. The remnant magnetism thus developed depends (a) on the presence and character of suitable magnetic carrier phases (such as the mineral magnetite), and (b) on the strength and direction of the then-prevailing magnetic field.

Inasmuch as the carrier phase is linked to lithology, which responds to climate and oceanic change, oscillations in the carrier phase may be expected to reflect orbital (as well as other) sorts of lithic forcing. Hence it is not surprising that the detailed magnetic investigations of the Piobbico core (Napoleone et al., 1991, 1992) find the 100 ka eccentricity cycle, dominant in Fourier spectra of lithic variation, to be present in the magnetic intensity spectrum as well (Fig. 4). It is not so easy to explain why it should also appear in the inclination and declination spectra. It is even more difficult to understand why a 39 ka periodicity - that of the obliquity cycle - should dominate the magnetic intensity spectra and should also appear in the inclination and declination spectra, when it appears as only a very weak component of the various spectra related to lithology. There would thus appear to be a possibility that the magnetic field is affected by orbital variations - a suggestion that has been made previously, but has never been taken very seriously by the paleomagnetic community. If it were to be true, then paleomagnetic studies might provide a record of orbital cycles that is independent of transmission through climatic and oceanic dynamics - a possibility worth pursuing.

Paleontological criteria play a large role in the recognition of these cycles (1a, 1b, 2, 4, 6) - which should not be surprising, considering the great sensitivity of organic communities to climatic and oceanographic change.

5 Theoretical Considerations

Complications arise from the following factors:

- 1. The cycles may be overprinted and swamped out by grosser lithic changes in response to tectonic-geomorphic events. This is particularly the case in marine settings near major sources of detrital sediments, and is minimized in carbonate platforms and pelagic settings.

- 2. Cycles may be only partially preserved or totally lost owing to interruptions in deposition and continual reshuffling of sediments such as occurs in the "tempestite regime." This implies that many stratigraphic facies are never likely to lend themselves to the establishment of a "cyclostratigraphy."

- 3. Cycles of the higher frequencies may be largely or entirely destroyed by the burrowing activities of organisms (bioturbation). This is likely to be the case in slowly deposited facies, such as the "red clay" of the very deep ocean floor, accumulated at mean rates of $1mm/10^3 = 1m/10^6$years.

- 4. Cycle patterns are hierarchical and therefore complex (Figs. 2, 4, 5). The earliest workers sought to identify stratigraphic cycles with only one forcing period, such as that of the precession. Subsequent studies such as those by Schwarzacher (1947), Van Houten (1964), Herbert and Fischer (1987) found hierarchical patterns. The hierarchy most commonly encountered is the grouping of ca 5 bedding couplets into sets (bundles, Figs. 2, 5), which may in turn be grouped into superbundles of 4 (Fig. 2). On the other hand, the patterns can become complicated when members of the hierarchy shift phase relative to the others, and vary in strength of expression.

- 5. The different orbital forcing functions affect climate and oceanic behavior in quite different ways, and impinge upon a specific depositional setting via different pathways. The northern and southern hemispheres, for example, respond to the obliquity cycle in phase, but to the precessional cycle 180° out of phase. When this complication is combined with the observation that the climatic-oceanographic forcing of any given depositional setting contains both globally averaged effects such as sea level and locally imposed effects such as variations in the amount and timing of insolation, the likelihood of a wide range of possible combinations and variations emerges. When these effects take different pathways that impose different lag times (such as global oceanic turnover), further complications may result. On the one hand this may be daunting for a first recognition of cycle patterns, but on the other such complexities, once resolved, provide a wealth of additional information.

6 Identification of Specific Cycles

Vital to development of a cyclostratigraphy is the identification of oscillations observed in the stratigraphic record with specific cyclic forcing functions. This revolves largely around timing the cycle period. The following approaches have been used.

6.1 Varving.

The varve method, employed by Bradley (1929), Fischer and Roberts (1991), Ripepe, Roberts and Fischer (1991), and Anderson (1982, 1984). Some sedimentary sequences - in particular those of deep-water evaporites and those of meromictic lakes - retain a fine lamination which can with reasonable probability be assigned to the annual cycle, (varving). Continuous varving permitted Anderson to plot variations in sulfate precipitation for a 200,000 year record, which provided a remarkable record of the precession in late Permian time. Episodic varving in lake sediments, extrapolated to the non-varved intervals, permitted Bradley to recognize the precession in lacustrine Eocene sediments of the Rocky Mountain region (see also Fischer and Roberts, 1991; Ripepe, Roberts and Fischer, 1991). Varved sediments are, however, rare, and generally do not form time-series long enough to be useful in timing cycles in the Milankovitch frequency band.

6.2 Radiometry

Radiometric approaches are fairly accurate in the radiocarbon range (the last 30 ka, possibly extendable to 100 ka), and are applicable to many sediments, but for the vast bulk of geological time (Harland et al., 1990) radiometry depends on the dating of specific geological events, such as the emplacement of an ash layer or an intrusion, which are then extrapolated to the stratigraphy at large. Stratigraphical stage-boundaries dated in this manner generally have confidence limits of one or two million years for the last 100 Ma or so, but beyond this the uncertainties increase toward the 10 Ma level, and, in Cambrian time, beyond that. The durations of Mesozoic stages, averaging 3-10 Ma long, have errors in the range of 1-5 Ma. Rhythmic time series studied to date generally occupy fractions of such a stage, and extrapolating the assumed stage duration down to the level of the time-series in question involves further errors depending on accuracy of stratigraphic correlations and uniformity of sedimentation rate. As a result, such calculations are approximations with confidence limits in the range of a factor of 1.5 to 2. This generally serves to ascertain whether a given rhythm falls within the confines of the Milankovitch frequency band, but generally does not identify it definitively with one of the specific orbital variations.

6.3 Magnetic reversal stratigraphy

Magnetic reversals since the Late Jurassic have now been identified on the sea-floor, and can be recognized in many stratigraphic sequences. Through biostratigraphy these reversals have been tied to the radiometric scale. The width of the corresponding magnetic anomalies on the deep- sea floor provides a means of refining the radiometric time- scale, assuming relatively constant sea-floor spreading rates. At times of frequent reversals, the polarity zones are only a few million years long, commonly shorter than stages, and may thus afford a better basis for estimating the periods of cycles. Whereas much of our work has been in the "Cretaceous long normal" polarity chron which lacks the requisite reversals, work in the Tertiary (Schwarzacher, 1987; Herbert and d'Hondt, 1990) have used reversal stratigraphy to good effect in dating cycles.

6.4 Ratios

As pointed out above, stratigraphic cycles commonly occur in hierarchies. A grouping of ca 5 bedding couplets into bundles, in Triassic platform emergence cycles has now been well documented (Schwarzacher, 1947; Goldhammer et al., 1987; Hinnov and Goldhammer, 1991). It has been found in Triassic-Jurassic lacustrine sequences (Van Houten, 1964; Olsen, 1986), and occurs in Eocene (Fig. 5) and Cretaceous (Fig. 1, 2) pelagic sequences (Fischer et al., 1990). Furthermore, the Triassic-Jurassic lacustrine beds and the Cretaceous pelagic sequence of the Scisti a Fucoidi show a grouping of the 100 ka bundles into 400 ka superbundles.The geochronology based on radiometric data shows that these examples all lie within the Milankovitch frequency band, and thus the case of identifying bedding couplets with the ca, 20 ka precession, the bundles with the ca 100 ka eccentricity cycle, and the superbundles with the ca 400 ka eccentricity cycle becomes compelling.The ratios between cycle levels in the hierarchy thus emerge as an important clue to cycle identity. It is noteworthy, however, that to date no such good ratios have been found in the Paleozoic. Such studies are as yet in their infancy, but the 5;1 ratios, commonly visually striking in the Cenozoic and Mesozoic, have not emerged (cf. Boardman and Heckel, 1989; Goldhammer et al., 1991).

7 Present Status of Global Cyclostratigraphy

At this stage, the case for a pre-Quaternary record of orbital variations has been made in principle. The main stratigraphic facies showing heirarchical periodicities of the orbital variations are:

- (1) Deep-water evaporites (Permian, Anderson 1982, 1984). Their varving, offers the best age control. They suffer from (a) being too short to

apprehend the longer cycles, (b) from difficulties in tying them chronologically to other facies, and (c) in being scarce. Nevertheless, work on these sequences should be pursued. In particular, it now becomes essential to restudy the Castile sequence by means of instrumental scans. Studies should also be carried on to other sequences of this type, such as the varved anhydrites of the Zechstein Formation of Germany.

- (2) Lacustrine facies: Primarily the Triassic-Jurassic Newark Group sequences studied by Van Houten (1964) and Olsen (1986). Lakes as closed systems provide continuity of deposits and a record responding mainly and sensitively to local/regional climatic change (wet vs. dry). The disadvantages of lacustrine studies lie mainly in poor ties to the marine record and global geochronology. The most significant work being carried on at this time is that of Paul Olsen (Lamont). Other large and persistent lake systems of this sort include an unstudied Devonian complex in Nova Scotia, which would perhaps provide entry to the presently enigmatic Middle and Lower Paleozoic.

- (3) Biogenic pelagic facies such as those explored in the Piobbico Core (Fischer et al., 1991) in deep-sea cores (Herbert and co-workers). The not-so-deep pelagic sediments appear to have recorded (a) changes in the aeration state of the bottom waters, and (b) carbonate productivity in the surface waters. These parameters presumably reflect changes in circulation and in the general productivity patterns of the oceans, and a combination of local and global effects. Deep pelagic facies are complicated by the superposition of dissolution events, and by the effects of bioturbation on slowly accumulated muds.

- (4) Carbonate platform facies such as those studied by Schwarzacher (1947), Fischer (1964), Goldhammer et al., (1987), and Hinnov and Goldhammer (1991). Such facies monitor small-scale sea-level fluctuations - a globally integrated signal in contrast to lacustrine cycles. Whereas Milankovitch cyclicity has been well substantiated, uncertainties about the origin of sea-level oscillations pose a problem (I lean toward small-scale glacial effects). Also, like the evaporite and lacustrine records the platform rocks generally lack the means of close correlation into the global stratigraphy, based mainly on pelagic fossils.

8 My Own Researches

8.1 Piobbico Core

I have been working primarily with orbital cyclicity in the pelagic facies - and in recent years mainly with the Piobbico core, cut by an Italo-American consortium

(Premoli Silva-Fischer-Napoleone) in the mid-Cretaceous Scisti a Fucoidi of the central Apennines. We have used this core as a means of exploring various techniques of extracting continuous time-series data of various parameters from rocks. Figs. 2-4 are a summary of the work to date. We are continuing work on this core.

8.2 Eocene of Angola

Some of my Italian colleagues, working in Angola, have discovered there what appears to be a truly extraordinary Milankovitch sequence in Eocene chalks, in which the shale-chalk couplets appear even better defined than in the Albian of Italy, as is their bundling into sets of ca 5 (Fig. 5). We hope to make a detailed photographic record of these exposures in 1992, and to sample the sequence in more detail.

The regional setting of this sequence - between the extremely nutrient- rich upwelling belt of southwest Africa and the tropical waters of the Gulf of Guinea - may well have provided an ideal site for recording lateral displacements of the boundary, of the sort that might be driven by orbital cycles.

The Eocene, like the Mid-Cretaceous, was a time of Greenhouse Climate, and this could well turn out to be the most dramatic expression of orbital/Milankovitch cyclicity in greenhouse times. We do not presently have support for this study. Eocene time contains numerous magnetic reversals, well tied into the planktonic fossil record, and if Angolan sequence retains its original remnant magnetism then it should be possible to define the cycle periods with a higher degree or precision than has theretofore been achieved.

8.3 Project Albicore

It is one thing to establish the effects and a record of orbital forcing in principle, in isolated sequences. Such work may indeed help to define the relative changes in cycle periods through time. But they will not shed light on geological problems by providing refined chronologies, nor will they illuminate the problems of ancient climates. For this it will be necessary to study cyclicity globally and for restricted time-slices, which will provide a general view of changes in cycle patterns as related to latitude, continent-ocean distribution etc.

Toward this end I hope to generate a global attack on the pelagic facies of one time-slice - the Ticinella praeticinesis subzone of the Albian, about 100 million years ago, at about the peak of the Cretaceous greenhouse. We chose this zone because (1), it shows such striking cyclicity in Italy (Fig. 2, 3, 4), (2) it is readily recognized by foraminifera and nannofossils, and (3) it stems from a time when high sea- levels left a widely distributed record of pelagic sediment. We expect to find such sediments in about 15-20 countries. My plan is to carry on studies modelled somewhat (with improvements) on those we have developed in Italy (Piobbico core), which will produce comparable data. The

work in individual countries would be financed and carried out by groups of concerned scientists, advised and aided by an international steering committee.

Our first step in this direction will be an international workshop, organized by Premoli Silva, Fischer and Napoleone, to be held on October 4-9, 1992, in Perugia, Italy. The reason for choosing that locale is that it lies within striking distance of the outcrops in which our model - the cyclicity in the Scista a Fucoidi - can be displayed.

This workshop will be largely combined with another, the APTICORE conference of Larson and Erba. This will attempt to organize a parallel project to focus on the slightly earlier (early Aptian) events - the eruption of enormous quantities of basalt in the mid-Pacific region, and the widespread development of oil shales the Selli Bed - which is also very well displayed there. A vital part of the participants - that of the world's Mid- Cretaceous stratigraphers - will be equally involved in both workshops.

The aim of the ALBICORE workshop will include (a) alerting the Mid-Cretaceous stratigraphers to the opportunities provided by these approaches, which provide a focus very different from the conventional one, (b) educating them in the general background, in the need for extended interdisciplinary approaches, (c) providing a general forum of exchange on these matters, (d) organizing some international "action groups" who would set out to undertake such studies at specific locales, and (e) organizing a supporting organization that would provide advice, and support such as providing laboratory facilities for specific types of analyses.

We expect 50-75 people for the combined workshops. Larson has asked NSF Ocean Sciences for support, through JOIDES, and this may help to cover travel expenses for the 15 or so US participants, but is limited to supporting US workers. Our dependence on other nations, many of whose scientists do not have travel money, makes it imperative to find funds no thus restricted. I hope that the NSF Global Change program will allow for this, but we are likely to fall short of support for non-US participants.

9 References

ANDERSON, R.Y., 1982, A Long Geoclimatic Record From the Permian, Journal of Geophysical Research, v. 87, p. 7285- 7294.

BERGER, A., 1980, Milankovitch Astronomical Theory of Paleoclimates: A Modern Review, Vistas in Astronomy, v. 24, p. 103-122.

BERGER, A., 1988, Milankovitch Theory and Climate, Reviews of Geophysics, v. 26, p. 624-657.

BERGER, A., LOUTRE, M.F., AND DEHANT, V., 1989, Influence of the Changing Lunar Orbit on the Astronomical Frequencies of Pre-Quaternary Insolation Patterns, Paleoceanography, v. 4, p. 555-564.

BOARDMAN, D.R. II, AND HECKEL, P.H., 1989, Glacial-Eustatic Sea-Level Curve for Early Late Pennsylvanian Sequence in North-Central Texas and Biostratigraphic Correlation With Curve for Midcontinent North America, Geology, v. 17, p. 802-805.

BRADLEY, W.B., 1929, The Varves and Climate of the Green River Epoch, U.S. Geological Survey Professional Paper, 158, p. 87-110.

DUFF, P.M., HALLAM, A. AND WALTON, E.K., 1967, Cyclic Sedimentation, Elsevier, 280 pp.

FISCHER, A.G., 1964, The Lofer Cyclothems of the Alpine Triassic, Kansas Geological Survey Bull., v. 169, p. 107- 149.

FISCHER, A.G., 1984, The Two Phanerozoic Supercycles: in Berggren, W., and Van Couvering, J., eds., Princeton Univ. Press pp. 29-150.

FISCHER, A.G., 1986, Climatic Rhythms Recorded in Strata, Ann. Rev. Earth & Planet. Sci., 14, 351-376.

FISCHER, A.G., deBOER, P., & PREMOLI SILVA, I., 1990, Cyclostratigraphy, In Ginsburg, R.N., & Beaudoin, B., eds., Cretaceous Resources, Events and Rhythms, Dordrecht-Boston-London, Kluwer Publ., p. 139-172.

FISCHER, A.G., HERBERT, T.D., PREMOLI SILVA, I., NAPOLEONE, G., & RIPEPE, M., 1991, Albian Pelagic Rhythms (Piobbico core), Jour. Sedimentary Petrology, v. 61, No. 7, (in press).

FISCHER, A.G., & ROBERTS, L., 1991, Cyclicity in the Green River Formation (Lacustrine Eocene), Wyoming, 1991, Jour. Sediment, Petrol., v. 61, No. 7, (in press).

GILBERT, G.K., 1895, Sedimentary Measurement of Geological Time, Journal of Geology, v. 3, p. 121-125.

GOLDHAMMER, R.K., DUNN, P.A., AND HARDIE, L.A., 1987, High-Frequency Glacioeustatic Oscillations With Milankovitch Characteristics Recorded in Middle Triassic Platform Carbonates in Northern Italy, Amer. Jour. Sci., 287, 853- 892.

GOLDHAMMER, R.K., OSWALD, E.J., AND DUNN, P.A., 1991, in Franseen, E.K., Watney, W.L., Kendall, C. St. C., and Ross, W.C., (eds.), Sedimentary Modeling: Computer Simulations and Methods for Improved Parameter Definition, Kansas Geological Survey, in press.

HARLAND, W.B., ARMSTRONG, R.L., COX, A.V., CRAIG, L.E., SMITH, A.G., AND SMITH, D.G., A Geologic Time Scale 1989, 1990, Cambridge University Press, 280 pp.

HAYS, J.D., IMBRIE, J., AND SHACKLETON, N.J., 1967, Variations in the Earth's Orbit: Pacemaker of the Ice Ages, Science, v. 194, p. 1121-1132.

HERBERT, T.D., AND FISCHER, A.G., 1986, Milankovitch Climatic Origin of Mid-Cretaceous Black Shale Rhythms in Central Italy, Nature, 321, 739-743.

IMBRIE, J., 1985, A Theoretical Framework for the Pleistocene Ice Ages, Jour. Geol. Soc., London, 142, 417- 432.

IMBRIE, J., AND IMBRIE, K., Ice Ages: Solving the Mystery, Harvard Univ. Press, 224 pp.

MILANKOVITCH, M., 1941, Kanon der Erdbestrahlung und Seine Anwendung auf das Eiszeitenproblem, Serbian Academy of Science, v. 133, 633 pp.

NAPOLEONE, G., & RIPEPE, M., 1990, Cyclic GeomagneticChanges in Mid-Cretaceous Rhythmites, Italy, Terra Nova, 1, 437-442.

NAPOLEONE, G., RIPEPE, M., ALBIANELLI, A., LANDI, S., AND POMPEO, R., 1992, Variazioni Cicliche del Campo Magnetico Terrestre ne'll Albiano Superiore della Seria Umbra, Bol. Societa Geol. Ital., in press.

OLSEN, P., 1986, A 40-million Year Lake Record of Early Mesozoic Orbital Forcing, Science, v. 234, p. 842-848.

RIPEPE, M., ROBERTS, L., AND FISCHER, A.G., 1991, ENSO and Sunspot Cycles in Eocene Oil Shales: An Image Analysis Study, in Franseen, E.K., Watney, W.L., Kendall, C. St. C., and Ross, W.C., (eds.), Sedimentary Modeling: Computer Simulations and Methods for Improved Parameter Definition, Kansas Geological Survey, in press.

ROCC GROUP, 1986, Rhythmi Bedding in Upper Cretaceous Pelagic Carbonate Sequences: Varying Sedimentary Response to Orbital Forcing, Geology, 14, 153-159.

SAVRDA, C.E., AND BOTTJER, D.J., 1989, Trace-fossil Model for Reconstructing Oxygenation Histories of Ancient Marine Bottom Waters: Application to Upper Cretaceous Niobrara Formation, Colorado, Paleogeography, Paleoclimatology, and Paleoecology, v. 74, p. 49-74.

SCHWARZACHER, W., 1947, Ueber die Sedimentaere Rhythmik des Dachsteinkalkes von Lofer, Geologische Bundesanstalt, Wien, Verhandlungen, 1947, No. 10-12, p. 175-188. SCHWARZACHER, W., 1987, Astronomically Controlled Cycles in the Lower Tertiary of Gubbio, Earth & Planet. Sci., Letters, 84, 22-26.

SCHWARZACHER, W., 1990, Milankovitch Cycles and the Measurement of Time, Terra Nova, 1, 405-408.

VAN HOUTEN, F.B., 1964, Cyclic Lacustrine Sedimentation, Upper Triassic Lockatong Formation, Central New Jersey and adjacent Pennsylvania, Kansas Geological Survey, Bulletin, v. 169, p. 497-531.

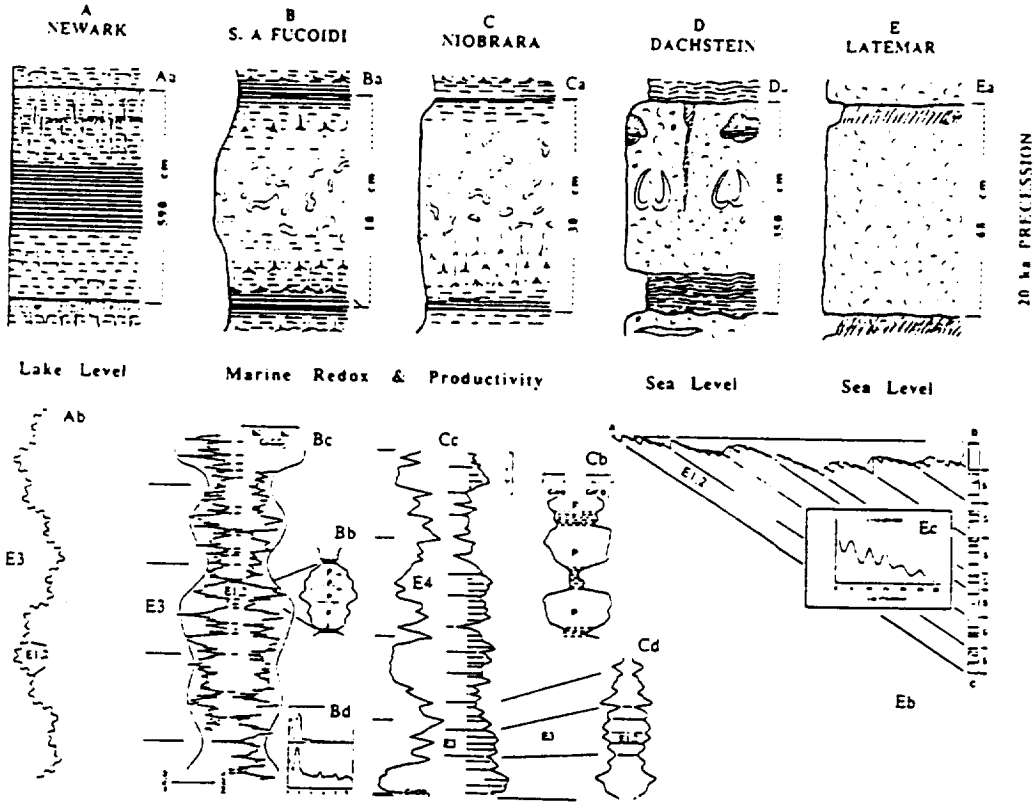

Five stratigraphic sequences showing hierarchical rhythmicity identified with orbital cycles. *Upper tier* comparison of precessional cycles. Note variations in scale. *Lower tier* eccentricity cycles. A Lacustrine facies, Triassic-Jurassic Newark Supergroup, eastern North America. Aa Precessional cycle lake- shore mudstones etc., followed by lacustrine fish-bearing shale (commonly black), succeeded by playa mudstones a lake-level cycle. Ab Eccentricity cycles. E1,2 cycle: fluctuations in carbonate and analcime content, attributed to degree of basin flushing by periodic attainment of overflow E3 cycle is a modulation in oxidation level, resulting in alternation of drab and red colors. B Pelagic, Albian Scisti a Fucoidi, Italy. Ba Precessional cycle black, more or less laminated shale (anaerobic) succeeded by Chondrites marls (dysaerobic) followed by Planolites-bearing limestone (aerobic). Cycle attributed to fluctuations in planktonic carbonate productivity linked to degree of bottom aeration. Bb An E1,2 bundle of precessional cycles expressed in calcium carbonate values (*mirror plot*) and in occurrence of black shales. Piobbico core, Bc Instrumental profiles of 8 m (1600 ka) of Piobbico core, showing darkness curve (*left*) and calcium carbonate curve (*right*). Black shales in center. High-frequency signal is that of precessional couplets; these are grouped into E1,2 bundles, and these into E3 superbundles. (After Herbert and Fischer 1986). Bd multitaper spectra of darkness curve and calcium carbonate curve, showing the E1,2 peak (Park and Herbert 1987). C Hemipelagic Coniacian–Campanian Niobrara Formation. Colorado, USA. Ca Precessional signal: shale, dark, nonbioturbated, anaerobic?, followed by Chondrites chalk (dysaerobic), succeeded by Planolites- bearing chalk (aerobic). Cb Precessional couplets defined by detailed calcium carbonate profiles and organic carbon content. Berthoud No. 1 State. (Pratt et al. 1990). Cc Entire Niobrara Formation, Berthoud No. 1 State. *Left* calcium carbonate curve, general; *right* gamma ray log. Precessional cycles not resolved. E1,2 cycles, at lower limit of resolution, are grouped into E3 superbundles in sets of 4, and these into a yet longer cycle which may represent E4 or a still longer (1600 ka) cycle. (After Pratt et al. 1990). Cd Fort Hays Member. Adobe Oil & Gas Co. Johnson Taylor 11-22, mirror plot of resistivity laterolog. Precessional cycles not resolved. E1,2 cycles grouped into E3 "superbundles". (After Lafferiere et al. 1987). D Platform facies, Late Triassic Dachstein Limestone, Northern Alps. Precessional signal: massive neritic limestone containing large clams etc. alternates with peritidal algal laminites. Evidence that a eustatic oscillation commonly led to full emergence of platform is furnished by occasional presence of relic soils (clayey red to greemudstones) and common mudstone-filled

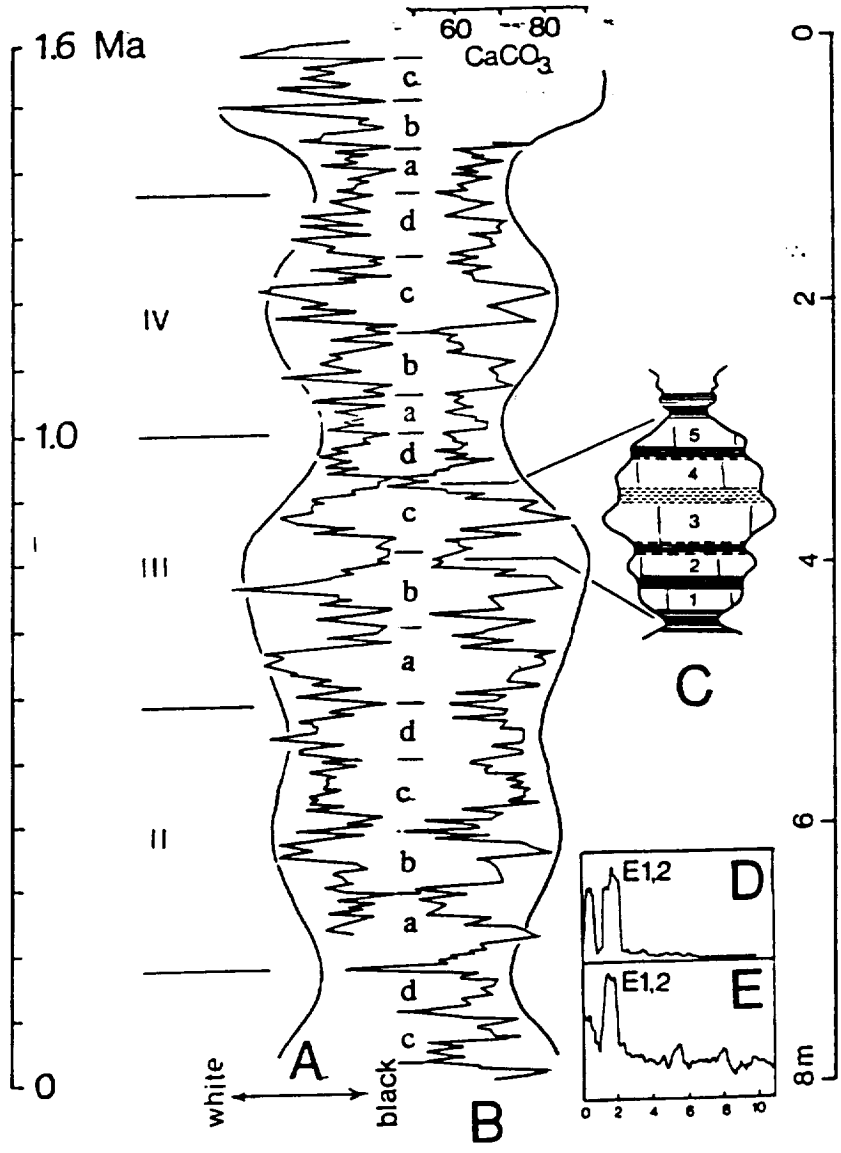

Fig. 2--Quantitative expression of hierarchical Milankovitch cyclicity patterns in the pelagic Mid-Cretaceous (Scisti a Fucoidi) of Italy (Fig. 1). Left curve: variations of gray-scale darkness, by microdensitometry of diapositives; right curve: calcium-carbonate values. High-frequency dark-light (low-carbonate/high-carbonate) bedding couplets (a,b,c,d,e) represent the precessional cycle (productivity and redox cycles combined). A baseline variation in carbonate content (and thickness of carbonate beds) groups these couplets into sets of ca. 5, representing the ca. 100-ka eccentricity cycles (1,2,3,4). The enveloping trace shows the grouping of bundles into sets of 4, representing the ca. 400-ka eccentricity cycle (A,B,C,...). From Fischer et al., 1991.

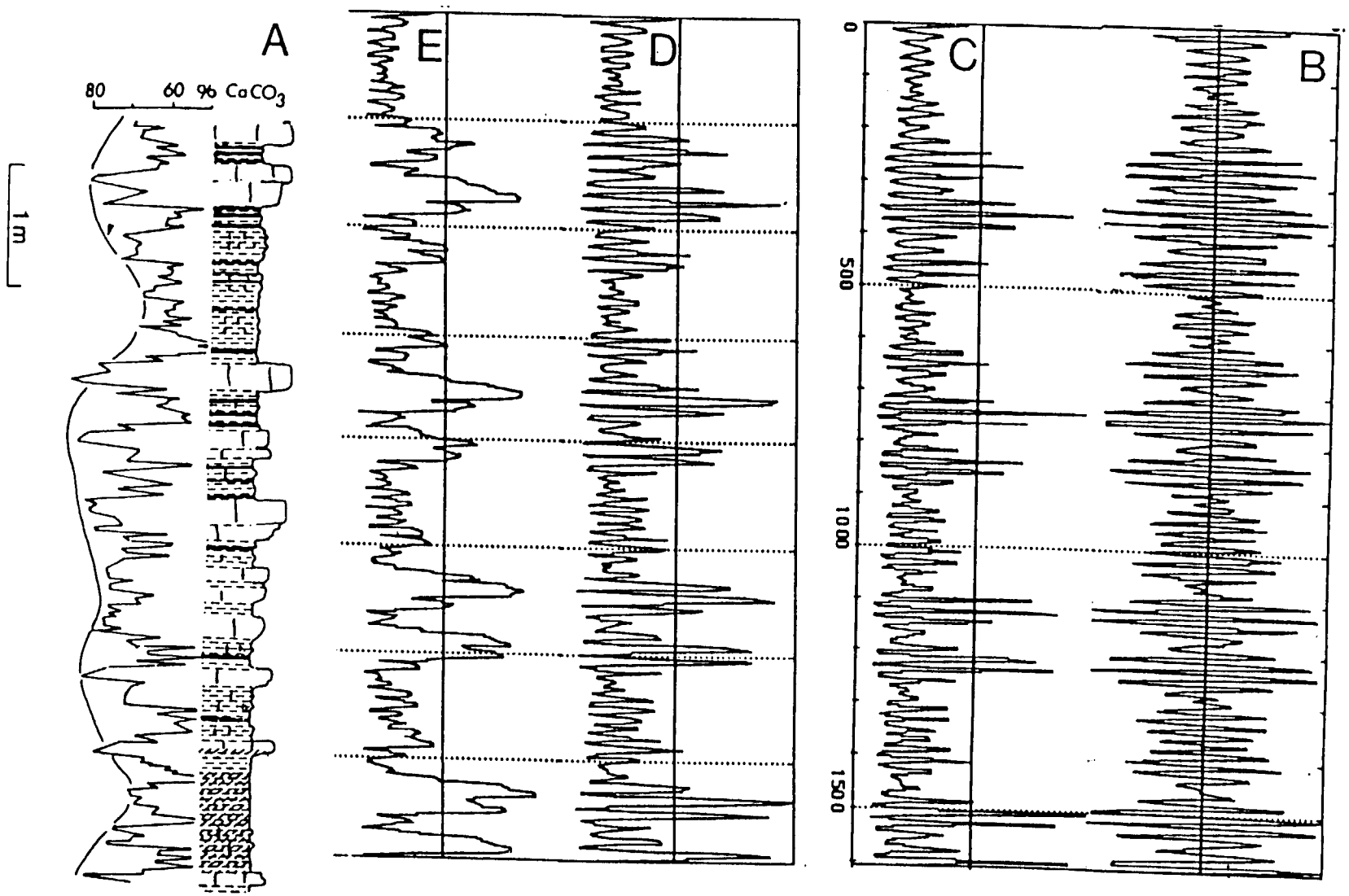

Fig. 3
(A), calcium carbonate profile in m 9-16 of Cretaceous Piobbico core, compared to outcrop expression at Erma, 800 m distant. Time represented ca. 1,400 ka.
(B-E), successive steps in computer simulation of 1,600 ka:
(B), precession index calculated for 1450 ka BP- 150 ka AP.
(C), biogenic rock accumulation rate, obtained by varying skeletal production as a logistic function of B.
D), curve C converted to stratigraphy by converting time-axis to stratigraphic thickness according to accumulation rate.
(E), burrow-mixing to depths varying from 0 to 12 cm as a logistic function of B.
For Fourier spectra, see Fig. 4.

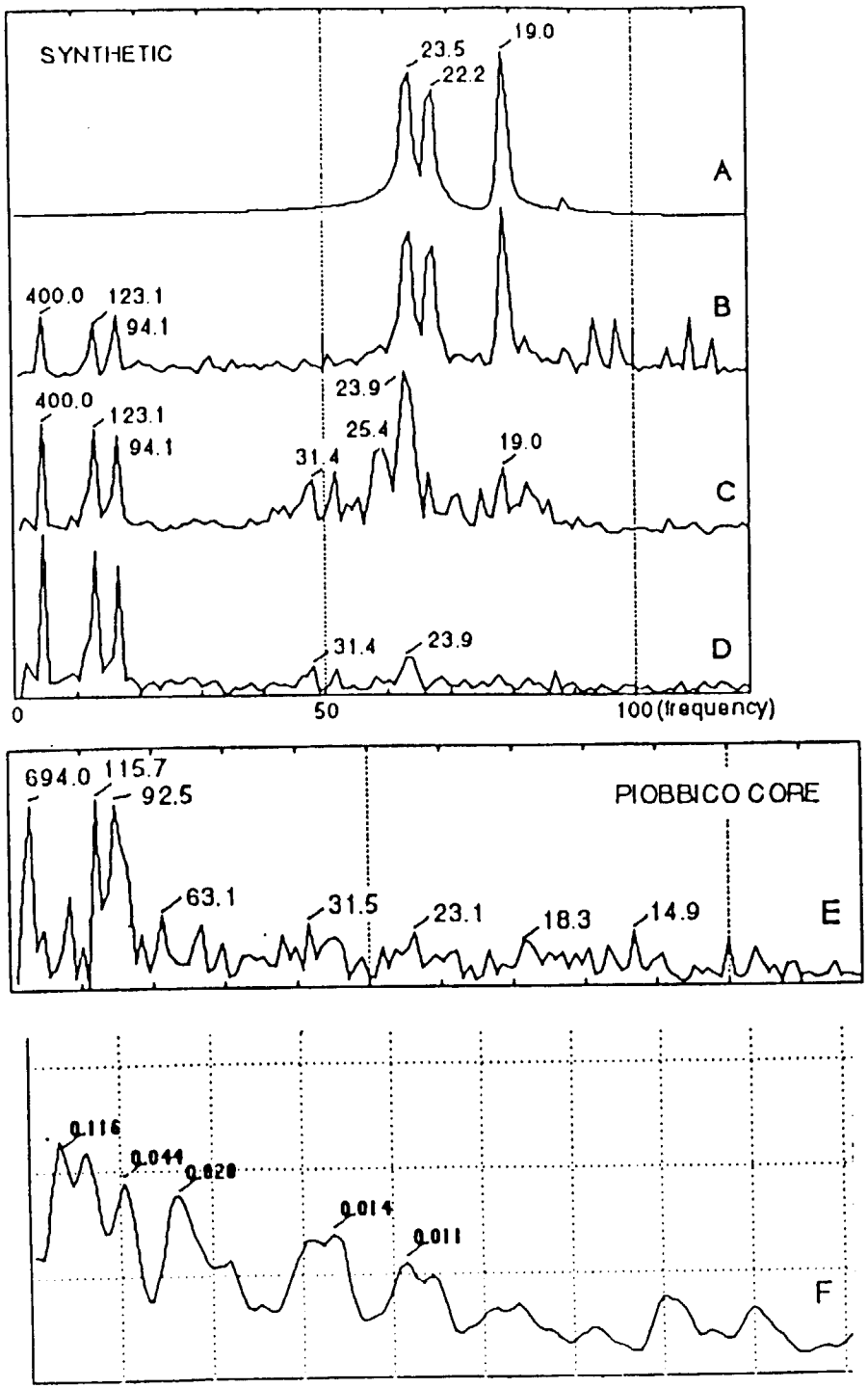

Fig. 4.- Fourier (FFT) spectra. (A), precession index (Fig. 3 B); (B), first step in simulation (Fig. 3C); (C), second step in simulation (Fig. 3D); (D), Synthetic stratigraphy (Fig. 3 E); (E), actual sequence in Piobbico core (calcium carbonate, Fig. 3A). (F), spectrum of foraminiferal abundance. Piobbico core m 10.3-14.2. (G)-(I) magnetic parameters, core m 10.4-12.7, sample spacing 2.5 cm, demagnetized at 200 °C. From various sources.

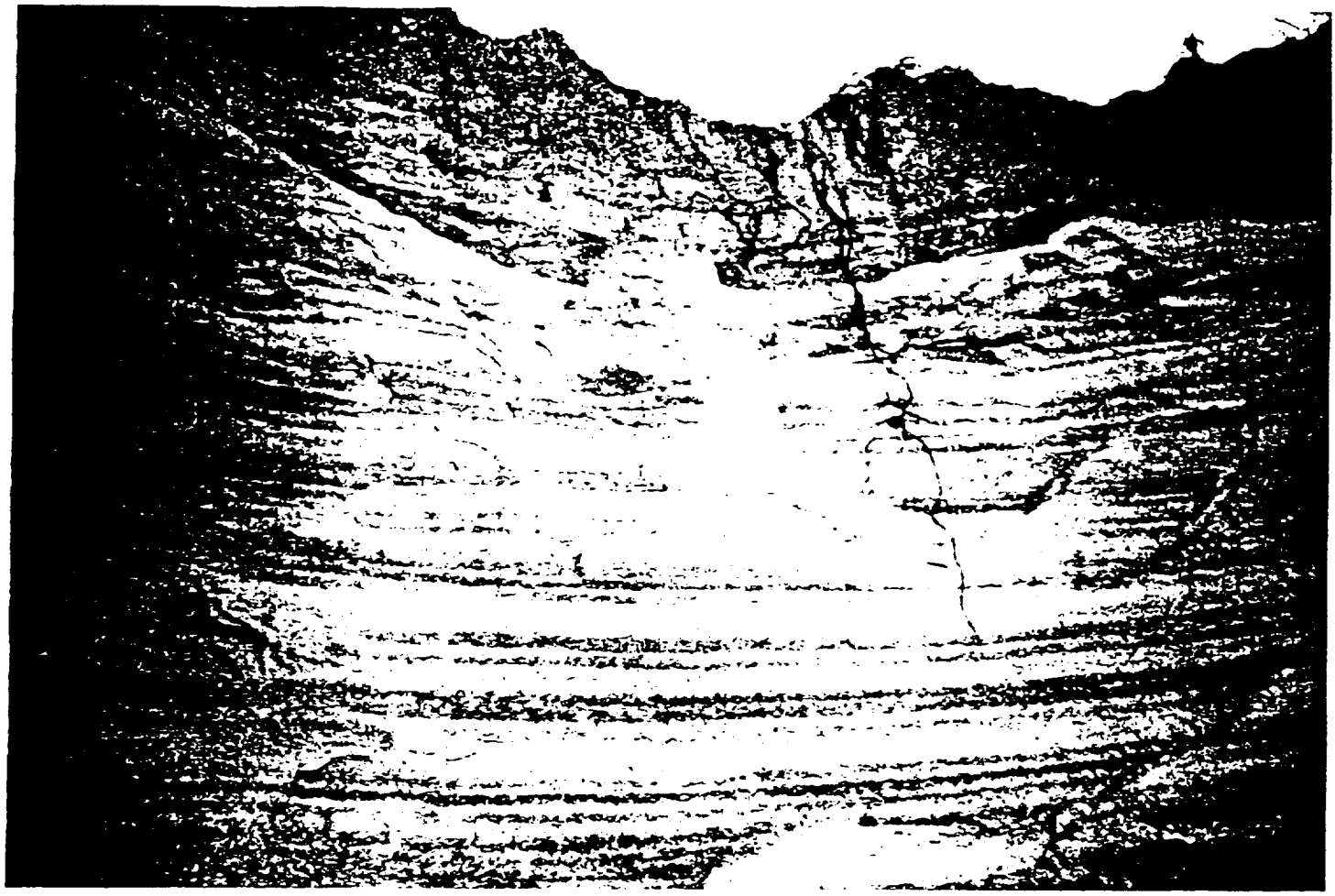

Fig. 5--Pelagic chalk-marl sequence in Eocene of Angola. This is the most dramatic visual stratigraphic record of Milankovitch cyclicity known to me, but has yet to be studied. By analogy with the Scisti a Fucoidi cycles (Figs. 1, 2 and 3), I would interpret the high-frequency chalk-marl bedding couplets as alternations of (a) calcareous plankton blooms combined with bottom aeration, and (b) reduction of carbonate productivity combined with bottom stagnation. This appears to be a record of the precession. They are bundled in sets of ca. 5 into what would have to be the ca. 100-ka eccentricity cycle. The number of bundles in the 20-km strip of coastal cliffs is estimated at ca. 100, which implies a 10-million-year record of Milankovitch cyclicity. Study is being planned.

Evidence of Orbital Forcing in 510 to 530 Million Year Old Shallow Marine Cycles, Utah and Western Canada

Gerard C. Bond
Lamont-Doherty Geological Observatory
Palisades, NY 10964

Michelle A. Kominz
Department of Geology
University of Texas
Austin, TX 78713

John Beavan
Lamont-Doherty Geological Observatory
Palisades, NY 10964

William Devlin
Exxon Production Research Co.
Houston, TX 77252

We have completed spectral analyses of two sequences of shallow marine sedimentary cycles that were deposited between 510 and 530 million years ago. One sequence is from Middle Cambrian rocks in southern Utah and the other is from Upper Cambrian rocks in the southern Canadian Rockies. In spite of the antiquity of these strata, and even though there are differences in the age, location and cycle facies between the two sequences, both records have distinct spectral peaks with surprisingly similar periodicities. A null model constructed to test for significance of the spectral peaks and circularity in the methodology indicates that all but one of the spectral peaks are significant at the 90% confidence level. When the ratios between the statistically significant peaks are measured, we find a consistent relation to orbital forcing; specifically, the spectral peak ratios in both the Utah and Canadian examples imply that a significant amount of the variance in the cyclic records is driven by the short eccentricity (~ 109 ky) and by the precessional (~ 21 ky) components of the Earth's orbital variations. Neither section contains a significant component of variance at the period of the obliquity cycle, however.

In the Utah example, the spectral separation between the short eccentricity and precessional peaks

is longer (by about 30%) than expected for the frequencies of the modern orbital parameters. This result is intriguing because a shift in the separation of the peaks by this magnitude is consistent with the recent estimate by Berger of the changes in the frequencies of orbital parameters for the early Paleozoic.

We were able to extract these results from poorly dated rocks of great age only after applying a new method we have developed, which we call the gamma method, for scaling relative time in sedimentary strata. The gamma method works only for well developed cyclic sequences. It makes use of the fact that if the cycles are periodic, there will be a predictable relation between the duration of the cycles and the durations of the facies that compose the cycles. This relation is tested by applying least squares procedures to data from sections measured through the cyclic strata. The most important advantage of our method is that it does not require a high-resolution numerical time scale; it can be applied to strata of any age, even Precambrian, provided that they have the right type of cyclicity.

The results of our initial experiments suggest to us that our new method has much promise and that the record of orbital forcing in sedimentary rocks, particularly in cyclic strata, may be much more robust over geologic time than is generally thought. To test this idea, we are applying the same methodology to other examples from older and younger parts of the geologic record. One recent result of this work is very encouraging evidence of orbital forcing of shallow marine siliciclastic cycles of Cretaceous age in part of the Western Interior Basin in Wyoming. If we continue to be successful in this ongoing project, we will be in a unique position to address some long-standing questions about the stability of the Earth's orbital system and about long-term changes in the Earth's orbital parameters.

The Cyclic Carbonates of the Latemar Massif: Evidence for the Orbital Forcing of a Carbonate Platform during the Middle Triassic

Linda Hinnov
Department of Earth and Planetary Sciences
The Johns Hopkins University
Baltimore, Maryland 21218

The Latemar Massif is an exhumed carbonate platform in the Dolomites of Northern Italy that was deposited during the Ladinian stage of the Middle Triassic. The platform interior is comprised of hundreds of vertically stacked, meter scale, subtidal limestone/vadose dolostone cap carbonate cycles ("Latemar couplets") arranged into upward thinning bundles of 5. The individual couplets are interpreted as the products of sea level oscillations occurring with a ~ 20,000 year periodicity; the 5:1 bundling is indicative of a lower order ~ 100,000 year modulating component. This combination of cycling is interpreted as a platform response to precession forcing with the 5:1 bundling an expression of modulation by the eccentricity.

Spectral analysis confirms the significance of the 5:1 bundling, and identifies other significant bundling components related to other components of the eccentricity. The results show that the Latemar bundling spectrum is complex, with a splitting of components around the 1:% bundling frequency, suggestive of the multiple component eccentricity in the 100,000 year range. On the other hand, there is no direct evidence for the major 400,000 year eccentricity component, although there is a dominant ~ 700,000 year cycling in the buildup (a 35:1 bundling period). Other higher frequency bundling components may be related to obliquity forcing. Simple models are presented to argue for and against an astronomical origin of these cyclic platform carbonates.

REPORT DOCUMENTATION PAGE

Form Approved
OMB No. 0704-0188

1. AGENCY USE ONLY *(Leave blank)*	2. REPORT DATE	3. REPORT TYPE AND DATES COVERED
	December 1992	Conference Publication

4. TITLE AND SUBTITLE

Orbital, Rotational and Climatic Interactions

5. FUNDING NUMBERS

Code 921

6. AUTHOR(S)

Bruce G. Bills, Editor

7. PERFORMING ORGANIZATION NAME(S) AND ADDRESS(ES)

Goddard Space Flight Center
Greenbelt, Maryland 20771

8. PERFORMING ORGANIZATION REPORT NUMBER

93B00004

9. SPONSORING/MONITORING AGENCY NAME(S) AND ADDRESS(ES)

National Aeronautics and Space Administration
Washington, D.C. 20546-0001

10. SPONSORING/MONITORING AGENCY REPORT NUMBER

NASA CP-3185

11. SUPPLEMENTARY NOTES

12a. DISTRIBUTION/AVAILABILITY STATEMENT

Unclassified - Unlimited
Subject Category 46

12b. DISTRIBUTION CODE

13. ABSTRACT *(Maximum 200 words)*

This document contains the report of an international meeting on the topic of Orbital, Rotational and Climatic Interactions, which was held July 9-11, 1991 at the Johns Hopkins University. The meeting was attended by 22 researchers working on various aspects of orbital and rotational dynamics, paleoclimate data analysis and modeling, solid-Earth deformation studies, and paleomagnetic analyses. The primary objective of the workshop was to arrive at a better understanding of the interactions between the orbital, rotational and climatic variations of the Earth. This report contains a brief introduction and 14 contribued papers which cover most of the topics discussed at the meeting.

14. SUBJECT TERMS

Paleoclimate, Precession, Obliquity, Orbital Eccentricity, Milankovitch Cycles

15. NUMBER OF PAGES

124

16. PRICE CODE

A06

17. SECURITY CLASSIFICATION OF REPORT	18. SECURITY CLASSIFICATION OF THIS PAGE	19. SECURITY CLASSIFICATION OF ABSTRACT	20. LIMITATION OF ABSTRACT
Unclassified	Unclassified	Unclassified	Unlimited

NSN 7540-01-280-5500

Standard Form 298 (Rev. 2-89)
Prescribed by ANSI Std. 239-18, 298-102

NASA-Langley, 1993

National Aeronautics and
Space Administration
Code JTT
Washington, D.C.
20546-0001

Official Business

Penalty for Private Use, $300

BULK RATE
POSTAGE & FEES PAID
NASA
Permit No. G-27

POSTMASTER: If Undeliverable (Section 158 Postal Manual) Do Not Return